Investigating cannabinoids and endocannabinoid receptors as drug targets for pain and inflammation.

A thesis submitted to Rhodes University

by

Sinobomi Zamachi Marwarwa

In fulfilment of the requirements for the degree of

Master of Science in Chemistry

RHODES UNIVERSITY

Where leaders learn

September 2020

Acknowledgements

"*The fear of the Lord is the beginning of all wisdom*"

Proverbs 9:10

I would like to express my sincere gratitude to my supervisor Prof RWM Krause for his enthusiasm, knowledge and belief in my ability to conduct this research. Thank you to Prof P Kaye, Prof K Lobb and Prof C Frost for assisting me with your knowledge and resources. I am extremely grateful Dr MP Ngoepe, for always being there to encourage and support me, you have been a mentor and a friend.

Dr A Sarron, Dr FI Khan, Jarmo Kalinski, Judith Webber, and Luxolo Joji, thank you for your knowledge and support. To Thanduxolo Mtshare, I am humbled by the amount of support that you have given me throughout the process of perusing this degree. To my colleagues in my research group and labmates, your support is appreciated.

I am appreciative to Rhodes University and the Rhodes University chemistry department Staff. The Library Staff and colleagues for their support. I am grateful to the National Research Fund (NRF) for funding this research.

Finally, I would like to thank family and friends for all their support. I am extremely grateful to my parents Mr WS and Mrs SG Marwarwa for their prayers, love, and support. To my siblings maNcayiyana amahle, your ability to take my sense of humour seriously gave me the strength to pull through, you have been very supportive, thank you.

Abstract

Cannabinoids and the endocannabinoid system have been studied in the past decades but have yet to be fully understood. An insight into interactions that occur between cannabinoid compounds and their receptors is important for understanding the cannabinoids and the endocannabinoid system. Cannabinoids are natural products found in some cannabis plants, and they have similar effects to endocannabinoids, which are chemicals in the body that are involved many aspects of health from appetite, memory, and movement to pain, inflammation and response to cancer. Cannabinoids have a high impact on the treatment of pain and inflammation, they show different antinociceptive mechanisms to existing drugs like opioids, also, they have antimigraine properties better than those achieved by aspirin. The CB1 and CB2 human receptors have been the most studied cannabinoid receptors. In this project, we used a combination of mass-spectrometry to generate plausible chemical fragments and computational techniques to assess the binding of these fragments to these two main CB receptors. CB1 was adapted from the protein data bank (PBD), file 5U09 and the CB2 model was predicted using the hierarchical protocol I-TASSER, starting from the amino acid sequence in UniProt (P34972 CNR2_HUMAN). The proposed active site for CB1 was reported in a publication accompanying the 5U09 PDB model, which was originally generated with a pre-existing ligand in the active site. However, CB2 had to be built from a homology model and the active site determined using a combination of I-TASSER, Maestro, and CASTp the more favourable binding energies were determined by CASTp, leading to the use of the CASTp coordinates as default for docking in the CB2 human receptor. The molecular docking of cannabinoids THC, CBD, CBDV, CBG and CBN on both the CB1 and CB2 proteins was performed to identify the amino acids that interact with these compounds at their active sites. This would provide a guide to a future fragment-based drug discovery (FBDD) synthesis project. The docking in this work showed adequate accuracy with binding energies between -8.23 kcal/mol and -9.97 kcal/mol for CB1 and between -6.78 kcal/mol and -7.74 kcal/mol for CB2. An observation made was that binding energies of the CB1 human receptor docking were higher than those of the CB2 human receptor, which could support the widely held belief that CB1 is more important in cannabinoid interactions. The cannabinoids were then subjected to collision-induced dissociation to produce fragment structures predicted in chapter 2. These hypothetical fragments were docked in the CB1 and CB2 human receptor, the general trend

again being the binding energies for the CB1 receptor was again around 10% higher than those of the CB2 receptor. As expected, larger fragments tended to have better binding, with the fragment proposed from *m/z* 259 with binding energies -9.62 kcal/mol in CB1 and -6.26 kcal/mol. Those fragments with significant lipophilic side chains or some aromatic moiety also showed good binding or around -6.00 kcal/mol, similar to the intact cannabinoids. In our case, this fragment was proposed from *m/z* 223 with binding energies -7.71 kcal/mol in CB1 and -6.5 kcal/mol in CB2. The results from the fragment dockings were favourable in that they have binding affinities lower than -6.0 kcal/mol which is good enough for the structures to be leads in the creation of fragment libraries. The docking was performed with Autodock 1.5.6 and data visualization with a discovery studio.

Table of contents

List of Abbreviations

2-AG	2-Arachidonoylglycerol
AC	Adenyl cyclase
ACN	Acetonitrile
AEA	Anandamide
BPC	Base peak Chromatogram
CASTp	Computed atlas of surface topography of proteins
CB1	Cannabinoid receptor 1
CB2	Cannabinoid receptor 2
CBC	Cannabichromene
CBCA	Cannabichromene acid
CBCAS	Cannabichromenic acid synthase
CBCVA	Cannabichromenevarinic acid
CBCVA	Cannabichrovarinic acid
CBD	Cannabidiol
CBDA	Cannabidiolic acid
CBDAS	Cannabidiolic acid synthase
CBDMA	Cannabidiolic acid monoethyl ether
CBDV	Cannabidivarin
CBDVA	Cannabidivarinic acid
CBG	Cannabigerol
CBGA	Cannabigerolic acid (3-geranyl olivetolate)
CBGAS	Cannabigerolic acid synthase
CBGVA	Cannabigerovarinic acid
CBN	Cannabinol
CBNA	Cannabinol acid
CBNRA	Cannabinerolic acid (cis-CBGA)
CBR	Cannabiripsol
CBTA	Cannabitriol acid
CID-	Collision induced dissociation
CNS	Central nervous system
DOR	delta opioid receptor

ECS	Endocannabinoid system
ESI	Electrospray ionisation
EI	Electron ionisation
FAAH	Fatty-acid amide hydrolase
FBDD	Fragment based drug design
Glu	Glutamate
HPC	High performance computing
I-TASSER	Iterative Threading ASSEmbly Refinement
KOR	Kappa opioid receptor
LC-MS	Liquid chromatography- mass spectrometry
m/z	mass-to-charge ratio
MAGL	Monoacylglycerol
MAPK	Microtubule associated protein kinase
MeOH	Methanol
mGluRs	Metabotropic glutamate receptor
MOR	Mu opioid receptor
MS1	Mass spectrometry 1
MS2	Mass spectrometry 2
rt	Retention Time
THC	Tetrahydrocannabinol
THCA	Tetrahydrocannabinolic acid
THCAS	Tetrahydrocannabinolic acid synthase
THCV	Tetrahydrocannabivarin
TIC	Total ion chromatography
ToF	Time –of- Flight
TRPV1	Transient receptor potential vanilloid type-1

List of Figures

List of Tables

List of Schemes

Chapter 1
Introduction and Review

1.1 Introduction

Cannabis taken here to mean plant parts or extracts has long been used for its medicinal properties and therefore has a history beyond formal scientific research (1). Cannabis use has been diverse worldwide, with some cannabinoid research being influenced by the knowledge of its use in traditional healing and its use as an illicit drug. The status of cannabis as an illicit drug in many countries has contributed to its colossal stigma and ensured that cannabis research has fallen behind many other plants. A body of research that dates to the 1930s, along with the research by people like Raphael Mechoulam in the 1960s, has made a great impact on the recognition of the cannabis plant as a medicinal plant (2). Raphael Mechoulam and colleagues were the first to have research that includes structure identification of phytocannabinoids like tetrahydrocannabinol (THC) and cannabidiol (CBD), the discovery of the endocannabinoid system (ECS) and endocannabinoids (e.g. anandamide) (1). These discoveries led to research on structure-activity relationships (SAR) of cannabinoids and work reaching clinical trials for different diseases (3). The importance of the cannabis plant for treating diseases has brought attention to the different cannabis strains which are *Cannabis Sativa, Cannabis Indica*, and *Cannabis Ruderalis* (Figure 1.1) (4).

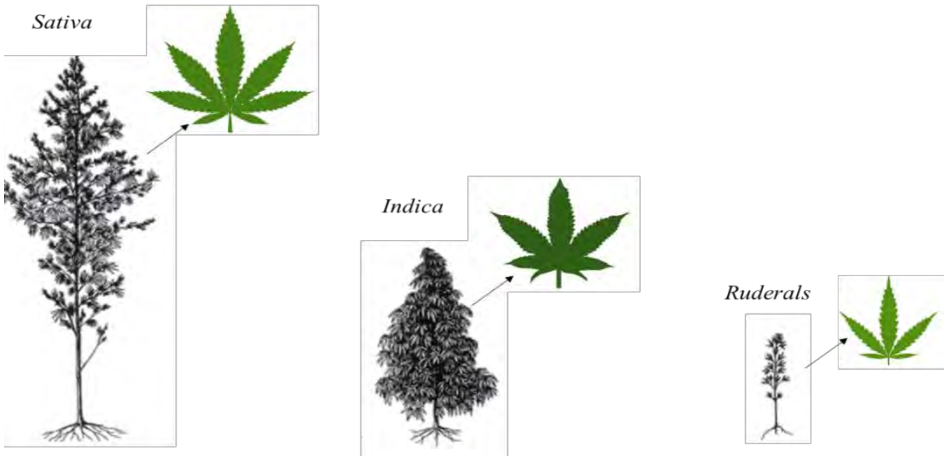

Figure 1.1: A visual representation of *Cannabis Sativa*, *Cannabis Indica*, and *Cannabis Ruderalis*.

The most researched cannabis plant is the *Cannabis Sativa* with multiple cannabinoids extracted and analyzed leading to the identification of multiple cannabinoids including tetrahydrocannabinol (THC), cannabidiol (CBD), cannabidivarin (CBDV), cannabinol (CBN), cannabigerol (CBG) to name a few (5). The identified cannabis compounds (cannabinoids) have been found to have an impact on the treatment of pain and inflammation among other clinical diseases (6). Another plant that has been found to have an impact on the treatment of pain is called *Papaver somniferum* (Figure 1.2), which is also known as the poppy plant (7). *Papaver somniferum* is the source of many alkaloids and among the natural opioids, morphine is perhaps the most well-known (8).

Figure 1.2: The *Papaver somniferum* plant (photograph: http://botanika.wendys.cz/).

Compounds extracted from the opium plant are called opioids and are known to bind opioid receptors in the endogenous opioid system (9). The cannabis plant compounds (cannabinoids) also bind to an endogenous cannabinoid system (ECS) consisting of cannabinoid receptors (CB1 and CB2). The endogenous opioid system has a mu-opioid receptor (MOR) distributed in similar areas to the CB1 receptor with not much restriction in its distribution. On the other hand, cannabinoid receptors are restricted in their distribution towards the delta-opioid receptor

(DOR) and kappa-opioid receptor (KOR) (10). Cannabinoids have been researched individually and synergistically with opioids for a variety of diseases and the results have been promising (11). However, cannabis research has to date lacked clinical trials which could lead to the use of cannabinoids for treatment.

Chronic pain is a problem globally usually followed by inflammation that is the body's attempt at self-protection to remove harmful stimuli (12). Chronic pain, however, is a sensory experience that extends beyond a minimum of 12 weeks (13). Chronic pain is significant healthcare and economic challenge affecting people of all ages and with many causes. Recently, chronic pain has been described as a disease based on the complex functional and structural pathological changes (14). Pain has not been approved to be classified as a disease, this is based on the grounds of confusion of pain as a symptom, a cause and a pathological feature (14). Several diseases may be worsened as a result of inflammation, acute bronchitis, infective meningitis, rheumatoid arthritis, sore throat from cold or flu and other physical traumas (15). A challenge for clinical pain management has been the association of chronic pain and impairment of cognitive functions (16). This is said to be caused by pain-related sensory inputs competing for the attention of the resources required for cognitive functions (17). Neurochemical mediators may have a role in altering neural circuitries that interfere with normal cognitive functions, as proposed by Hart *et al*, (2000) (18).

Research has shown that some autonomic nervous system functions are associated with the endogenous opioid system. It has some control in the gastrointestinal motility, breathing and in the modulation of the immune response (19). The endogenous opioid-system modulates the ascending and descending pathways in pain; hence it is essential in the control of nociceptive response in the peripheral and central levels. An example of a condition characterized by chronic pain and inflammation is osteoarthritis (20). Analysing similarities between the opioid and cannabinoid endogenous systems may lead to an improvement in cannabis research for pain and inflammation because opioids have proved effective for pain relief. The similarities between opioids and cannabinoids are that they both uke have G-coupled receptors associated with the Gi/o protein and are broadly distributed in the nervous system and peripheral tissues (21). This knowledge can be useful in understanding the endocannabinoid system as an analgesic. The mechanisms of action between opioids and cannabinoids differ, this difference could explain the reason cannabinoids are not major addictive agents compared to opiates and cocaine (9).

This review aims to discuss the evidence provided in clinical research about the role of cannabinoids in anti-nociception. The studies include models of chronic pain inflammatory pain including the sites that the sites and mechanisms involved. An objective is to know the position of receptors in the endocannabinoid system and their distribution in the pain pathway. Mechanisms that have been studied as analgesic compounds, give useful information that can be used in proposing how cannabinoids can be effective in the treatment of pain and inflammation.

1.2 Pain and inflammation

The brain and nervous system have cells called neurons, which have a cell body that runs the activity of the neurons (22). The cell body has dendrites which are fibres responsible for transmitting and receiving signals between neurons (23) (24). Attached to the cell body is an axon a long fibre that sends messages from the cell body to the dendrites on other cell bodies (25). Axons are present in other tissues such as muscles performing the same function of transmitting commands as needed (25). This communication is called neurotransmission playing a major role in pain pathways (26). Neurotransmission is the release of chemical messages called neurotransmitters across the spaces between cells which are called synapses (27). Receptors pick up chemicals released from axons as a response to stimuli which is either temperature or mechanical different receptors send the chemical messages to the brain (28). Stimuli interpreters become noxious, meaning they cause damage to occur on tissues (29). Specialised receptors called nociceptors located throughout the body send the message to the brain (30). It is important to note that nociceptors are not as we think located topically on the skin and between joints (31). This makes the understanding of the difference between resolved or non-resolved causative factors between chronic pain and acute pain easier (21). Nociceptors are the first step in interpreting and sending the message to the brain (7).

When we encounter a noxious stimulus like heat (high temperature), an electrical signal is sent up to a primary afferent neuron to a part of the spinal cord called the dorsal route ganglia where their electrical current causes a release of neurotransmitters that pass the pain from the primary afferent neuron to a secondary excitatory neuron (25). Pain signalling involves several neurotransmitters, but the major players are glutamate and substance P. The message is then sent up the spinal cord to different parts of the brain where it is interpreted as pain (32). The thalamus also receives the signal which helps give context to the message. The thalamus relays

the message to the hypothalamus and limbic system and helps us learn to avoid noxious stimuli (29). A disadvantage of this that this receipt of these messages by our brains can modify our behaviours (27). Pain does not only have long-term physical effects it also has physiological consequences (33). The background knowledge on pain and inflammation suggests the importance of the location of cannabinoid receptors along the pain pathway (Figure 1.3).

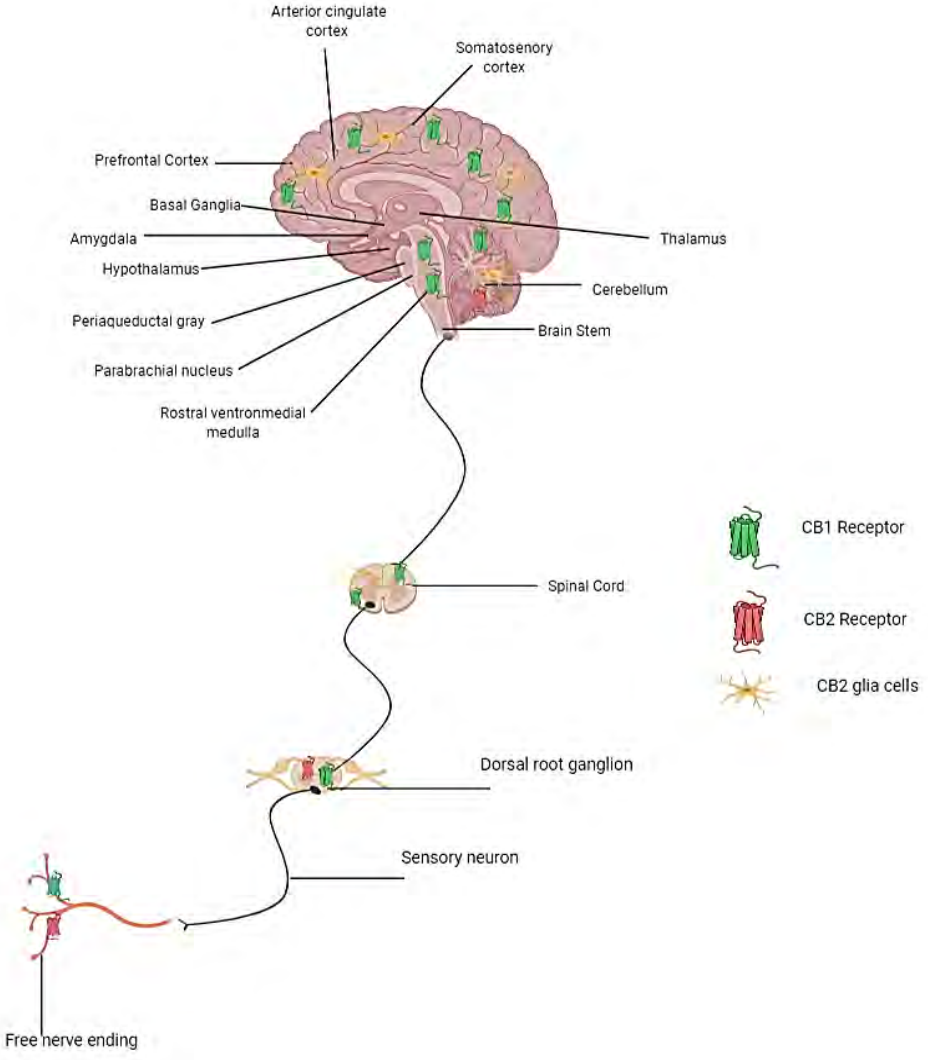

Figure 1.3: Representation of the pain pathway and position of CB1 and CB2 receptors (created with biorender @biorender.com).

The position of cannabinoid receptors in the pain pathway shows the potential role of cannabinoids in pain and inflammation relief. The receptor-ligand interactions that could occur at these points could induce a therapeutic effect (33).

1.2.1 Pain

The cannabinoids can be administered in different ways to ensure they have the desired pharmacological effect (34). The endocannabinoid system has recently been investigated for its role in pain relief (21). Pathways for pain relief display a few main points to consider, firstly the cannabinoid receptor agonists can retard electrochemical reactions at the peripheral receptors (35) (36). Secondly, agonists can induce interruption of the pain signals at the dorsal root ganglia as well as the neuron (37). Thirdly CB2 receptors are activated at the leukocytes which give major anti-inflammatory responses (38) (39). Lastly, there are psychoactive and euphoric effects associated with cannabinoid receptor agonists, reduction of short-term memory in addition to alleviation of the stress response to pain (21). Where there is pain, visually inflammation is observed, and this leads to the need to understand inflammation as well as pain.

1.2.2 Inflammation

Inflammation is the body's way of protecting itself from major damage caused by noxious stimuli (40). It is a response to defend the body allowing the healing process to begin (41). The inflammation defence mechanisms are characterized by tissue destruction and attempt to repair occurring simultaneously (42). Chronic inflammation leans towards being slightly swollen and firm, lasting for a few days to weeks (39).

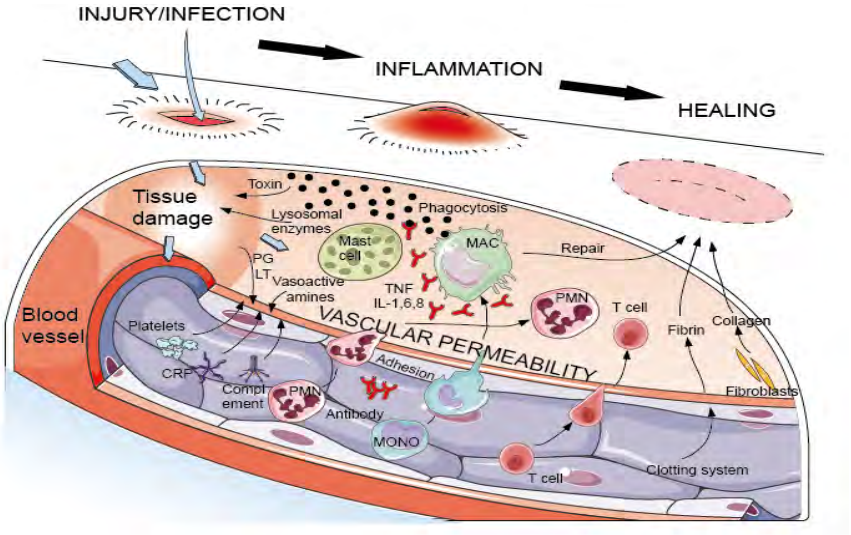

Figure 1.4: Model representing a generic chronic inflammatory (Creative-diagnostics.com).

Above the figure shows the basic characteristics of inflammation involve the discriminatory and sequential movement of blood cells into tissues and then local activation and interaction of these blood-based cells with resident tissue cells (23). Chronic inflammation may be involved in the worsening degenerative neurological diseases such as Alzheimer's and Parkinson's (43). Apart from noxious stimuli and bacterial infections inflammation is also caused by dietary choices (40). This form of inflammation can last longer periods which can then be classified as chronic inflammation (9). Cannabinoid regulation of inflammation relies on the expression of the CB2 receptor in leukocytes, they are in the peripheral nervous system (PNS) where inflammation is most likely to occur and be visible. It is important to understand the endocannabinoid system (ECS) to suggest ways in which healing can occur.

1.3 Endocannabinoid system

The endocannabinoid system (ECS) is a biological system that has receptors that bind endocannabinoids and produce a biological response (44). The discovery of the endocannabinoid system was sparked by the discovery of THC which in turn led to the discovery of AEA as one of the first endocannabinoids (45). Endocannabinoid system studies were done in mice and have verified the physiopathological processes in the nervous systems and peripheral organs (16).

The CBR1 and CBR2 receptors are G-coupled proteins and represent the most studied of the ECS receptors (1). They have seven transmembrane domains associated with the $G_{i/o}$ protein (46). Other receptors cannabinoid receptors include TRPV1, GPR3, GPR6 and GPR12 that are sphingolipid receptors (47). Cannabinoids have different affinities for cannabinoid receptors. This, however, does not negate the necessity of the ECS. CB1 is in the presynaptic terminals, they modulate the release of a variety of neurotransmitters mainly glutamate and gamma-aminobutyric acid (GABA). It also modulates dopamine, serotonin, acetylcholine (48) (16). Cannabinoids found in plants are phytocannabinoids, synthetic cannabinoids are a product of organic synthesis and the cannabinoids in the body are endocannabinoids (49) (50). These different types of cannabinoids are potential agonists or antagonists to various cannabinoid receptors. The distribution of the CB1 and CB2 cannabinoid receptors can be seen in Figure 1.5. The CB1 and CB2 receptors have been used in this because there is more information available on these receptors. In chapter 3 docking studies were conducted using the CB1 and CB2 models.

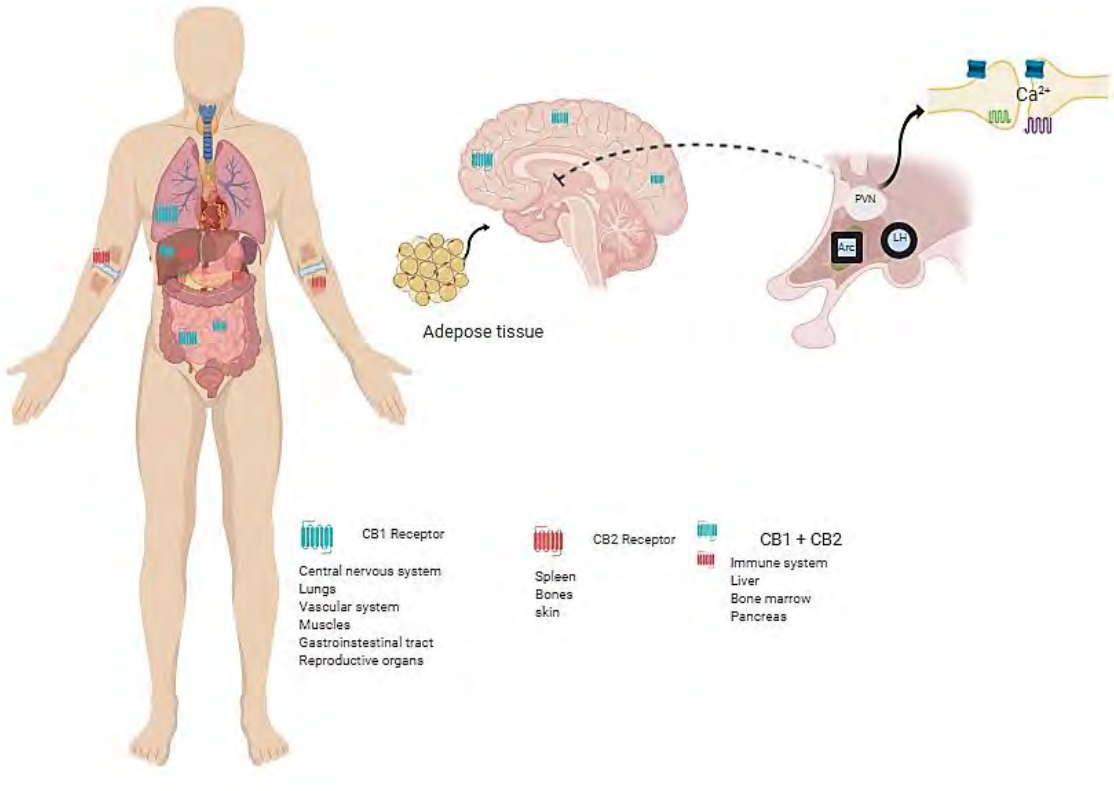

Figure 1.5: A representation of the endocannabinoid system (created with @biorender.com).

1.3.1 Endocannabinoid receptors

The CB1 and CB2 cannabinoid receptors have become ideal for research due to the increasing interest in cannabinoid pharmacology (51). Cannabinoids have been found to have therapeutic potential to control pain, obesity, epilepsy and many other disorders (45). These receptors are G-Coupled proteins found in the peripheral nervous system (PNS), central nervous system (CNS) and the brain (27). They are distributed across the body in areas that are nociceptive and addictive pathways (35)(29). The CB1 receptor explains the psychoactive effects of THC and they work in the periphery, gut and the brain (3). These receptors are the most abundant in the brain, involved in mediating pain (52). They are expressed in the nociceptive areas, limbic system, cerebellum, basal ganglia and reward pathways (27) (26). The CB1 receptors are potent in the substantia nigari and periaqueductal grey, being distributed in a limited fashion in the brainstem (39). They are not potent in the medullary respiratory centres, which supports the hypothesis that cannabinoids do not cause respiratory problems no matter how high the dosage. The CBR2 are mainly found in the peripheral organs and is an immunomodulatory receptor with an important role in pain, inflammation and physiological defence (15) (53). The drugs that affect CB2 would be drugs that cure fibrotic diseases such as scaring in the liver or other organs (54). The ECS has a role in regulating physiological and cognitive processes such as mood, pain sensation and pharmacological effects of cannabinoids (55).

1.3.2 CB1 and CB2 receptor signalling

To understand the effect of cannabinoids on the ECS, a suggestion is to pay attention to the signal pathways involved. The pathway activated is determined by the environment of the cells the G-coupled proteins, ligands and enzymes involved (56). CB1 is capable of being activated in more signal pathways than CB2, this is likely due to its abundance in biological systems (34). Cannabinoids receptor stimulation causes different effects cannabinoid receptors CB1 and CB2 activate heteromeric $G_{i/o}$ proteins ($\alpha\beta\gamma$) to mediate their biological effects (57). They activate a variety of signal transduction pathways, activating pathways that cause the inhibition of adenyl cyclase activity and decrease of cyclic adenosine monophosphate(cAMP) and protein kinase (PKA) activity (56) (28).

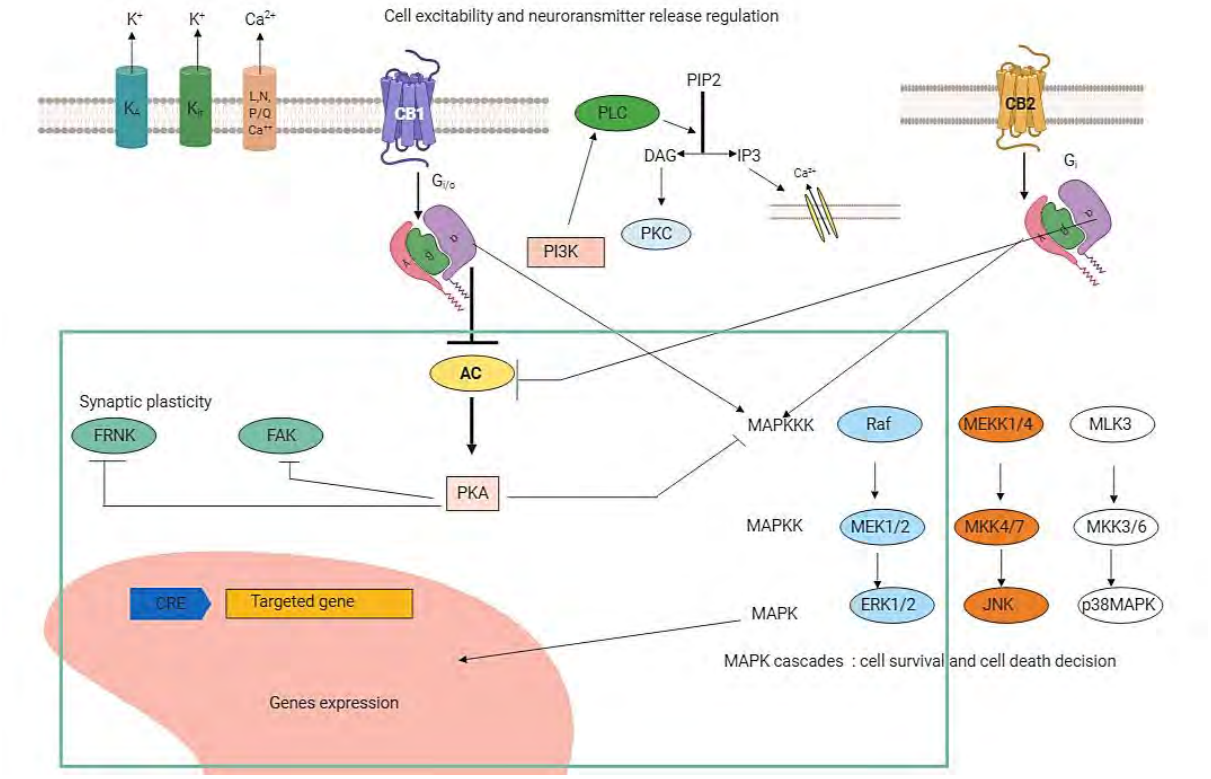

Figure 1. 6: Endocannabinoid system, cannabinoid receptors and signalling pathways (created with @biorender.com).

Bosier *et al* (2010), reviewed and discussed cannabinoid receptors and mechanisms allowing for specificity in responses, based on interaction with cannabinoids this is represented in Figure 1.6, where activities that occur in the signalling pathways are also depicted. As observed above, the CB1 and CB2 receptors show that they can be linked to their similarity to $G_{i/o}$ G-coupled proteins. $G_{i/o}$ – dependent inhibitions of adenyl cyclase (AC) activity along with Gβγ-dependent activation of different MAPK signalling cascades (56). The CB1 protein is involved in regulating the voltage-gated Ca^{2+} channels negatively, while positively regulating inwardly rectifying K^+ channel, therefore, inhibiting neurotransmitter release. This shows that these pathways can affect each other because they require cannabinoid-mediated inhibition of PKA (56). Ligands that have given much insight into understanding the endocannabinoid system are endocannabinoids which we have discussed in detail, hence the performance of docking studies on the CB1 and CB2 receptors in chapter 3.

1.4 Endocannabinoids

Endocannabinoids are compounds that are synthesized in the body that regulates the ECS, unlike phytocannabinoids that are produced by cannabis plants. In the ECS, there is constant synthesis and biodegradation of these compounds. They play a crucial role in researchers' ability to map out the ECS. In the process of the discovery of THC, N-arachidonoylethanolamine (Anandamide, AEA) was the first to be discovered in the 1960s by Dr Raphael Mechoulam (50). Anandamide is a compound that acts like THC and shares its properties like stimulus effects at the receptor and cellular level (1). AEA and THC are both agonists of CB1 and CB2 receptors. They affect appetite, pain, and memory (50). Other endocannabinoids were also identified such as 2-arachidononylglycerol (2-AG), 2-Noladin ether), arachidonyldopamine (NADA) and o-arachidononylethanolamine (Virodhamine) Figure 1.7). Their physiological relevance is not yet known (58).

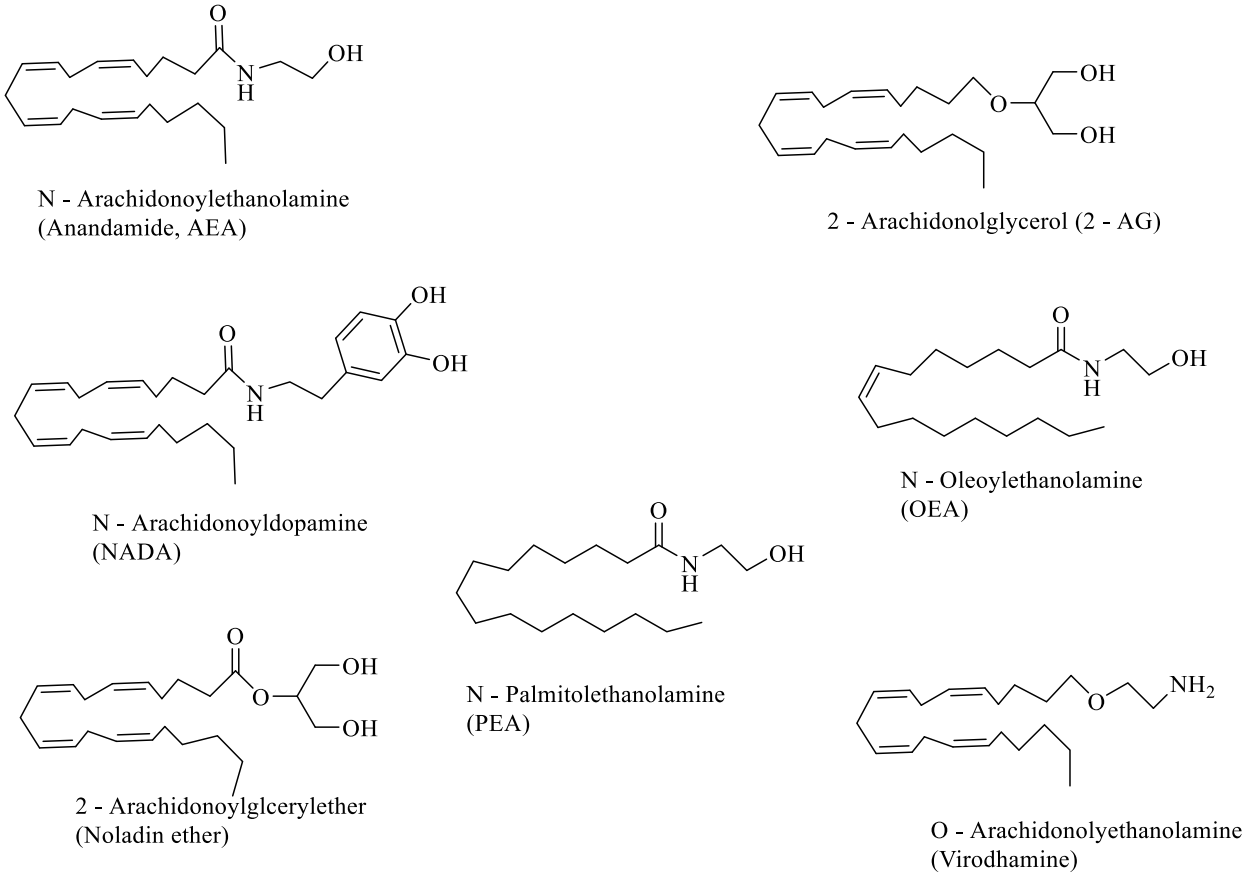

Figure 1.7: Structures of some endocannabinoids identified as part of the endocannabinoid system.

According to Wilson *et al* (2002), endocannabinoids are synthesized rapidly when needed (59). This happens in the postsynaptic neuron, where they act as retrograde messengers regulating the release of neurotransmitters at the presynaptic level. Homeostasis is maintained by endocannabinoids because they are neuromodulators that prevent the presence of excessive neural activity (34). Cell membrane lipids produce AEA and 2-AG from biosynthetic pathways (48). The diacylglycerol lipase (DGL) enzyme mediates the synthesis of 2-AG from diacylglycerol. According to Grotenhermen (2004), enzymes N-acyltransferase and phospholipase D synthesize AEA from the precursor N-arachidonic-phosphatidylethanolamine (38). Degradation of anandamide is by fatty-acid amide hydrolase (FAAH) (38) (Figure 2) and 2-AG is metabolised by monoacylglycerol lipase (MAGL) (60). In the brain 2-AG is the most abundant endocannabinoid and it as an agonist on CB1 and CB2. The life cycle of anandamide may lead to understanding how other cannabinoids would interact with the endocannabinoid receptors (see Figure 1.8).

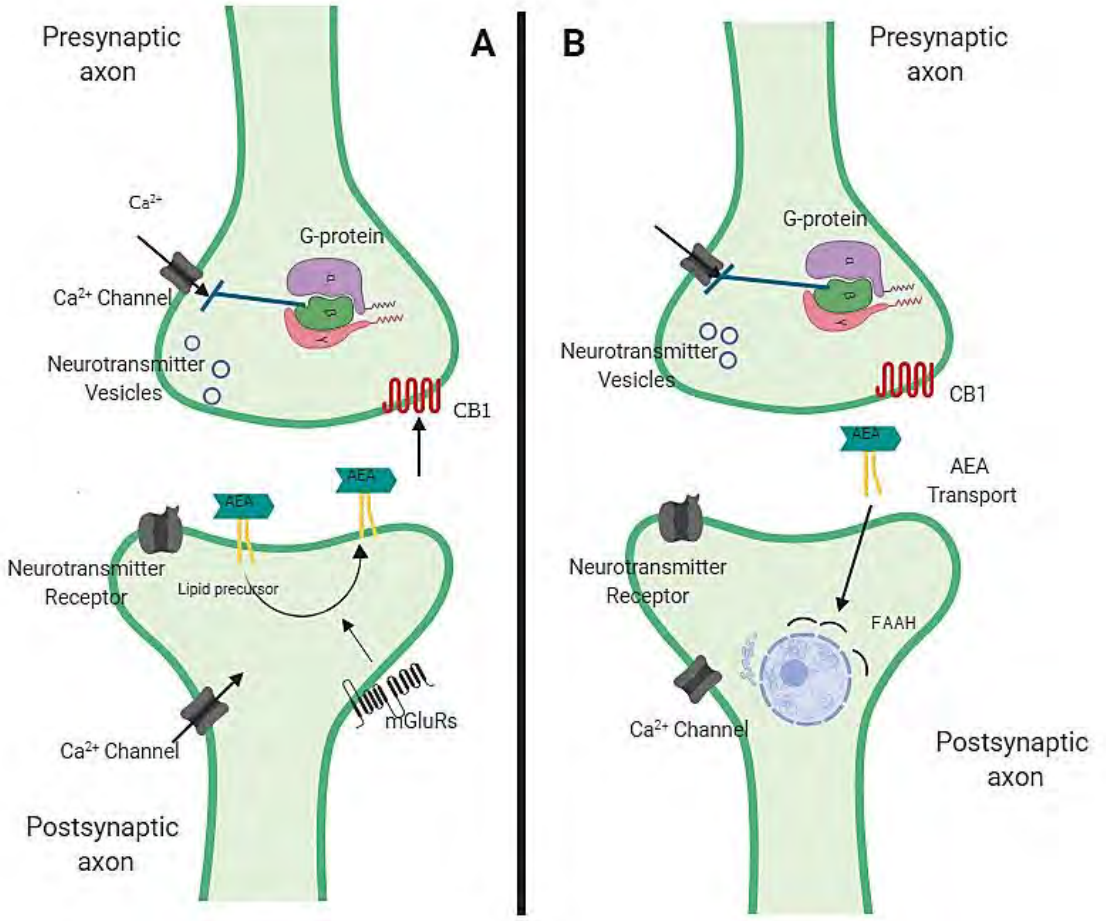

Figure 1.8: Pathway and degradation of endocannabinoids (created @biorender.com), A and B show the life cycle of anandamide.

(A). The synthesis of AEA from lipids by neurons is a response to the depolarization of lipids and the influx of Ca^{2+} (35). The synthesized AEA is transported to the presynaptic neuron from the postsynaptic neuron by simple diffusion (50). The CB1 receptor has seven helices and AEA is thought to bind in the binding site formed between the 7 helices, this results in the inhibition of Ca^{2+} channels in the presynaptic cell (38). The activation of CB1 receptors is responsible for preventing the release of neurotransmitters from vesicles, this is due to the dependency of cationic neurotransmitter release on Ca^{2+} (61). This process decreases the chances of a local response of synaptic vesicles and has some similarities to opioid pharmacology as it relates to the pain pathway that is Ca^{2+}-dependent (61). Endocannabinoids may be independent of cellular uptake, this does not mean that current findings are null and void (61). **(B)** This process is one that involves an enzyme called fatty-acid amide hydrolase (FAAH) localized in the endoplasmic reticulum (61). This enzyme is classified as an enzyme that is either reversible or irreversible inhibitor based on the mechanism it is involved. The role of FAAH is to breakdown AEA after cellular uptake (61). The AEA is taken up after interaction with the CB1 receptor and is then broken down into arachidonic acid and ethanolamine.

1.5 Phytocannabinoids

Cannabis plants synthesize cannabinoids, called phytocannabinoids in different quantities, there are approximately 300 phytocannabinoids that have been identified (62). The *Cannabis Sativa* strain has been investigated, with extractions leading to structure elucidations, synthesis of synthetic cannabinoids and performance of clinical trials on phytocannabinoids found (1). Phytocannabinoids are secondary metabolites in cannabinoids in plants, that act as ligands to cannabinoid receptors (CB1 and CB2).

In *Cannabis Sativa*, the biosynthetic pathway of phytocannabinoids has been researched and cannabigerolic acid (CBGA) has been identified as the central precursor of phytocannabinoids synthesis (14). Phytocannabinoids synthesis usually involves enzymes but the decarboxylation of the acid versions of the compounds involves heat. Some phytocannabinoids are known as a product of decarboxylation e.g. tetrahydrocannabinol acid (THCA) to tetrahydrocannabinol (THC) (Figure 1.9). The major enzymes involved in the synthesis of phytocannabinoids are cannabigerolic acid synthase (CBGAS), tetrahydrocannabinolic acid synthase (THCAS), cannabidiolic acid synthase (CBDAS) and cannabichromene acid synthase (CBCAS). Isomerization and oxidation are also non-enzymatic reactions that lead to new

phytocannabinoids (63). Figure 1.9 below is an example of the reactions that occur when an enzyme is involved, and this process is similar for the above-mentioned cannabinoids with their respective enzymes.

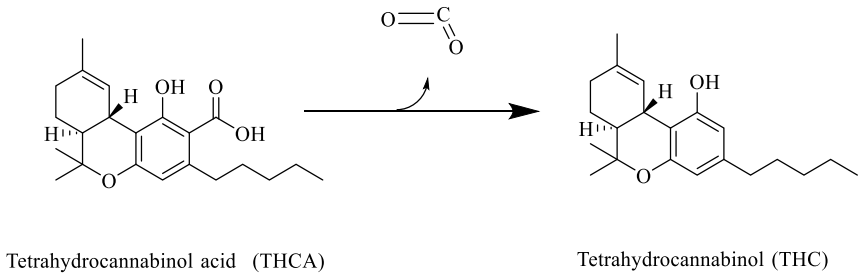

Tetrahydrocannabinol acid (THCA) Tetrahydrocannabinol (THC)

Figure 1.9: Decarboxylation of THCA to THC.

Beyond the discovery of phytocannabinoids, their effects have been researched. Cannabidiol (CBD) is has a structure like THC but is not cyclized (Figure 1.10). It is a non-psychoactive compound. Pharmacological activity anti-inflammatory anti-nociceptive, anti-convulsive, antioxidant anti-psychotic effects (39). Cannabidiol counteracts other effects caused by other cannabis compounds e.g. THC is psychoactive, causes hunger and sedation (38). Sativex® is a pharmaceutical product that has CBD and been approved by the food and drug administration (FDA) (2). THC is the most studied of the cannabinoids, with thousands of publications on its possible recreational use and has anti-inflammatory and antinociceptive effects in assays with laboratory animals (64). THC has less psychoactive effects when used along with CBD, terpenes or when its structure has been modified (65). When plants containing THC are burnt (smoking of the plant) or used as a tea, cannabinoids may be decarboxylated due to the heat. This is an example enzymatic decarboxylation of THCA to THC which is a neutral psychoactive compound (Figure 1.10) (65). Cannabigerol (CBG), this compound was purified the same year as THC, it has no psychoactive effects, it is also known as a parent cannabinoid, although it has been reported to have a weak agonistic effect on CB1 receptors (38). CBG has remarkable anti-cancer properties (66). In terms of the effect on pain and inflammation, there is evidence of CBG behaving as a potent α2-adrenoreceptor agonist. Cannabinol (CBN), is a nonenzymatic by-product of THC, predicted to be discovered when THC degraded while being transported for analysis (67). Cannabinol (CBN) might cause sleepiness because it is a by-product of the degradation of THC (67). Cannabidivarin (CBDV) is a CBD homolog that possesses potential treatment for nausea and vomiting (67). CBDV has been shown to cross the blood-brain barrier (BBB), it was found to be able to activate or block several ion channels (68). It can be hypothesized that, because CBDV competes with CBD as a therapeutic agent it

can act as an analgesic and anti-inflammatory drug (69) (Figure 1.10). In multiple drug discovery efforts, different cannabinoids have been isolated from cannabis plants, identified and synthesized (66). Figure 1.10 represents some of the most researched phytocannabinoids.

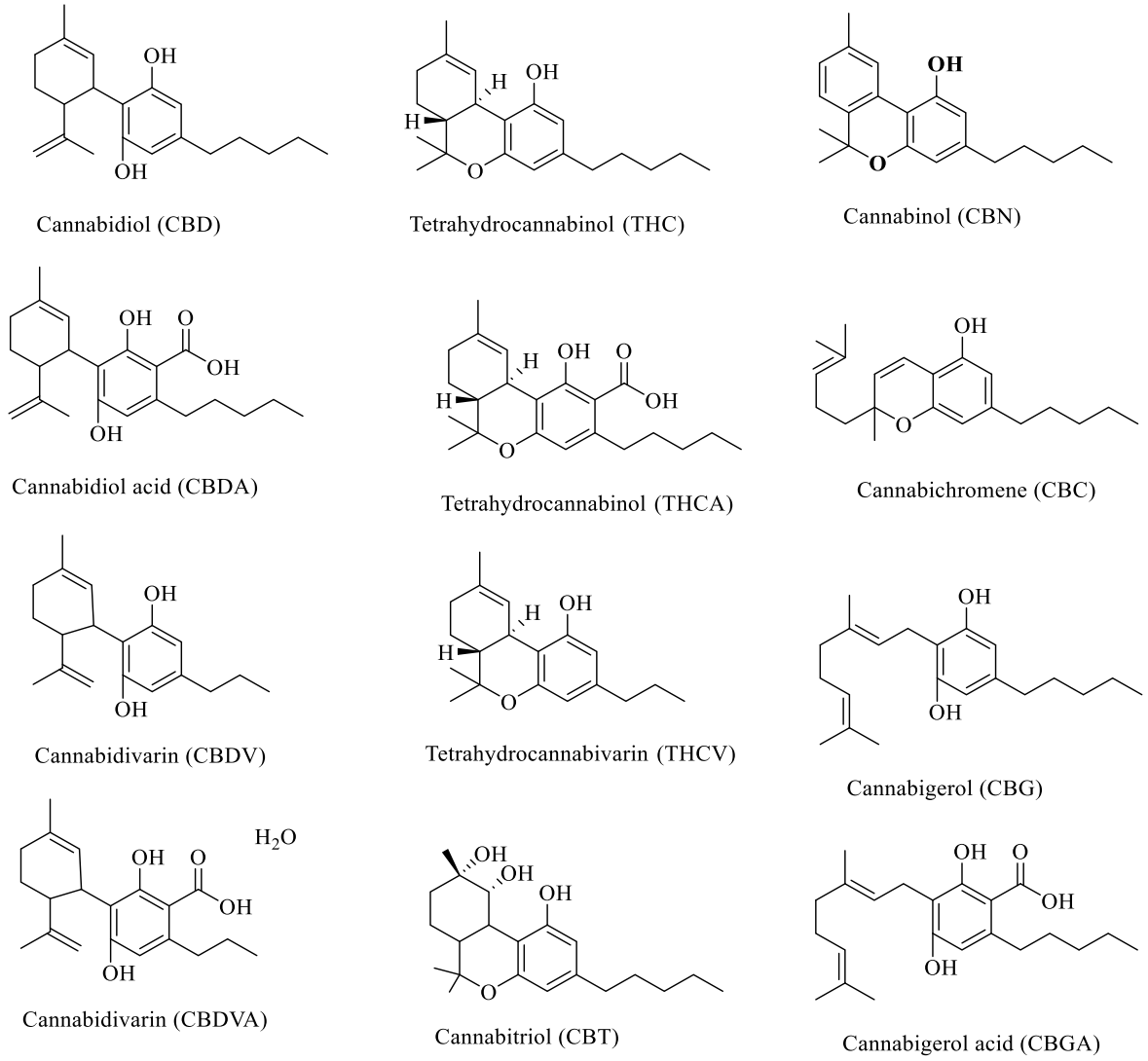

Figure 1.10: Structures of some phytocannabinoids synthesized directly from the cannabis plant.

The phytocannabinoids in Figure 1.10 is infused in cannabis products because of their potential benefits. In chapter 2, the liquid chromatography-mass spectrometry (LC-MS) is used to analyse THC, CBD, CBDV, CBG and CBN, and cannabinoids that are found in cannabis products. Cannabis plants are not only composed of phytocannabinoids but also with terpenes, terpenoids, and other compounds. Terpenes and terpenoids have been reported to have anti-inflammatory and anti-nociceptive effects. Some terpenes and terpenoids are structurally

related to phytocannabinoids suggesting that there can be a degradation of cannabinoids to give terpenes and terpenoids. We discuss some terpenes in detail.

1.6 Terpenes and Terpenoids

Terpenes are a large class of compounds consisting of short and long hydrocarbon chains, made from isoprene units and terpenoids are derived from terpenes and they contain the oxygen group (70). Terpenoids are produced by a variety of plants, they are aromatic compounds present in plants that, plants use for protection from predation and attraction of pollinators (71). The figure below shows the structures of terpenes and terpenoids (Figure 1.11).

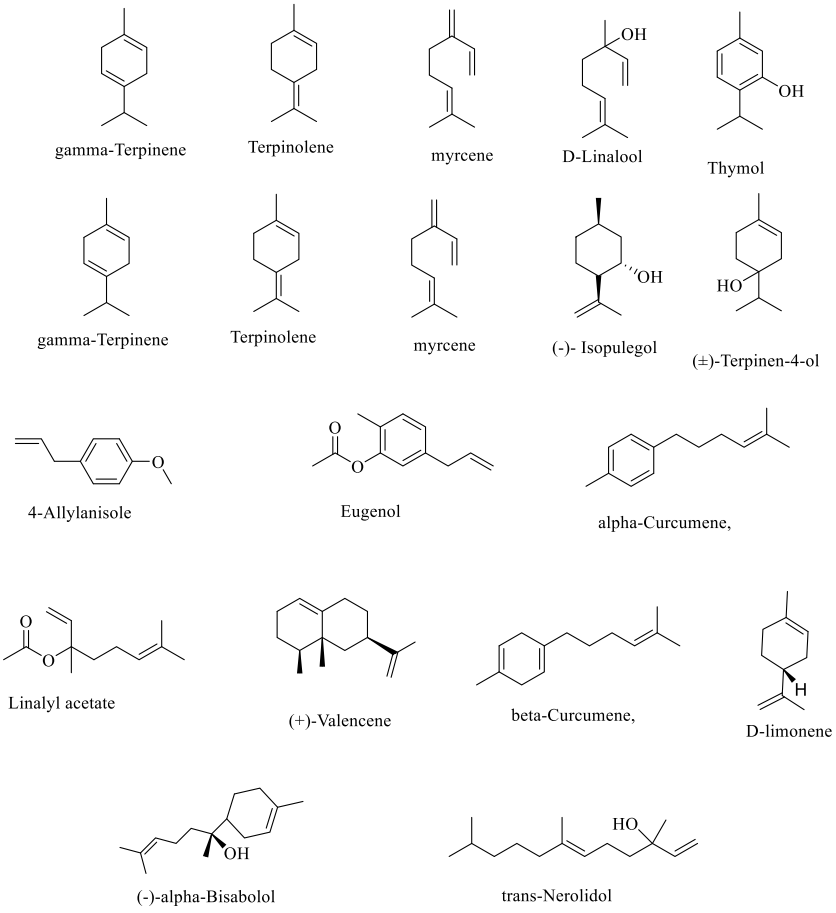

Figure 1.11: Structures of some terpenes and terpenoids.

A terpene that has been studied well is limonene, also found in lemons and other plants. Limonene has shown to enhance some of the effects of cannabinoids (72). Limonene can be found in cannabis along with other terpenes which also have a synergistic relationship with cannabinoids along with their own (72). Limonene added to THC enhanced a 'cerebral euphoric' experience and reduced inflammation scores (73). Limonene reduces inflammation

scores, limonene could synergise with CBD and THC, because it is an agonist at A_{2A} adenosine receptors (74). γ-Terpinene is a terpene that also has broad anti-inflammatory effects (72). The use of pepper which also has terpenes can activate CB2 receptors, which are highly effective in the process of reducing inflammation (8).α-Pinene is an anti-inflammatory compound in humans at low exposure (72). Linalool has analgesic, sedative, anti-depressant (45). Terpinolene is a sub active antinociceptive and anti-inflammatory dosage (8). The terpenoid 1.8- Cineole is also an anti-inflammatory terpene (65). Terpenes and terpenoids have been discussed further in chapter 2, because of their presence in cannabinoid products.

1.7 Conclusion

An argument for the use of cannabinoids for the treatment of pain and inflammation has been made based on the position of the cannabinoid receptors on the pain pathway and the body, based on previous reviews. The understanding of the role of the endocannabinoid system, cannabinoids, terpenes, and terpenoids is still developing, with the discovery of more phytocannabinoids, terpenes, and terpenoids as well as multiple receptors in the endocannabinoid system besides the CB1 and CB2. Further analysis and discussion of phytocannabinoids, terpenes and terpenoids can be seen in Chapter 2. Thereafter, protein-ligand interactions between phytocannabinoids and fragment structures predicted in chapter 2 and the CB1 and CB2 receptors will be discussed in Chapter 3. This will give more understanding beyond reviewing the topic of the cannabinoids and the endocannabinoid system.

1.8 References

1. Pertwee R.G. Cannabinoid pharmacology: The first 66 years. *Br J Pharmacol*. 2006;147: 163 - 171.

2. Peters M., Murillo-Rodriguez E, and Hanus LO. Cannabidiol – Recent Advances. *Chemistry & Biodiversity.*2007;4:1678–92.

3. Thakur G.A, Nikas S.P, Makriyannis A. CB1 cannabinoid receptor ligands. *Mini Rev Med Chem*. 2005;5(7):631–40.

4. Lewis M.M, Yang Y., Wasilewski E., Clarke H.A and Kotra L.P. Chemical Profiling of Medical Cannabis Extracts. *ACS Omega*. 2017;2(9):6091–103.

5. Degenhardt F., Stehle F., and Kayser O. The Biosynthesis of Cannabinoids *Handbook of Cannabis and Related Pathologies: Biology, Pharmacology, Diagnosis, and Treatment. Elsevier Inc.*; 2017. 13–23. .8

6. Devinsky O., Whalley B.J, and Di Marzo V. Erratum to Cannabinoids in the Treatment of Neurological Disorders. *Neurotherapeutics*. 2015;12(4):910–910.

7. Lemke L.T and Williams DA. Foye's Principles of Medicinal Chemistry, 6th Edition, Lippincott Williams and Wilkins, Philadelphia, 2007, Chapter 24:653- 676.

8. Russo E.B. Cannabinoids in the management of difficult to treat pain. *Ther Clin Risk Manag*. 2008;4(1):245–59.

9. Hill K.P, Palastro M.D, Johnson B., and Ditre J.W. Cannabis and Pain: A Clinical Review. *Cannabis Cannabinoid Res*. 2017;2(1):96–104.

10. Felder C.C, Joyce K.E, Briley E.M, Mansouri J., Mackie K., Blond O, Lai Y., Ma A.L and Mitchell R.L. Comparison of the pharmacology and signal transduction of the human cannabinoid CB1 and CB2 receptors. *Mol Pharmacol.* 1995;48(3):443–50.

11. Cichewicz D.L. Synergistic interactions between cannabinoid and opioid analgesics. *Life Sci.* 2004;74(11): 1317–24.

12. Walker S.P, Odendaal C.L, Esterhuyse K.G.F. Biographical, pain, and psychosocial data for a South African sample of chronic pain patients Correspondence : *South African J Anaesth Analg.* 2006;(6):62–6.

13. Igumbor E.U, Puoane T., Gansky S.A, and Plesh O. Prevalence and risk indicators of chronic pain in a rural community in South Africa. *J Rural Trop Public Heal*. 2011;10(1994):61–9.

14. Hua1 T., Vemuri K., Pu M., Qu L, Han G.W, Wu Y., Zhao S, Shui W., Li S, Korde A, Laprairie R.B, Stahl E.L, Ho J.H, Zvonok N, Zhou H, Kufareva I, Wu B, Zhao Q, Hanson MA, Bohn L.M, Makriyannis A, Stevens R.C, and Liu Z.J, Crystal Structure of the Human Cannabinoid Receptor CB1. *HHS Public Access*. 2017;39(1):55–64.

15. Ashley N.T, Weil Z.M, and Nelson R.J. Inflammation: Mechanisms, Costs, and Natural

Variation. *Annu Rev Ecol Evol Syst*. 2012;43(1):385–406.

16. Pertwee R.G, and Ross R.A. Cannabinoid receptors and their ligands. *Prostaglandins Leukot Essent Fat Acids*. 2002;66(2–3):101–21.

17. Meyers J.E. Chronic pain and neuropsychological assessment. A*PA Handb forensic Neuropsychol*. 2017;10(3):263–77.

18. Hart A.J, Whalen P.J, Shin L.M, McInerney S.C, Fischer H and Rauch S.L. Differential response in the human amygdala to racial outgroup vs ingroup face stimuli. *Neuroreport.* 2000;11(11):2351–4.

19. Raff M, Crosier J, Eppel S, Meyer H, Sarembock B., and Webb D. South African guideline for the use of chronic opioid therapy for chronic non-cancer pain. *South African Med J.* 2014;104(1):78–89.

20. Hodkinson B, Musenge E, Ally M, Meyer P, Anderson R and Tikly M. Functional disability and health-related quality of life in South Africans with early rheumatoid arthritis. S*cand J Rheumatol*. 2012;41(5):366–74.

21. Reiman A, Welty M, Solomon P. Cannabis as a Substitute for Opioid-Based Pain Medication: Patient Self-Report. *Cannabis Cannabinoid Res.* 2017;2(1):160–6.

22. Styrczewska M, Kulma A, Ratajczak K, Amarowicz R and Szopa J. Cannabinoid-like anti-inflammatory compounds from flax fiber. *Cell Mol Biol Lett*. 2012;17(3):479–99.

23. Hunter P. The inflammation theory of disease. the growing realization that chronic inflammation is crucial in many diseases opens new avenues for treatment. *EMBO Rep*. 2012;13(11):968–70.

24. Ayoub S.S, Ward P.A and Ayoub S.S. Acute and Chronic Inflammation. *Fundam Inflamm*. 2014;1–16.

25. Yam M.F, Loh Y.C, Tan C.S, Adam S.K, Manan N.A and Basir R. General pathways of pain sensation and the major neurotransmitters involved in pain regulation. *Int J Mol Sci*. 2018;19(8).

26. Iffland K and Grotenhermen F. An Update on Safety and Side Effects of Cannabidiol: A Review of Clinical Data and Relevant Animal Studies. Cannabis Cannabinoid Res. 2017;2(1):139–54.

27. Irving A.J, Rae MG and Coutts A.A. Cannabinoids on the Brain. *Sci World J* . 2002;2(April 2002): 632–48.

28. Ji R.R and Woolf C.J. Neuronal plasticity and signal transduction in nociceptive neurons: Implications for the initiation and maintenance of pathological pain. *Neurobiol Dis*. 2001;8(1):1–10.

29. Guindon J and Hohmann A. The Endocannabinoid System and Pain. *CNS Neurol Disord - Drug Targets*. 2009;8(6):403–21.

30. Kogan N.M, Mechoulam R. Cannabinoids in health and disease. *Dialogues Clin Neurosci.* 2007;9(4):413–30.

31. Prabu C, Latha S, Selvamani P, Ahrentorp F. Layer-by-layer assembled magnetic prednisolone microcapsules (MPC) for controlled and targeted drug release at rheumatoid arthritic joints. J *Magn Magn Mater*. 2017;427(11):258–67.

32. Hua T, Vemuri K, Pu M, Qu L, Han G.W, Wu Y, Zhao S, Shui W, Li S, Korde A, Laprairie RB, Stahl EL, Ho J, Zvonok N, Zhou H, Kufareva I, Wu B, Zhao Q, Hanson MA, Bohn LM, Makriyannis A, Stevens RC and Liu Z. Crystal Structure of the Human Cannabinoid Receptor CB 1. *Cell*. 2016;167(3):750-762.e14.

33. Downer E.J, Finn D.P. Cannabinoids: Clearing the smoke on pain, inflammation and neurodegeneration. *Br J Pharmacol*. 2014;171(6):1341–4.

34. Cabral G.A and Griffin T.L. Emerging role of the cannabinoid receptor CB2 in immune regulation: therapeutic prospects for neuroinflammation. Reviews in *Molecular Medicine*, 2009;11(804):1–31.

35. Manzanares J, Julian M, Carrascosa A. Role of the Cannabinoid System in Pain Control and Therapeutic Implications for the Management of Acute and Chronic Pain Episodes. *Curr Neuropharmacol.* 2006;4(3):239–57.

36. Meyer H.P, Marcus TS, Becker PJ. The impact of chronic pain on the quality of life of patients attending primary healthcare clinics. *South African J Anaesth Analg*. 1995;20(2):122–6.

37. Stern E, Muccioli G.G, Millet R, Goossens J.F, Farce A, Chavatte P, Poupaert P.H, Lambert D.M, Depreux P and He´nichart J.P. Novel 4-oxo-1,4-dihydroquinoline-3-carboxamide derivatives as new CB 2 cannabinoid receptors agonists: Synthesis, pharmacological properties and molecular modelling. *J Med Chem.* 2006;49(1):70–9.

38. Grotenhermen F. Pharmacology of cannabinoids. *Neuroendocrinol Lett.* 2004;25(1–2):14–23.

39. Starowicz K and Finn D.P. Cannabinoids and Pain: Sites and Mechanisms of Action. 1st ed., *Advances in Pharmacology. Elsevier In*c.; 2017. 80: 437–475.

40. Maskrey B.H, Megson I.L, Whitfield P.D, Rossi AG. Mechanisms of resolution of inflammation: A focus on cardiovascular disease. *Arterioscler Thromb Vasc Biol.* 2011;31(5):1001–6.

41. Libby M.D. Inflammatory Mechanisms: The Molecular Basis of Inflammation and Disease. *Nutr Rev.* 2007;65(12):140–6.

42. Sherwood E.R and Toliver-Kinsky T. Mechanisms of the inflammatory response. *Best Pract Res Clin Anaesthesiol*. 2004;18(3):385–405.

43. Bruni N, Pepa C Della, Oliaro-Bosso S, Pessione E, Gastaldi D and Dosio F. Cannabinoid delivery systems for pain and inflammation treatment. *Molecules*. 2018;23(10).

44. Edwards G and Mechoulam R. Conversation with Raphael Mechoulam. *Addict Mak Prof Careers*. 2018;93–9.

45. Russo E, Guy G.W. A tale of two cannabinoids: The therapeutic rationale for combining tetrahydrocannabinol and cannabidiol. *Med Hypotheses*. 2006;66(2):234–46.

46. Childers S.R, Deadwyler SA. Role of cyclic AMP in the actions of cannabinoid receptors. *Biochem Pharmacol*. 1996;52(6):819–27.

47. Pĩeiro R, Maffucci T and Falasca M. The putative cannabinoid receptor GPR55 defines a novel autocrine loop in cancer cell proliferation. *Oncogene*. 2011;30(2): 142–52.

48. Howlett A.C. The cannabinoid receptors. *Prostaglandins Other Lipid Mediat*. 2002;68–69:619–31.

49. Berman P, Futoran K, Lewitus GM, Mukha D, Benami M, Shlomi T and Meiri D. A new ESI-LC/MS approach for comprehensive metabolic profiling of phytocannabinoids in Cannabis. *Sci Rep*. 2018; 8(1):1–15.

50. Reggio P.H. Endocannabinoid binding to the cannabinoid receptors: what is known and what remains unknown. *Curr Med Chem*. 2010;17(14):1468–86.

51. Pertwee R.G. Pharmacology of cannabinoid CB1 and CB2 receptors. *Pharmacol Ther.* 1997;74(2):129–80.

52. Smith F.L, Cichewicz D, Martin Z.L and Welch S.P. The enhancement of morphine antinociception in mice by Δ9- tetrahydrocannabinol. *Pharmacol Biochem Behav.* 1998;60(2):559–66.

53. Rajput S, Kumari R and Mishra BN. Molecular modeling studies and structure-based virtual screening for identification of potent ligands for Cb2 receptor. *International Journal of Chemical Studies.*2016;4(1):24–36.

54. Jhaveri M.D, Sagar D.R, Elmes S.J.R and Kendall D.A, Chapman V. Cannabinoid CB2 receptor-mediated anti-nociception in models of acute and chronic pain. *Mol Neurobiol*. 2007;36(1):26–35.

55. Frank B, Serpell M.G, Hughes J, Matthews J.N.S and Kapur D. Comparison of analgesic effects and patient tolerability of nabilone and dihydrocodeine for chronic neuropathic pain: Randomised, crossover, double-blind study. *Bio Med Journ.* 2008;336(7637):199–201.

56. Bosier B, Muccioli G.G, Hermans E and Lambert D.M. Functionally selective cannabinoid receptor signalling: Therapeutic implications and opportunities. *Biochem Pharmacol.* 2010;80(1):1–12.

57. Di Luccio E and Koehl P. A quality metric for homology modeling: The H-factor. *BMC Bioinformatics* .2011;12(1):48.

58. Matias I., and Di Marzo V. Endocannabinoids and the control of energy balance. Trends Endocrinol Metab. 2007;18(1):27–37.

59. Wilson R.I and Nicoll R.A. Endocannabinoid signalling in the brain. *Science* (80-) .2002;296(5568):678–82.

60. Dinh T.P, Carpenter D., Leslie F.M, Freund T.F, Katona I., Sensi S.L, Kathuria S. and Piomelli D. Brain monoglyceride lipase participating in endocannabinoid inactivation. *Proc Natl Acad Sci*. 2002;99(16):10819–24.

61. Zou S, Kumar U. Cannabinoid receptors and the endocannabinoid system: Signaling and function in the central nervous system. *Int J Mol Sci*. 2018;19(3).

62. Citti C, Battisti U.M, Braghiroli D, Ciccarella G, Schmid M, Vandelli MA and Cannazza G. A Metabolomic Approach Applied to a Liquid Chromatography Coupled to High-Resolution Tandem Mass Spectrometry Method (HPLC-ESI-HRMS/MS): Towards the Comprehensive Evaluation of the Chemical Composition of Cannabis Medicinal Extracts. *Phytochem Anal*. 2018;29(2):144–55.

63. Rotherham D and Harbison S.A. Differentiation of drug and non-drug Cannabis using a single nucleotide polymorphism (SNP) assay. *Forensic Sci Int*.. 2011;207(1–3):193–7.

64. Martin J.H., Gordon M.R and Fitzwater ES. Iron Limitation? *Limnol Oceanogr.* 1991;36(8):1793–802.

65. Pavlovic R, Nenna G, Calvi L, Panseri S, Borgonovo G, Giupponi L, Cannazza G and Giorgi Annamaria. Quality traits of "cannabidiol oils": Cannabinoids content, terpene fingerprint and oxidation stability of European commercially available preparations. Molecules. 2018;23(5):1–22.

66. Hanuš L.O, Meyer SM, Muñoz E, Taglialatela-Scafati O, Appendino G. Phytocannabinoids: A unified critical inventory. *Natural Product Reports* 2016.33: 1357–1392 p.

67. Zimmerman A.M, Bruce W.R, and Zimmerman S. Effects of cannabinoids on sperm morphology. *Pharmacology*. 1979;18(3):143–8.

68. Reiss C.S. Cannabinoids and viral infections. *Pharmaceutical*s. 2010;3(6):1873–86.

69. Emerson R, Procópio D.L, Reis I, Kassawara M, Lúcio J, Azevedo D and de Araujo J.M. Review article Antibiotics produced by Streptomyces. *Brazilian J Infect Dis*. 2012;16(5):466–71.

70. Reusch W, Professor Emeritus (Michigan State U.), Virtual Textbook of Organic Chemistry carbon atoms (Terpenes). LibreTexts. 2019;1–2.

71. Waksmundzka-Hajnos M, Hawrył MA, Cieśla Ł. Analysis of Plant Material. *Instrum Thin-Layer Chromatogr.* 2014;505–53.

72. Pellati F, Brighenti V, Sperlea J, Marchetti L, Bertelli D, Benvenuti S. New Methods for the Comprehensive Analysis of Bioactive Compounds in Cannabis sativa L. (hemp). *Molecules*. 2018;23(10):2639.

73. Carlsson A., Lindberg S., Wu X., Dunne S., Josefsson M., Åstot C., and Dahlén J. Prediction of designer drugs: synthesis and spectroscopic analysis of synthetic cannabinoid analogues of 1H-indol-3-yl(2,2,3,3-tetramethylcyclopropyl)methanone and 1H-indol-3-yl(adamantan-1-yl)methanone

74. Durdagi S, Papadopoulos MG, Zoumpoulakis PG, Koukoulitsa C and Mavromoustakos T. A computational study on cannabinoid receptors and potent bioactive cannabinoid ligands: Homology modeling, docking, de novo drug design and molecular dynamics analysis. *Mol Divers*. 2010;14(2):257–76.

Chapter 2
LC-MS cannabinoid analysis and fragment structure elucidations

2.1 Introduction

There are various analytical techniques and instruments that are used in drug design and development. Liquid Chromatography-Mass Spectroscopy (LC-MS) is the technique of choice in this project as it combines two techniques namely Liquid Chromatography (LC) and Mass Spectroscopy (MS) (1). The combination of chromatography with mass spectroscopy was reported as a possibility as far back as 1967, leading to the introduction of the first commercial LC-MS system in the 1980s (2).

Chromatography was discovered in 1903 by Mikhail Tweet, it is a separation technique to isolate compounds from a mixture (2). The combination of the two has made an immense improvement in research most especially synthetic and analytical chemistry, by introducing rapid quantitative separation of compounds (1). In liquid chromatography, the affinity of the compound towards the stationary or mobile phase determines whether it is eluted quickly or slowly (2). The higher the affinity towards the stationary phase the slower the elution (2). A main characteristic of the LC domain is acquiring the retention time (rt), which is essential in data analysis (1) (2). Mass spectrometry helps determines the mass, elemental composition and structural elucidation of compounds (3). The ionization techniques applied in an MS vary considerably but are often characterized as soft or hard ionization (3). Hard ionization involves a substantial amount of internal energy being put into a molecule as the ion is generated. This defines electron ionization energy (EI) where internal energy in electron volts is transferred to a molecular ion depicted as M^+ (4). The fragmentation, in this case, leads to in source compound-specific fragmentation (4).

During soft-ionization techniques barely any energy is transferred to the molecule, protonation or deprotonation of the molecular ion occurs to give ions, depicted as $[M+H]^+$ or $[M-H]^-$, also, little or no in-source fragmentation occurs (5). Fragmentation in electrospray ionization (ESI) must be induced by increasing internal energy, this is usually done by performing MS/MS experiments that involve collision-induced dissociation discussed (CID) in this project (5).

ESI is an example of a liquid phase ionization technique and can be performed in the positive (ESI+) and negative mode (ESI-), with the former applied in this research project (5). Since in-source fragmentation is mostly absent, ESI- MS mostly gives information about the intact molecule, collision-induced fragmentation also tends to have low – energy rearrangements and bond cleavage, rather than the high energy single – electron versions like in electron ionisation mass spectrometry EI-MS. Fragmentation reactions in mass spectrometry ESI fragmentation for both $[M+H]^+$ and $[M-H]^-$ is mostly described as complete small molecule losses (6). The even-electron rule is a rule that has been used to understand the prediction of the mass spectral behaviour of organic compounds, this rule suggests that small molecule losses should only involve neutral losses and it prohibits the loss of radicals (7) (6). A positive mode of analysis was preferred because there are higher chances of ionization of compounds in a positive mode as opposed to negative mode (8). Negative mode, however, has been reported to have lower background noise (8).

This chapter will explain our approach in analysing cannabinoids with the aim of fragment-based drug design that will be discussed in chapter 3. Method development was aimed at eluting cannabinoids rapidly, efficiently and effectively for qualitative analysis. When a fast method is required for analysing samples with low concentration in a short time these methods will be effective. While drugs and derivatives are hard to make and require many steps, but pieces or fragments require fewer steps, so are cheaper, easier, faster to synthesize. Fragments are not perfect either because their binding to enzymes is much weaker etc, they are not drugs, but clues on how to make better drugs and how to design fragments, well, MS, ESI especially, gives stable fragments, to perhaps suggesting future fragment structures.

2.2 Experimental

2.2.1 Instrumentation

Bruker Compact Liquid Chromatography-Mass Spectrometry. Bruker Compact QToF mass spectrometer using an electrospray ionization (ESI) probe (Bruker, Bremen, Germany). The standard compound analysis was carried out in LC-MS/MS positive mode with a Dionex HPLC (Thermo Fisher Scientific, Sunnyvale, CA, USA), the voltage and experimental conditions listed later. Columns used were the Kinetex Evo C-18 column (2.1X 1.5 mm, 5 µm; Phenomenex, Torrance, CA, USA) and Kinetex polar C-18 column (3.0 × 100 mm, 2.6 µm; Phenomenex, Torrance, CA, USA). Software: MZmine 2.30 for data processing. Data Analysis 4.0 Bruker.

2.2.2 Solvent and reagents

Tetrahydrocannabinol (THC) standard was purchased at LECO Africa (Pty) Ltd. Cannabidiol (CBD), Cannabigerol (CBG), Cannabinol (CBN) and Cannabidivarin (CBDV) were purchased from LGC Analytical Ltd, additional standards were a kind donation from Prof C. Frost (NMU). HPLC-MS grade Acetonitrile (Merck, Johannesburg South Africa), HPLC-MS grade Methanol (Merck, Johannesburg South Africa), HPLC-MS grade MilliQ water and Formic acid (FA) purchased from Sigma Aldrich. Hemp seed by the Soaring Free brand and organic hemp powder by Nature Organic were purchased at Dischem. Cannabidiol oil was purchased from the Mastered Seed in Makhanda. Hemp oil (HEMP2820041) purchased from Essential Products, (Canada). To prepare the crude extract plant material was covered in methanol and sonicated for 30 minutes at room temperature (25˚C). The extract was filtered through a 0.2 µm syringe filter and used for analysis.

2.2.3 Sample Preparation

Five certified cannabinoid standards THC, CBD, CBDV, CBG, and CBN were dissolved in methanol to make 10 µg/ml for each standard. Cannabis products, CBD oil, hemp oil, hemp seed, hemp powder and crude extract were solubilized in methanol for analysis.

2.2.4 Methods

The analysis of samples was conducted with three different methods. We kept the mass spectrometry method parameters consistent for all the methods. An injection volume of 2 µl stayed the same, we relied on the sensitivity and selectivity of the instrument. The mass spectrometry was calibrated before each run. ESI positive mode was kept consistent because it is more sensitive than the APCI methods.

Liquid Chromatography Methods

We kept the Flow rate at 0.2 ml/min, column temperature 40°C, injection volume 0.2 µl and autosampler 25°C while adjusting the gradients.

Liquid Chromatography Method 1: The development of this method was aimed at analysing both the standards and cannabis products and standards. Mobile phase A – High purity grade water (0.1% formic acid). Mobile phase B- High purity HPLC grade acetonitrile (0.1% formic acid). Flow rate 0.2 ml/min, column temperature 40°C, injection Volume 0.2 µl and autosampler 25°C. Gradients 0min – 4 min: 50% B; 6 min – 16 min: 90% B; 16 min – 20 min: 50% B. The total run time was 20 minutes.

Liquid Chromatography Method 2: Mobile phase A – High purity grade water (0.1% formic acid) Mobile phase D- High purity HPLC grade acetonitrile (0.1% formic acid). Gradients 0 min – 10 min: 50% D; 10 min – 12 min: 90% D; 12 min – 15 min: 80% D. The total run time was 15 minutes.

Liquid Chromatography Method 3: Mobile phase A – High purity grade water (0.1% formic acid) Mobile phase B- High purity HPLC grade methanol (0.1% formic acid). Gradients 0 min – 10 min: 0% B; 10 min – 12 min: 100% B; 12 min – 15 min: 80%. The total run time was 15 minutes. The second and third method was used to compare acetonitrile and methanol as mobile phases in cannabinoid analysis (section 2.3.2).

Mass Spectrometry: Acquisition Parameters ionization mode electrospray ionization positive mode (ESI+). Other parameters were nebulizer gas pressure (N_2) 0.5 Bar at temperature 220 ° C, Capillary Voltage 4500 V, Scan range 50-2000 *m/z*. The collision energy was kept consistent at 40 eV.

Data Acquisition

The raw data acquired and viewed using the Bruker Compass software (Bruker, Bremen, Germany). Raw data were converted into mzXML, a preferred format for MZmine 2.30 software also compatible with other MS software. The following were routinely performed using MZmine. 1) Mass lists from the raw data were created, using the mass detection module. The parameters for this module were MS1 10 000 counts and MS2 4 000 counts for noise level 2).

By using the chromatogram builder module, we created a peak list. The parameters used to create a peak list were 0.10 min retention time range, a minimum peak height of 10000 and *m/z* tolerance of 0.01 Da or 5.0ppm. Parameters for chromatogram deconvolution were as follows: the smoothing algorithm used was the Savitzky Golay, minimum peak height 5 000, peak duration 2 min, derivative threshold 70%.

The MS2 range for MS2 scans pairing set to 0.01 Da. The retention time range for MS2 scan pairing was 0.5 min. 3). The deconvoluted peak lists were aligned with an *m*/*z* tolerance of 0.001 Da or 5ppm at a retention time tolerance set at 1 minute with the join aligner module. The score for perfectly matching weight for *m*/*z* and weight for retention time (rt) was set at the value 1. The scan retention time range was 0 -20 min and the *m*/*z* range of 100 - 400. 4) Filtering parameters was to retain only peaks with MS2 scan. 5) Gap filling intensity tolerance of 20% an *m/z* tolerance of 0.001 Da or 5 ppm.

2.3 Result and Discussion

2.3.1 Qualitative analysis of cannabis products.

The detection of cannabinoids in cannabis products was performed using parameters of the liquid chromatography method 1 along with the MS method (see section 2.2.4), the instrument equipped with the Phenomenex, (Torrance, CA, USA) with 2.1 × 1.5 mm, 5 µm particle size column. The total ion chromatograms above are a result of the first method with the cannabinoids eluting at 90% acetonitrile (0.1 formic acid) and 10% water and represented in Table 2.1 are the retention times of the standards. This analysis was used to determine the presence of cannabinoids in CBD oil, hemp oil, hemp seed, hemp powder, and a crude extract. This was done by comparing retention times of the precursor ion $[M+H]^+$ of each standard compound with the retention times of the precursor ion $[M+H]^+$ detected in each cannabis product. The cannabinoid standards used were THC, CBD, CBN, CBG, and CBDV. The precursor ions of interest observed being *m/z* 315.2214 for THC and 315.2258 for CBD, *m/z* 311.1986 for CBN, *m/z* 317.2397 for CBG, and *m/z* 287.1957 for CBDV positive ionization (Table 2.4). We observed the CBDV, CBG, CBD, CBN, and THC elution order, similarly to other reported analyses (9) (10) (11).

The focus was on the $[M+H]^+$ adduct is because soft ionization forms $[M+H]^+$ ions easily (12). Adduct formation is a result of gas-phase reactions between charged and neutral species inside the mass analyser yielding *m*/*z* values that are larger than precursor ions of neutral mass values (12). Adduct formation is highly dependent on the instrument used and compounds analyzed (4). There are difficulties in explaining the formation of adducts, they are reported to be formed in intramolecular gas-phase reactions in the mass analyser (12). Adducts can also form due to impurities in the solvent, calibration of the instrument needs to be considered (12). We refrained from making any conclusions based on the adduct observations in this work, besides $[M+H]^+$.

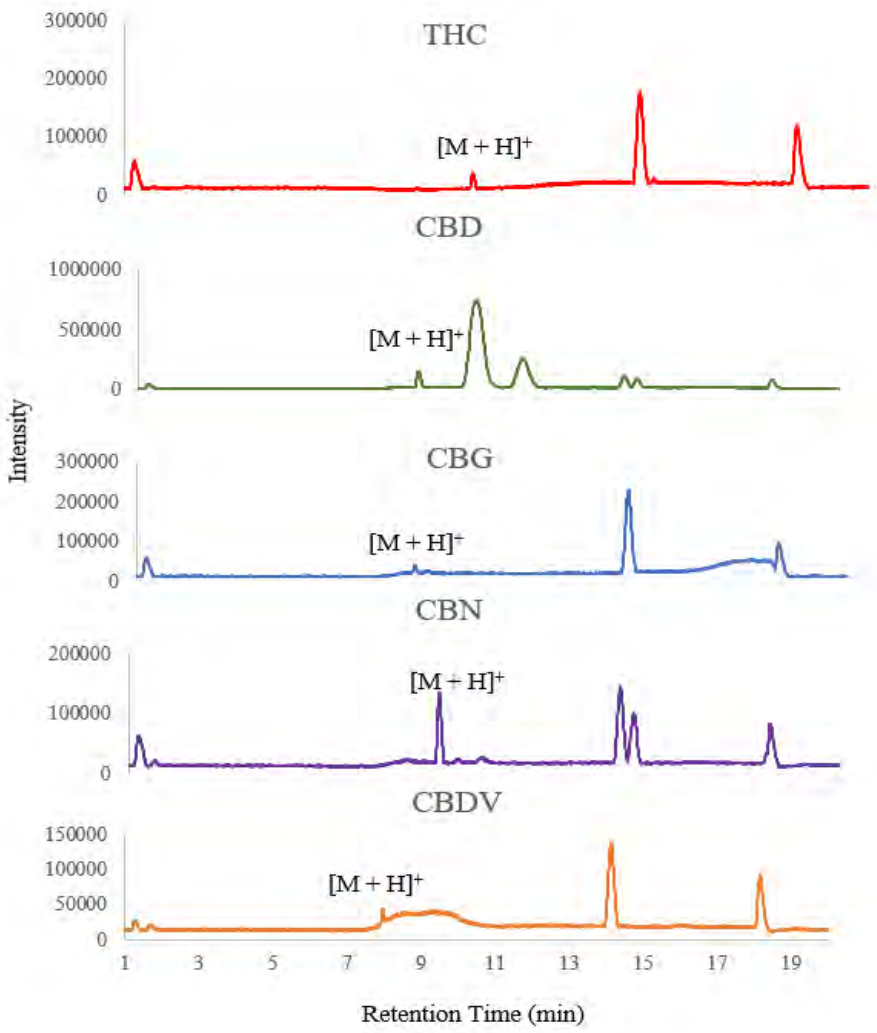

Figure 2.1: Total ion chromatograms obtained by LC-MS for the analysis of cannabinoid standards THC ($[M+H]^+$, 315.2214) , CBD ($[M+H]^+$,315.2258), CBN ($[M+H]^+$, 311.1958), CBG ($[M+H]^+$, 317.2397) and CBDV ($[M+H]^+$, 287.1957).

Figure 2.1 The chromatograms presented are reliable for comparison in cannabinoid product analysis, because of the distinguishability in retention times (Table 2.1). The main focus our work is the $[M+H]^+$ ion and these peaks are shown are well resolved enough to clearly state the retention times. The other peaks observed in the figure could be due to adduct formation, not in our interest in this work. The aim is to do structure elucidations of $[M+H]^+$ ionised structures.

Table 2.1: Cannabinoid compound retention times for qualitative analysis of cannabis products obtained by LC-MS.

Standard	Retention Time (min)
THC	9.88
CBD	8.57
CBN	9.30
CBG	8.42
CBDV	7.98

2.3.1.1 Cannabinoid product analysis

Cannabinoid containing products are manufactured and processed differently, this affects the concentrations of cannabinoids in products, as well as the cannabinoids present in the products (Table 2.2). Cannabidiol oil and Hemp oil are the leading oils currently in the market used for anxiety, pain relief, inflammation and other conditions (10). Cannabidiol (CBD) oil, is an oil made by infusing cannabidiol in oil of choice. CBD carrier oils usually carry a specific concentration of CBD, this is important for determining dosages what dosages of cannabidiol oil patients can consume (13). Cannabidiol is an effective component in these products (13). Hemp oil is an oil prepared from crushing hemp seeds, extracting compounds and carrying the seeds in the oil (10). Hemp is a different strain of *Cannabis Sativa*, hence the abundance and distribution of cannabinoids varies (10). Largely, hemp is not psychoactive as a result of the low concentration of THC and high concentration of other non-psychoactive cannabinoids like CBD (10). Hemp powder is simply made from grinding hemp seeds into a powder, which is then mixed with different carrier powders like plant-based protein powders for use, mostly in food (14).

The crude extract analyzed in this work is a product of soaking a crude of a plant in a solvent to extract the active compound of the plant into the solvent. The solvent becomes the carrier of the compounds of interest. In this case, the compounds in the plant used in was a *Cannabis Sativa* plant, the compounds of interest being phytocannabinoids.

These oils usually have distinctive scents like the cannabis plant, this scent is known to be as a result of the presence of terpenes and terpenoids in these oils (Table 2.3). Generally, cannabinoids on their own have no scents but they degrade into terpene-like compounds and aromatic fragments (15). The observation made after analysing products was that most cannabinoids were observed in the 6.00 to 12.00 min range as expected, because of the 90% acetonitrile (0.1% formic acid) and 10% water mobile phase in the elution gradient of the chromatographic method.

In the analysis of the chromatograms, only those components with both an MS1 and an MS2 spectrum were considered. The main concepts that guided us in distinguishing the peaks of interest were resolution and resolving power. Resolution is a separation of two *m*/*z* values leading to the formation of a real spectrum (1). Resolving power of peaks can be defined by the distance between peaks and the width of the peaks (1). Although there was a very low resolving power in the extracts evident in the total ion chromatograms, the resolution of peaks was reliable. The results and compound proposals made here are consistent with other research (10). Below are tables and figures representing cannabinoids detected in each product sample.

Table 2.2: Proposed cannabinoid compounds for $[M+H]^+$ precursor ions detected in cannabis products and retention times obtained by LC-MS.

Cannabis Product	Proposed cannabinoid compounds (*)	Formula	Retention Time (min)RT	[M+H] +
Cannabidiol (CBD) oil	Cannabidiol (CBD) [a]	$C_{21}H_{30}O_2$	8.51	315.2292
Hemp oil	Cannabinol acid (CBNA) [b]	$C_{22}H_{26}O_4$	8.29	355.2443
	Cannabiripsol (CBR) [b]	$C_{21}H_{32}O_4$	7.07	349.2334
	6,7-Epoxy Cannabigerol (CBGA) [b]	$C_{22}H_{32}O_5$	1.94	377.1923
	6,7-Epoxy Cannabigerol (CBG) [b]	$C_{21}H_{32}O_3$	8.40	333.2392
	Cannabinol (CBN) [a]	$C_{21}H_{26}O_2$	10.64	311.1967
	Cannabichromene (CBC) [a]	$C_{21}H_{30}O_2$	11.10	331.2805
	Cannabidiol (CBD-C_1) [b]	$C_{17}H_{22}O_2$	8.54	259.2026
Hemp Powder	Cannabinol acid (CBNA) [b]	$C_{22}H_{26}O_4$	9.83	355.2807
	Cannabinol (CBN) [a]	$C_{21}H_{26}O_2$	10.43	311.2548
	Cannabidiol acid/Tetrahydrocannabinol acid (CBDA/THCA) [b]	$C_{22}H_{30}O_4$	9.48	359.2179
Hemp seed	Cannabichromene (CBC) [b]	$C_{21}H_{30}O_2$	10.09	315.2284
	Cannabichromenevarinic acid (CBCVA) [b]	$C_{20}H_{26}O_4$	11.07	331.2806
	Cannabidiol acid /Tetrahydrocannabinol acid (CBDA/THCA) [b]	$C_{22}H_{30}O_4$	10.67	359.2180
	Cannabidiolic acid monomethyl ether (CBDMA) [b]	$C_{23}H_{32}O_4$	10.66	373.0959
	Cannabinol acid (CBNA) [b]	$C_{22}H_{26}O_4$	9.81	355.2806
	Cannabinol (CBN) [a]	$C_{21}H_{26}O_2$	10.46	311.2547
	Cannabitriol acid (CBTA) [b]	$C_{22}H_{28}O_6$	16.02	391.2809

Table 2.2 Continued

Cannabis Product	Proposed cannabinoid compounds (*)	Formula	Retention Time (min)RT	[M+H] +
Crude Extract (CE)	Cannabidiol (CBD) [a]	$C_{21}H_{30}O_2$	8.58	315.2281
	Cannabidiol acid (CBDA) [b]	$C_{23}H_{32}O_4$	7.26	359.1806
	Cannabidiol (CBDA-C_1) [b]	$C_{17}H_{22}O_2$	4.93	303.1190
	Cannabidiol (CBD-C_4) [b]	$C_{20}H_{28}O_2$	8.79	301.1754
	Cannabidiol acid (CBDA-C_4) [b]	$C_{21}H_{28}O_4$	8.45	345.2020
	Cannabidivarin (CBDV) [b]	$C_{19}H_{27}O_2$	8.77	287.1969
	Cannabidivarin acid (CBDVA) [b]	$C_{20}H_{26}O_4$	9.03	331.2225
	Cannabichromenevarinic acid (CBCVA) [b]	$C_{20}H_{26}O_4$	9.37	3311868
	Cannabigerol (CBG) [a]	$C_{21}H_{32}O_2$	8.45	317.2433
	Cannabigerol acid (CBGA) [b]	$C_{22}H_{32}O_4$	7.26	377.1914
	Cannabidiol acid monomethyl ether (CBDMA) [b]	$C_{23}H_{32}O_4$	7.71	373.1966
	Cannabinol (CBN) [a]	$C_{22}H_{26}O_2$	9.33	311.1975
	Cannabinol acid (CBNA) [b]	$C_{22}H_{26}O_4$	10.03	355.1857
	Cannabiripsol (CBR) [b]	$C_{21}H_{32}O_4$	7.04	349.2322
	Cannabitriol (CBT) [b]	$C_{21}H_{30}O_4$	7.58	347.2175
	Cannabitriol acid (CBTA) [b]	$C_{22}H_{28}O_6$	9.33	391.2442
	Tetrahydrocannabinol (THC) [a]	$C_{21}H_{30}O_2$	9.89	315.2284
	Tetrahydrocannabinol acid (THCA) [b]	$C_{22}H_{30}O_4$	10.78	359.2175
	Tetrahydrocannabinol acid (THCA-C_4) [b]	C_{20}H28o2	9.26	301.2124

* *a* -identified against standard

b- based on literature.

Table 2.1 above is representative of the cannabinoids detected in the samples beyond the cannabinoids standards we purchased, we based the findings on literature (10). The cannabinoids detected are mainly phytocannabinoids that are classical cannabinoids, because they are structurally related to THC (see Figure 1.11). These compounds are either acid derivatives or decarboxylated versions of the acid derivatives (10). These cannabinoids include constituents of raw cannabinoids evident in the crude extract and hemp seed products. Cannabinoids do not exist in isolation in the cannabis plant, they exist amongst other compounds generally found in plants for example terpenes and terpenoids (16).

2.3.1.2 Terpenes and Terpenoids

Terpenes and terpenoids occur naturally in plants and animals, they are hydrocarbon biomolecules (16). The difference between terpenes and terpenoids is that terpenes are simple hydrocarbon on the other hand terpenoids are oxidized hydrocarbons (16). In this work, no terpenes or terpenoids standards were used. The existing raw data from cannabinoid product samples were analysed using the *m*/*z* 100 - 300 range to detected smaller components that could match the ionised masses of terpenes or terpenoids (Table 2.3). Cannabinoid products are therapeutic depending on the components of the pharmacologically active metabolites present in the plant, these include phytocannabinoids, flavonoids, terpenes, and terpenoids (17). While other metabolites are known, from several classes, these were not the focus of this study, that of several reviews that have been done on constituents of these plants (18) (19).

The volatility of terpenes makes them extremely difficult to analyze, for this reason, they have mostly been analyzed using GC-MS methods (17). The LC-MS optimization includes the removal of solvents before MS detection that leads to a loss of many of the volatile compounds making electrospray ionization hard for volatile compounds, although possible (17). To validate the GC-MS/ LC-MS method used for terpene and terpenoid detection it is advised that the method must be compared to already accepted methods (17). The results in Table 2.3 propose detected terpenes and terpenoids in the cannabis products, the mass to charge ratios are compared with those obtained in recent research (13).

Table 2.3: Proposed Terpene precursor ion $[M+H]^+$ detected in cannabis products and retention times obtained by LC-MS.

Cannabis Product	Proposed Terpenes	Chemical Formula	Molecular Weight g/mol.	Retention Time (min)	$[M+H]^+$
CBD oil	4- Allylanisole	$C_{10}H_{12}O$	148.2012	9.23	149.0435
	(-)-Perillyl alcohol	$C_{10}H_{16}O$	152.2328	11.83	153.1265
	(±)-Terpinen-4-ol, (-)- Isopulegol	$C_{10}H_{18}O$	154.2486	6.70	155.1416
	trans-Terpin	$C_{10}H_{20}O_2$	172.2638	6.74	173.1518
	trans-Nerolidol, (-)-α-Bisabolol	$C_{15}H_{26}O$	222.3653	8.26	223.0615
				9.25	223.0622
Hemp oil	*trans*-Nerolidol, (-)-α-Bisabolol	$C_{15}H_{26}O$	222.3653	8.29	223.0612
				9.22	223.0611
				13.14	223.0616
Hemp seed	4- Allylanisole	$C_{10}H_{12}O$	148.2012	5.88	149.0214
	Linalyl acetate	$C_{12}H_{20}O_2$	196.2852	7.55	197.0936
	(+)-Valencene	$C_{15}H_{24}$	204.3501	8.42	205.0833
	trans-Nerolidol,	$C_{15}H_{26}O$	222.3653	13.15	223.0620
Crude Extract	4- Allylanisole	$C_{10}H_{12}O$	148.2012	9.12	149.1306
	Thymol	$C_{10}H_{14}O_2$	150.2170	4.69	151.1099
				8.52	151.1097
	Carvacryl acetate or β-Ionone	$C_{12}H_{16}O_2$	192.2536	8.47	193.1197
	α-Curcumene, β-Curcumene	$C_{15}H_{22}$	202.3343	8.43	203.1770
				9.02	203.1769
	(+)-Valencene	$C_{15}H_{24}$	204.3501	8.94	205.1925
	trans-Nerolidol or (-)-α-Bisabolol	$C_{15}H_{26}O$	222.3653	9.24	223.1307

Cannabinoids are hydrocarbons and they fragment into smaller compounds like terpenes and terpenoids. The molecular formula of the terpenes or terpenoids in Table 2.3 is representative of the possible fragments of cannabinoid compounds (see structures in Figure 1.12). During the fragmentation of cannabinoids, small molecule losses may lead to terpenes or terpenoids as products. We could not state with certainty which terpene or terpenoid was detected at each specific retention time., however, the above $[M+H]^+$ ions were detected in each sample and matched according to recently determined terpene and terpenoids (20). The ions were detected at different retention times using the same set of results in table 2.3, by using the *m/z* 100 – 300 range in our analysis to detect smaller ionised molecules. These small ionised terpenes could be traces of terpenes and terpenoids because the samples have scents.

Some ionised molecules for an example, in hemp oil, the terpenoid detected could be *trans*-Nerolidol or (-)-α-Bisabolol or any other terpenoid structurally related to compounds expected to be found in hemp products. In addition, the peaks of suggested *trans*-Nerolidol or (-)-α-Bisabolol with the *m/z* 223, appeared at different retention times, meaning it could be different compounds, compounds with the same molecular formula can elute at different times depending on their structures (20). Based on the retention times of the terpenes and terpenoid they elute mostly at high volumes of solvent like cannabinoids.

2.3.1.3 Precursor ion mass accuracy

Given the identification of the proposed cannabinoid compounds, this method fulfilled our aim to identify cannabinoids present in the products. To explore how much use, we could get out of this method, we went on to determine the mass accuracy of the $[M + H]^+$ precursor ions. The mass accuracy in this context is the closeness of the experimental value to the true value, we adapted terminology and formulae consistent with the work of Brenton *et al*, (2010) (21). The mass accuracy of the precursor ions is significant for structure elucidations of fragments in the MS2 spectrum of compounds. We used the term accurate mass (m_i) for an experimentally measured mass and exact mass (m_a) for the theoretical or calculated mass (21).

The formula used is as follows:

Formula 1

$\Delta m = m_i - ma$

$\Delta m_i = (m_i - m_a)$ in Da

$\Delta m_i = (m_i - m_a) \times 10^3$ in mDa

$\Delta m_i = \frac{(mi - ma)}{ma} \times 10^6$ in ppm

We applied this to our set of cannabinoid compounds for the $[M + H]^+$ ions and found that the values were above the 5-ppm expected for structure elucidations. The results are summarised in Table 2.4.

Table 2.4: Cannabinoid compound precursor ions $[M+H]^+$ mass accuracy measurement error.

	$[M+H]^+$	Accurate Mass m_i	Exact Mass	Δm (Da)	Δm_i(mDa)	$\Delta m/m_i x10^6$ (ppm)
THC	$C_{21}H_{31}O_2$	315.2214	315.2324	-0.011	-11	-34.89
CBD	$C_{21}H_{31}O_2$	315.2258	315.2324	-0.006	-6.6	-20.93
CBN	$C_{21}H_{27}O_2$	311.1958	311.2011	-0.005	-5.3	-17.03
CBG	$C_{21}H_{33}O_2$	317.2397	317.2481	-0.008	-8.4	-26.47
CBDV	$C_{19}H_{27}O_2$	287.1957	287.2011	-0.005	-5.4	-18.80

According ChemCalc a molecular formula finder website the mass errors of the compounds THC, CBD, CBN, CBG and CBDV for their $[M+H]^+$ ions are -34.911, -20.95, -17.04, -26.33 and -18.82 respectively (22). The results in Table 2.4 were obtained from a method calibrated by enhanced quadratic calibration, mass accuracies obtained were well above the required 5 ppm (21). The accuracy in the above results may have been acceptable for structure elucidation had the first two decimal points been the same, this would mean the results are treated as though they are from a lower resolution instrument, reporting precursor ion values to two decimal places (21). Calibrating the instrument repeatedly and ensuring that the scans made are not too far apart would have helped with the accuracy.

2.3.2 Chromatographic conditions effects on precursor ions.

The choice of the stationary and mobile phase is significant when analysing a class of compounds. In the previous section, we used acetonitrile based on reviewing literature that suggests advantages such as early retention times when used with a C18 column (23). The extracted base peak ion chromatograms of CBD is *m/z* 315,2421 in acetonitrile and *m/z* 315,2432 in methanol are depicted in Figure 2.2, they show the result of comparing acetonitrile (blue) or methanol (red) as a mobile phase of choice. The LC method parameters were as per liquid chromatography method 2 and 3 in section 2.2.4. The MS method parameters were kept consistent as stated in section 2.2.4, the instrument equipped with the Phenomenex, (Torrance, CA, USA) with 2.1 × 1.5 mm, 5µm column used in the previous section (2.3.1). The early retention of the standards in comparison to the previous method was attributed to the use of 80% mobile phase (acetonitrile and methanol) at the beginning of the method compared to the 50% mobile phase in the method used in section 2.3.1. The concentration of the standards was kept the same, the injections were from the standard sample and MS method parameters were kept the same with only changes in the mobile phases in the LC method. The concentration of the standards used was 10 µg/ml. This was done for all the standards and the pattern remained consistent with acetonitrile with lower intensity and methanol later with higher peak intensity.

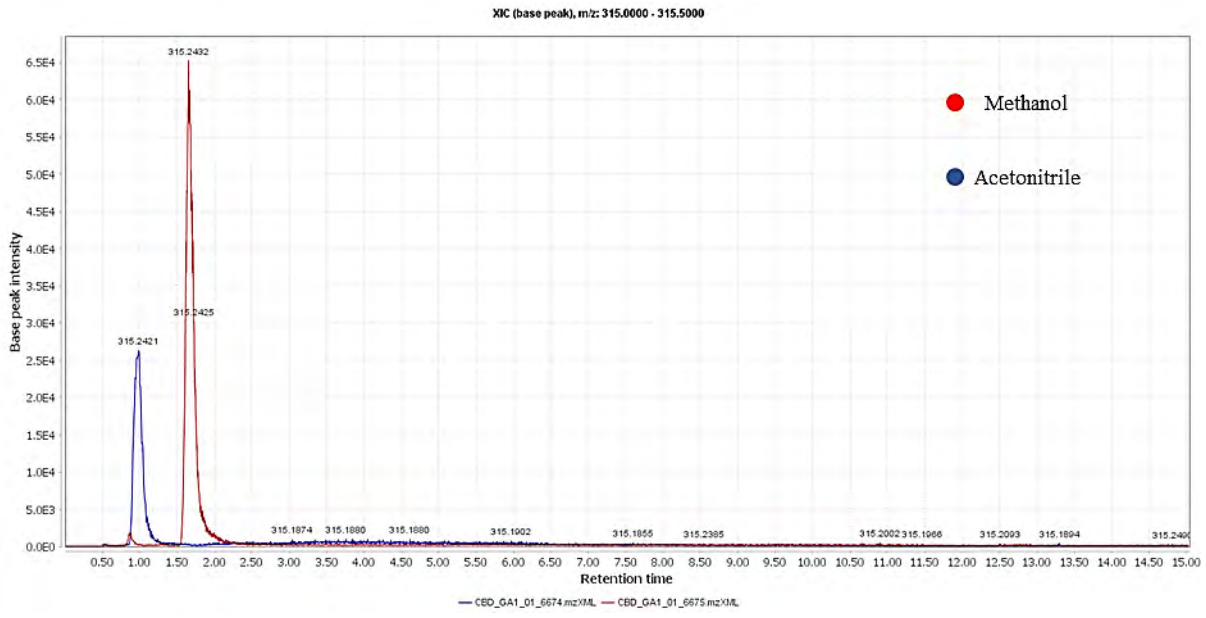

Figure 2.2: Extracted base peak ion chromatograms of Cannabidiol, acetonitrile (*m/z* 315.2421, rt 1.00) compared to methanol (m/z 315. 2432, rt 1.66) obtained by LC-MS.

Figure 2.2 shows the effect of acetonitrile and methanol on peak intensity and is significant because choosing methanol as a mobile phase when working with low concentrations can be beneficial when the priority is to have a high saturation of a specific $[M + H]^+$ ion for analysis

(21). On the other hand, if the priority is quick qualitative analysis, acetonitrile is a better mobile phase of choice. There is also a distinct difference in retention times with CBD retained at 1.00 minute in acetonitrile and 1.66 minutes in methanol. Another priority of this analysis was to observe changes in the mass accuracy of the $[M + H]^+$ precursor ion values, they differed only in the last two decimal points. The precursor ion values of CBD were *m/z* 315.2421 in acetonitrile and *m/z* 315.2432 methanol respectively. This led to considering the change from calibrating with an enhanced quadratic algorithm to a high-performance computing algorithm. The mobile phase in LC-MS is the carrier of the analyte which means its effect on the analyte must be considered.

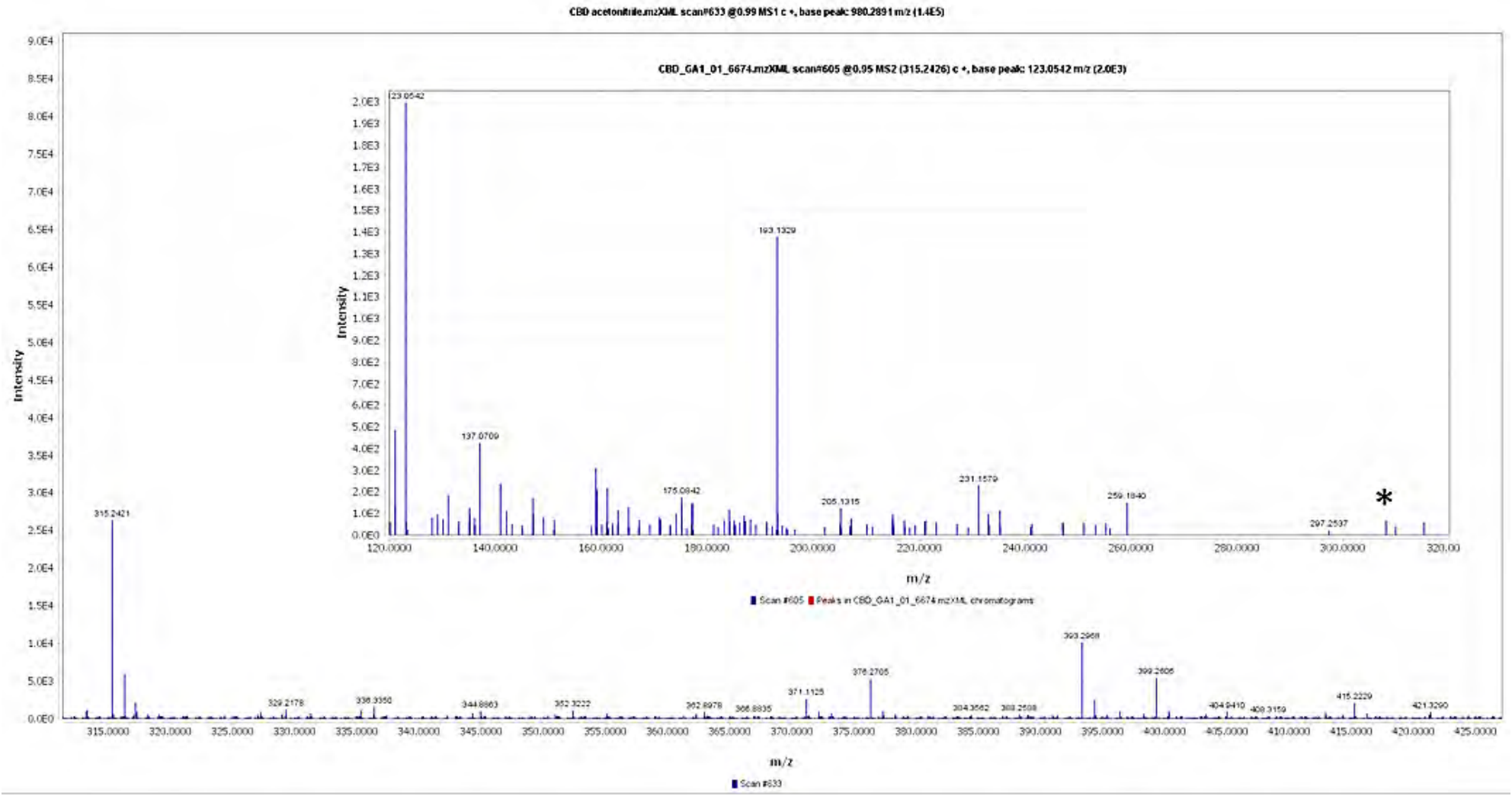

Figure 2.3: Cannabidiol MS1 and MS2 spectra with acetonitrile as mobile phase, *m/z* 315.2421 ion indicated by an asterisk (*) in the MS2 spectrum obtained by LC-MS.

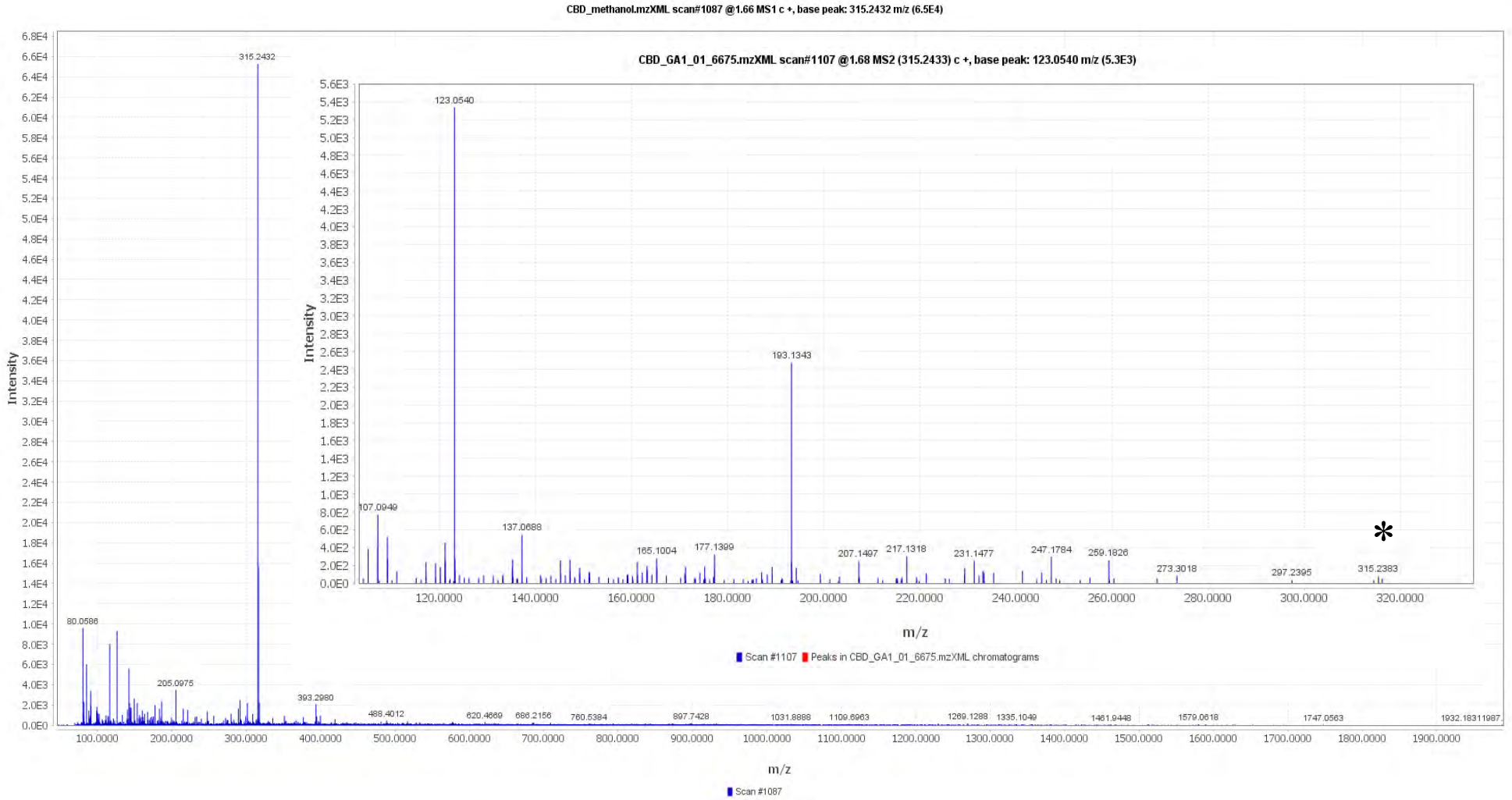

Figure 2.4: Cannabidiol MS1 and MS2 spectra with methanol as mobile phase *m/z* 315.2432 ions indicated by an asterisk (*) in the MS2 spectrum obtained by LC-MS.

Figure 2.3 and Figure 2.4 represent the effect of the mobile phase on the precursor ion (MS1) and the ion's fragmentation (MS2). The acetonitrile MS1 (Figure 2.3) indicates a higher intensity of other ions visible in the spectrum compared to the MS1 (Figure 2.4) of CBD with the methanol mobile phase. Also, the intensity of the *m*/*z* 315 precursor ions in both MS1 spectra has the highest intensity as expected. MS2 spectra in Figure 2.3 and Figure 2.4 are drastically different as a result of the intensity of precursor ion *m*/*z* 315 in the MS1 spectra Figure 3b MS2 spectra show fewer fragments with the precursor ion having a very low intensity close to complete dissociation (24). The impact of the other precursor ions present in an almost competing intensity may influence the intensity of the *m*/*z* 315 precursor ion. The methanol MS2 (Figure 2.4) showed more fragments than the acetonitrile MS2 (Figure 2.3), this may be due to the higher intensity of the precursor ion, and less interference from other precursor ions that are visible in the MS1 spectrum. The *m*/*z* 315 precursor ion was higher and more visible methanol MS2 spectrums. The more fragments there are the better the structural information that can be gathered, hence we then opted to continue with methanol as the mobile phase of choice for analysis.

2.3.3 Refining mass accuracy for fragment structure predictions.

Parameters that resulted in the development of the method in this section are as a result of the observations made in Section 2.3.1 and Section 2.3.2. Following the contrast between mobile phases, we used methanol as the mobile phase of choice, because of the higher intensities of the peaks of interest, (Liquid chromatography method 2, section 2.2.4). High-performance computing calibration was used to improve mass accuracies and enhance the fragment structure predictions. The column used in this section was the Kinetex polar C-18 column (3.0 × 100 mm, 2.6 µm; Phenomenex, Torrance, CA, USA), hence the difference in retention times in the standard total ion chromatograms. This column is a C-18 column different to the Phenomenex, Torrance, CA, USA, 2.1× 150 mm, 5 µm particle size and 100Å pore size, used in Section 2.3.1 and Section 2.3.2 because the resin in this column has a polar surface modification. In Section 2.3.2 we observe early retention of CBD, as early as 1.00 minute, while the retention time in acetonitrile and CBD in methanol were 0.66 and 1.66 minutes respectively. In Table 2.5, we observe the retention time of

CBD is 4.22 minutes in comparison to the 1.66 minutes retention time while using a different column. This increased rt allows for better resolution of standards.

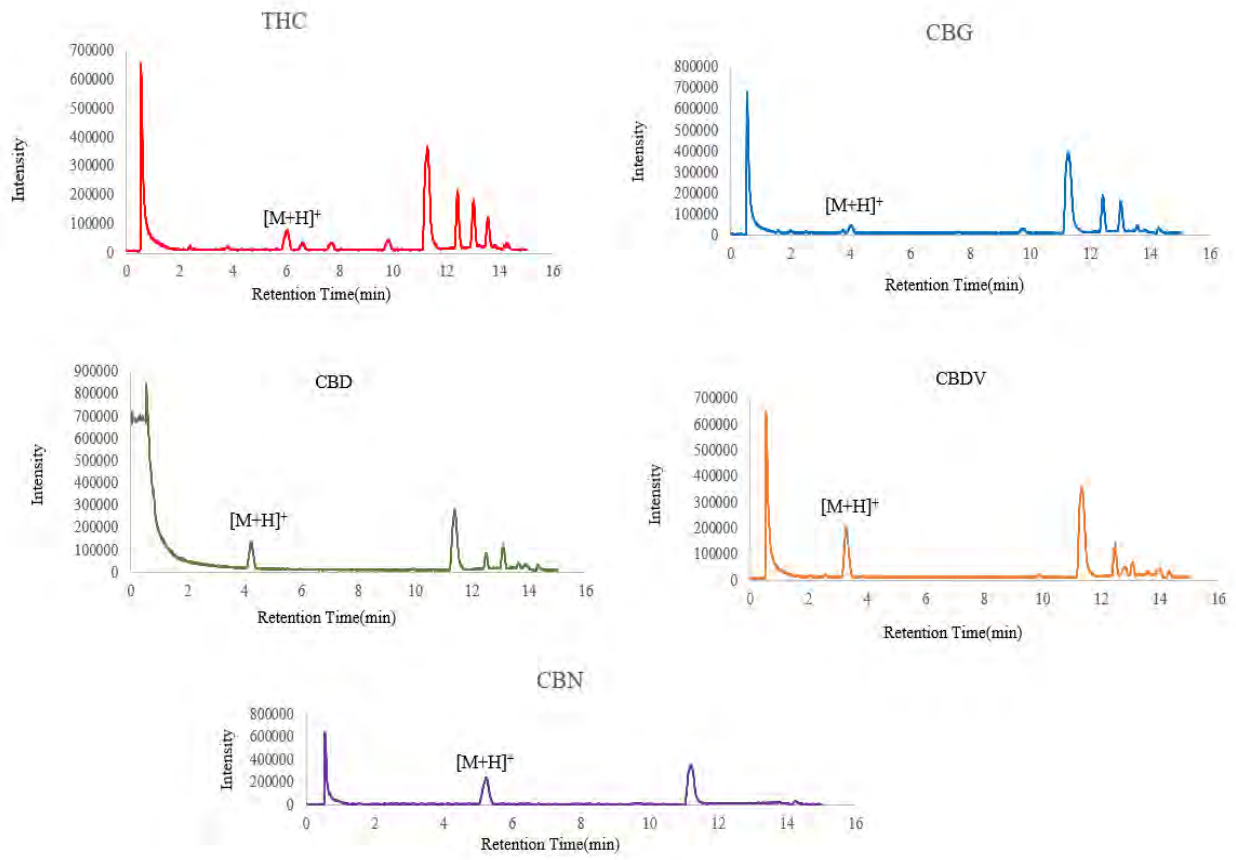

Figure 2.5: Total ion chromatograms obtained by LC-MS for the analysis of cannabinoid standards THC ($[M+H]^+$, 315.2305), CBD ($[M+H]^+$,315.2320) CBN ($[M+H]^+$, 311.1988), CBG ($[M+H]^+$,317.2451) and CBDV ($[M+H]^+$, 287.1999).

Figure 2.5 chromatograms show the distinct separation of the peaks of interest, which are the $[M+H]^+$ peaks only, because of our interest in proposing pathways for structure elucidations of fragments from these precursor ions. Summarised below in table 2.5 are the retention times of the $[M+H]^+$ ions of the standards.

Table 2.5: Cannabinoid compound retention times obtained by LC-MS.

Compound	Retention Time (min)
THC	6.04
CBD	4.22
CBN	5.22
CBG	4.01
CBDV	3.29

Retention times in this method are within 10.00 minutes, making this method a reasonable method to use for the rapid detection of cannabinoids. The elution order of the cannabinoids CBDV, CBG, CBD, CBN, and THC remained consistent with the one in section 2.3.1 and other published research on cannabinoids (9) (11). The total ion chromatograms of the cannabinoids in Figure 5 shows better resolution in comparison to the chromatograms in section 2.3.1 in Figure 2.1, note especially the improvement in the CBDV chromatograms in both figures.

As mentioned above, the results achieved were good resolution, with $[M+H]^+$ ions distinctly separated. Having achieved this, the focus was the ion mass accuracies of the precursor ions. Moreover, the option to use methanol as the mobile phase meant the possibility of more and better fragmentation which leads to more structural information (25). The high molecular abundance as a result of using methanol led to improved mass accuracies in Table 2.6 (in comparison to those in Section 2.3.1, Table 2. 4.

Table 2.6: Cannabinoid compound improved accurate masses for their $[M + H]^+$ precursor ions obtained by LC-MS.

Compounds	$[M+H]^+$	Accurate Mass (m_i)	Calculated Mass	Δm_i (Da)	Δm_i(mDa)	$\Delta m/m_i x10^6$ (ppm)
THC	$C_{21}H_{31}O_2$	315.2305	315.2324	0.0019	1, 9	6.03
CBD	$C_{21}H_{31}O_2$	315.2320	315.2324	0.0004	0.4	1.27
CBN	$C_{21}H_{27}O_2$	311.1988	311.2011	0,0023	2.3	7.39
CBG	$C_{21}H_{33}O_2$	317.2451	317.2481	0,0030	3.0	9.45
CBDV	$C_{19}H_{27}O_2$	287.1999	287.2011	0.0012	1,2	4.18

Although the expectation was that the mass accuracies would be 5 ppm or less with the use of high-performance computing, we did not achieve this for THC, CBN, and CBDV. The results obtained had a significant mass accuracy improvement in comparison to mass accuracy values obtained in Section 2.3.1 in Table 2.4, and these results were considered satisfactory for fragment structure predictions, where the aim was to achieve at least mass accuracy values lower than 10 ppm accuracy.

2.3.4 Proposed fragment structures and their elucidation pathways.

Information on cannabinoids and their structures are essential when performing soft ionization on compounds to give an MS1 spectrum, followed by collision-induced dissociation to give the MS2 spectrum is the key driver of this discussion. Knowledge of collision-induced dissociation is far less currently but we utilize the available knowledge for fragment structure predictions (26). To further emphasize the importance of MS in structure elucidation, in this research, proposed pathways have been presented, showing that structure assignment to fragments is possible. Charge retention fragmentations and charge migration fragmentations have been applied in the fragment structure predictions. Inductive cleavage and remote hydrogen rearrangement were utilized in predicting these structures, due to their regular prevalence in fragmentations of natural products (27).

In this section, the results are presented in spectra (Figure 2.6 to Figure 2.15) and schemes (Schemes 2.1 to 2.6). The mass spectra are a result of the analysis of 314.2245 g/mol THC, 314.2246 g/mol CBD, 287.1933 g/mol CBDV, 316.2402 g/mol CBG and 310.1933 CBN respectively. We added the ionised $[M+H]^+$ versions of the structures on the MS1 spectra, showing the suggested position of ionisation each compound. In the MS2 spectra, the ionised version of the structures was placed from the MS1 on to the MS2 spectra and added fragmentation lines colour coded to match the structure numbers placed near each signal, the actual fragment structures are seen in the schemes. However, this was not done for all fragments, it was done do represent the structures common in the cannabinoid MS2 spectra and fragment pathways.

2.3.4.1 Tetrahydrocannabinol

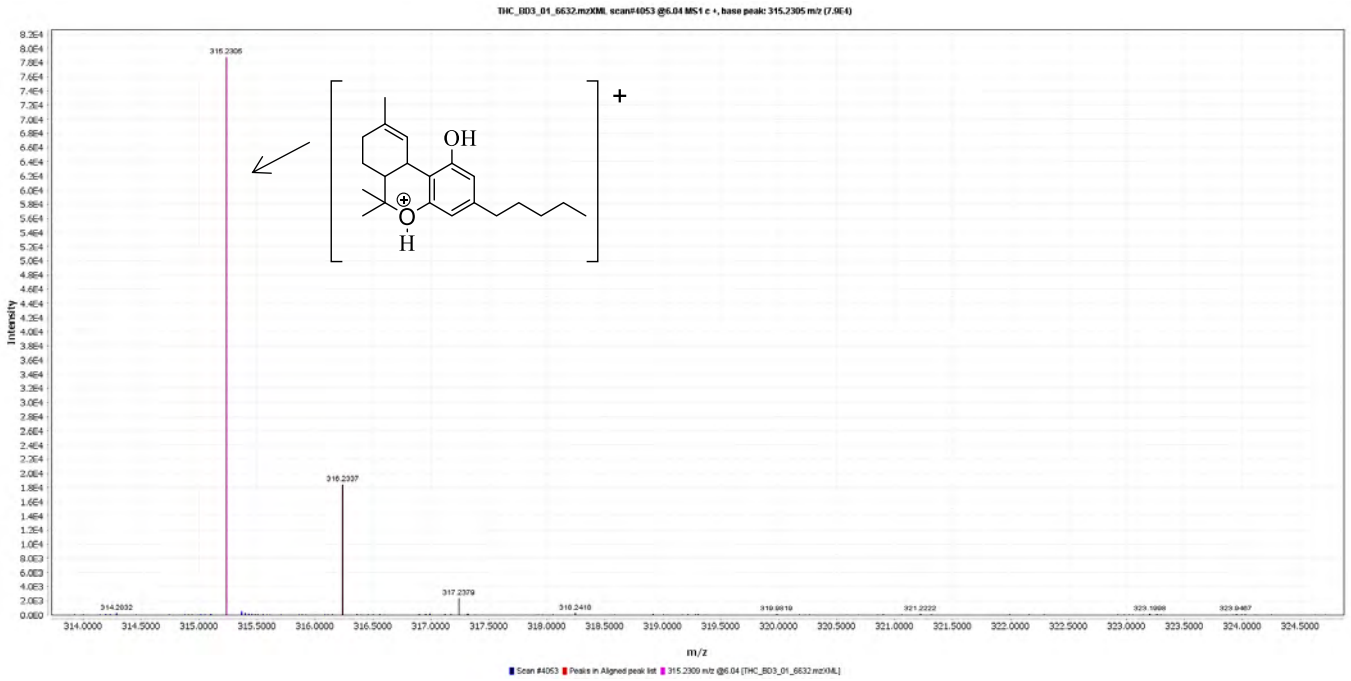

Figure 2.6: MS1 spectrum of Tetrahydrocannabinol $[M+H]^+$ *m/z* 315.2305, obtained by LC-MS.

The mass spectrum of THC shows the *m/z* 315.2305 precursor ion $[M+H]^+$ signal. Other ions in the spectrum intensity high enough to consider compared to *m/ z* 316.2337 and *m/z* 317.2379. The MS2 spectrum below shows the fragmentation pattern of the THC, $[M+H]^+$ precursor ion (Figure 2.7).

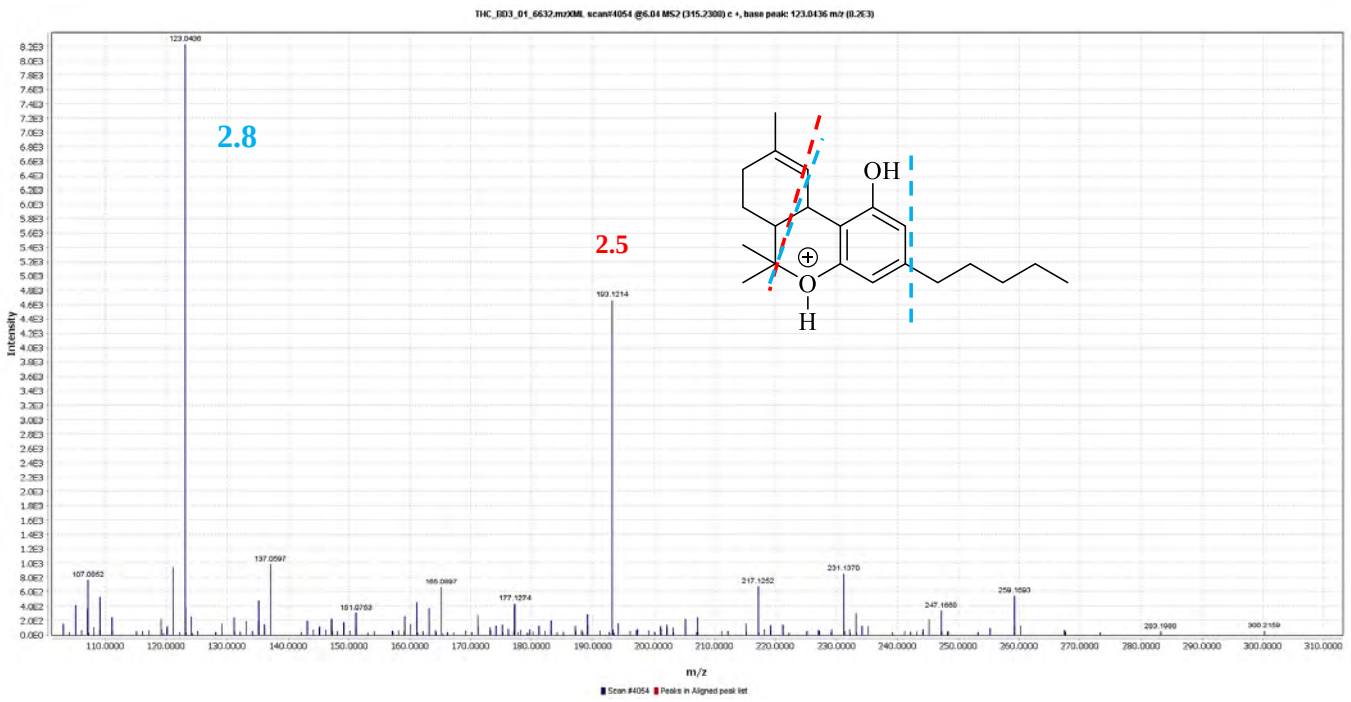

Figure 2.7: MS2 spectrum of Tetrahydrocannabinol $[M+H]^+$ precursor ion *m/z* 315.2305, obtained by LC-MS/MS.

The fragment ions *m/z* 123.0436 (structure 2.8) (Scheme 2.1). and *m/z* 193.1214 (structure 2.5) (Scheme 2.1). with the high intensity, as expected with the presence of *m/z* 259, this correlates with previous research on cannabinoids (9). Selected fragment ions structures in the above MS2 spectra have been predicted and shown in scheme 2.1. The precursor ion completely dissociated due to the use of the collision energy voltage of 40 eV, although this is the case, the results obtained, gave more fragment ions which are good for structure elucidations (Scheme 2.1).

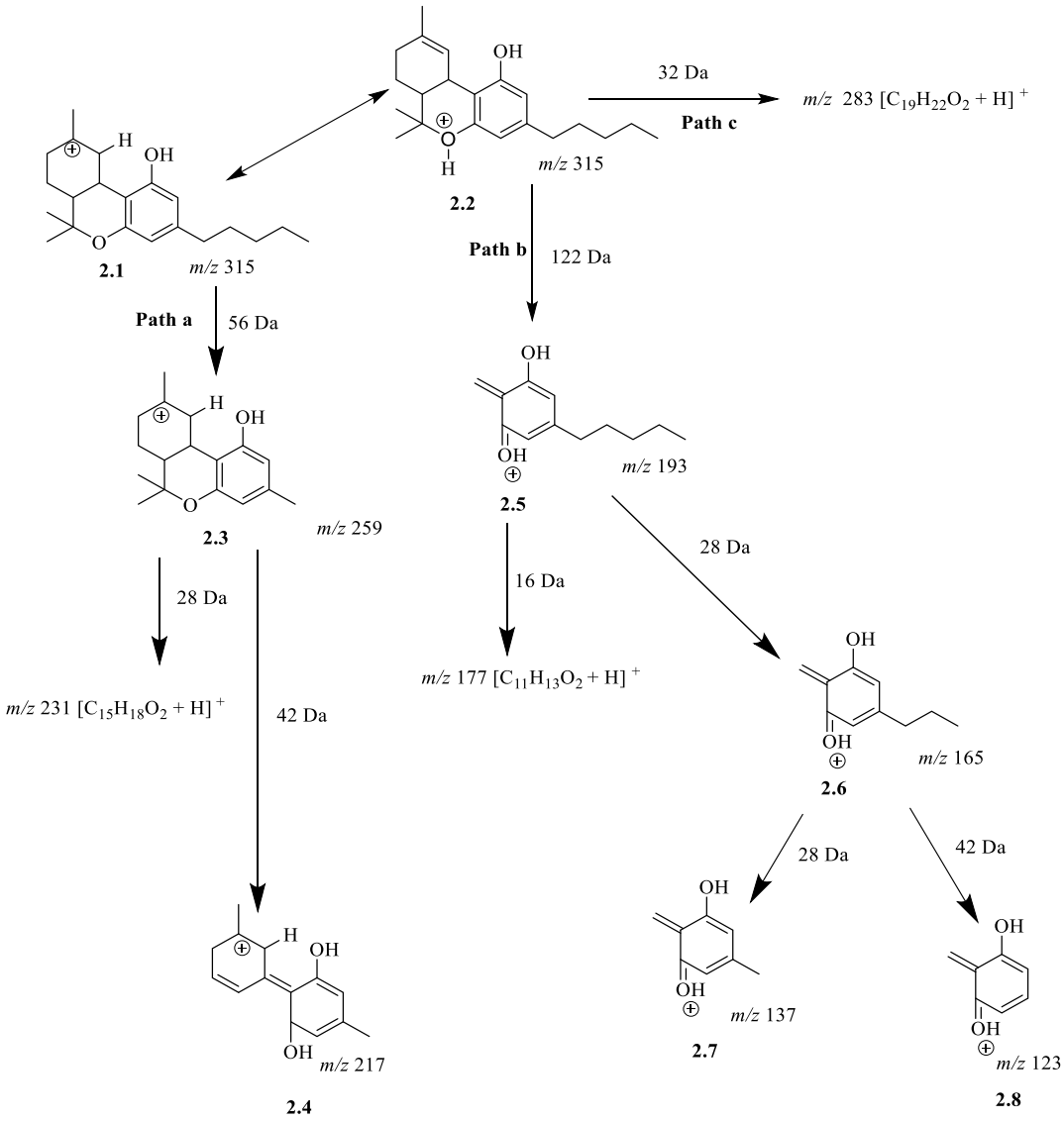

Scheme 2.1: Proposed fragment structures pathways of THC precursor ion $[M + H]^+$ *m/z* 315.2305.

The proposition of path a begins from structure **2.1** to **2.3** which shows loss of most of the pentyl side chain (C_4H_8) leads to fragment structure **2.3** (*m/z* 259) which has been observed in previous

research (9). This could be as a result of a retro Diels Alder reaction followed by a hydrogen rearrangement. The neutral loss of 28 Da (C_2H_4), in the transition of *m/z* 259 → 231 producing the ion *m/z* 231 $[C_{15}H_{18}O_2 + H]^+$ and the transition *m/z* 259 → 217 was, as a result, neutral loss of 42 Da (C_3H_6) producing the fragment ion *m/z* 217 $[C_{14}H_{17}O_2 + H]^+$ (Structure **2.4**). Path b, beginning at the *m/z* 315 $[C_{21}H_{30}O_2 + H]^+$ (Structure **2.2**) fragment ion, was proposed to begin with the neutral loss of 122 Da (C_9H_{14}) resulting in the fragment ion *m/z* 193$[C_{12}H_{16}O_2 + H]^+$ (Structure **2.5**). A neutral loss 16 Da (CH_4) from structure **2.5** in the transition (*m/z* 193 → 177) results in the fragment ion *m/z* 177 $[C_{11}H_{13}O_2 + H]^+$. Alternatively, a neutral loss of 28 Da (C_2H_4) in the *m/z* 193 → 165 transition could result the fragment ion *m/z* 165 $[C_{10}H_{12}O_2 + H]^+$ (Structure **2.6**). The neutral loss from *m/z* 193 to *m/z* 165 lead to more fragment structure propositions.

The transitions *m/z* 165 → 137 and *m/z* 165→ 123 with neutral losses 28 Da (C_2H_4) and 42 Da (C_3H_6) respectively resulting in the fragment ions *m/z* 137 $[C_8H_8O_2 + H]^+$ (Structure **2.6**) and *m/z* 123 $[C_7H_6O_2 + H]^+$ (Structure **2.7**) respectively. However, path c is representative of a transition (*m/z* 315 → 283) resulting in the precursor ion *m/z* 283 $C_{19}H_{22}O_2 + H]^+$ that could be due to a neutral loss of 32 Da (CH_3OH).

2.3.4.2 Cannabidiol

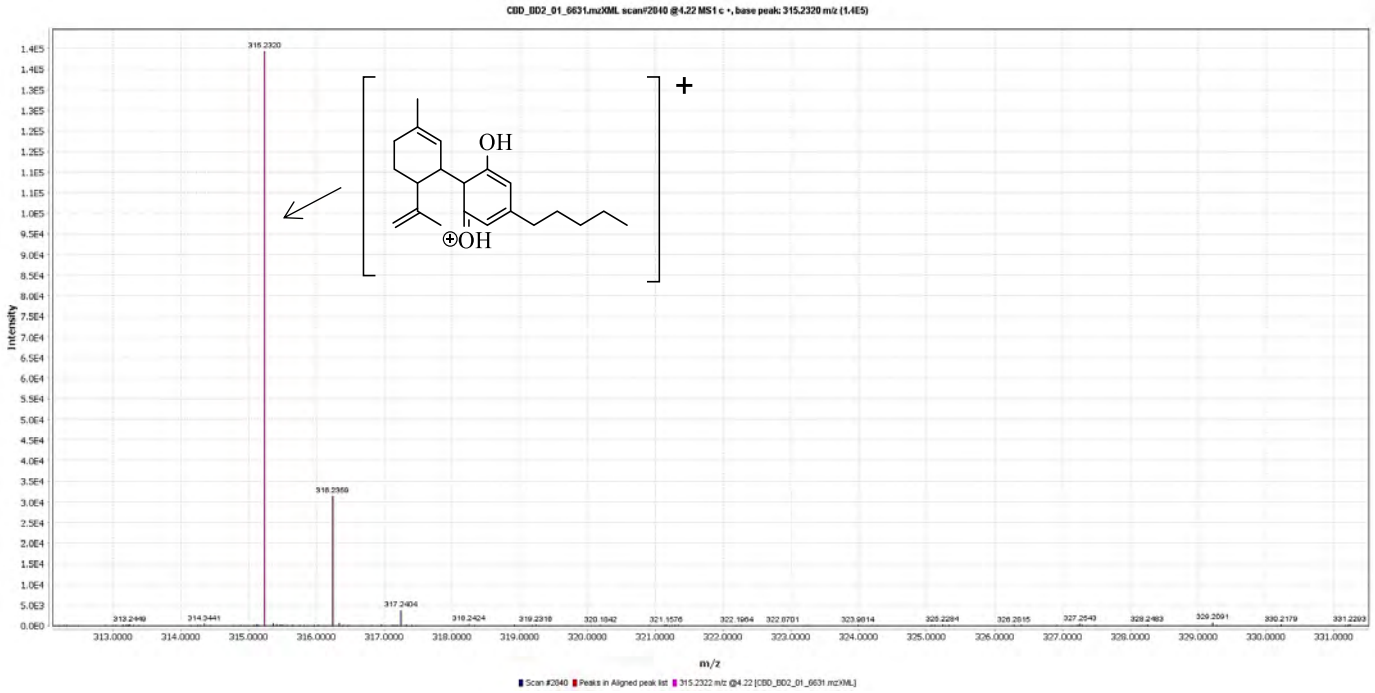

Figure 2.8: MS1 spectrum of Cannabidiol $[M+H]^+$, precursor ion *m/z* 315.2320 obtained by LC-MS.

The CBD mass spectrum shows the $[M+H]^+$, precursor ion with *m/z* 315.2320, as expected. The *m/z* 316.2359 and *m/z* 317.2404 are also visible in the spectrum in relative abundances.

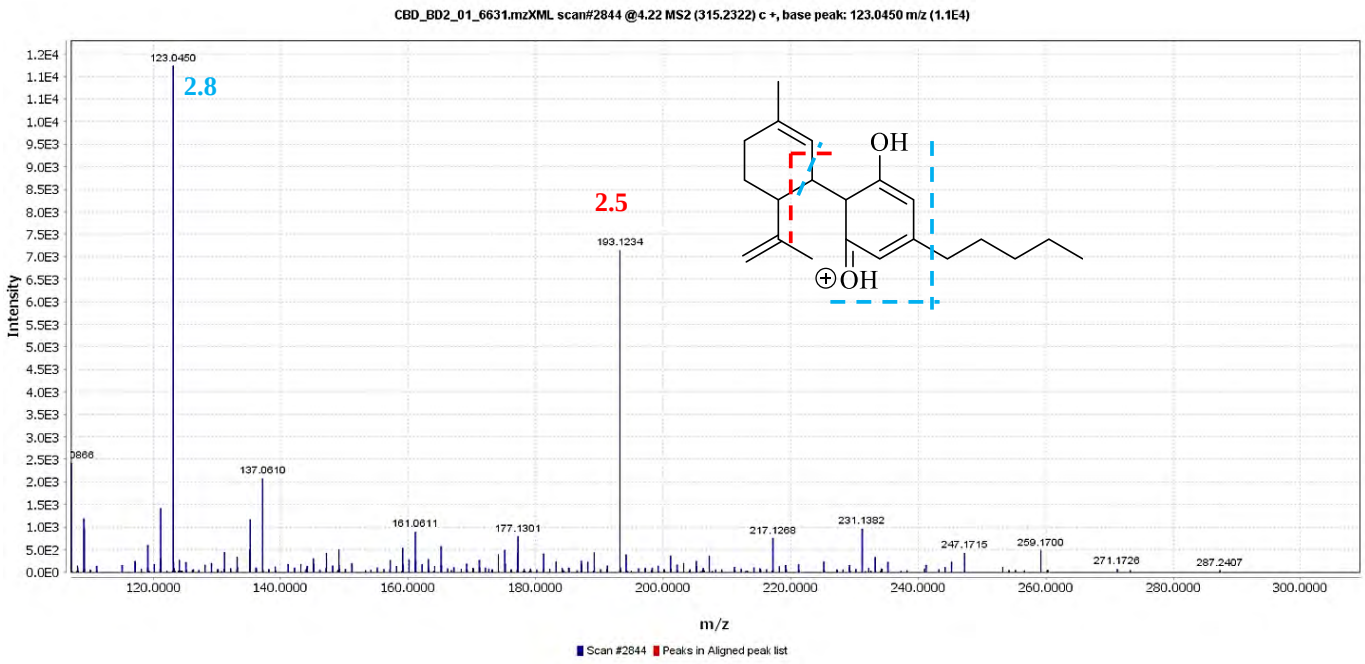

Figure 2.9: MS2 spectrum of Cannabidiol $[M+H]^+$ precursor ion *m/z* 315.2320, obtained by LC-MS/MS at 40 eV.

While THC (Figure 2.6 and 2.7) and CBD (Figure 2.8 and Figure 2.9) both have the same clear differences and some similarities. The fragment ions *m/z* 193.1234 and *m/z* 123.0450 with low intensity for *m/z* 259 as observed in previous work (9). Most fragment ions observed in the above MS2 spectrum are comparable to those observed in the THC MS2 spectrum (Figure 2.7) apart from the presence of *m/z* 161 instead of *m/z* and the presence of *m/z* 287 in the CBD MS2 spectrum (Figure 2.9). The precursor ion *m/z* 315 is not present in the MS2 spectrum due to complete dissociation at 40 eV. Structures of fragment ions in the above MS2 spectrum are in Scheme 2.2.

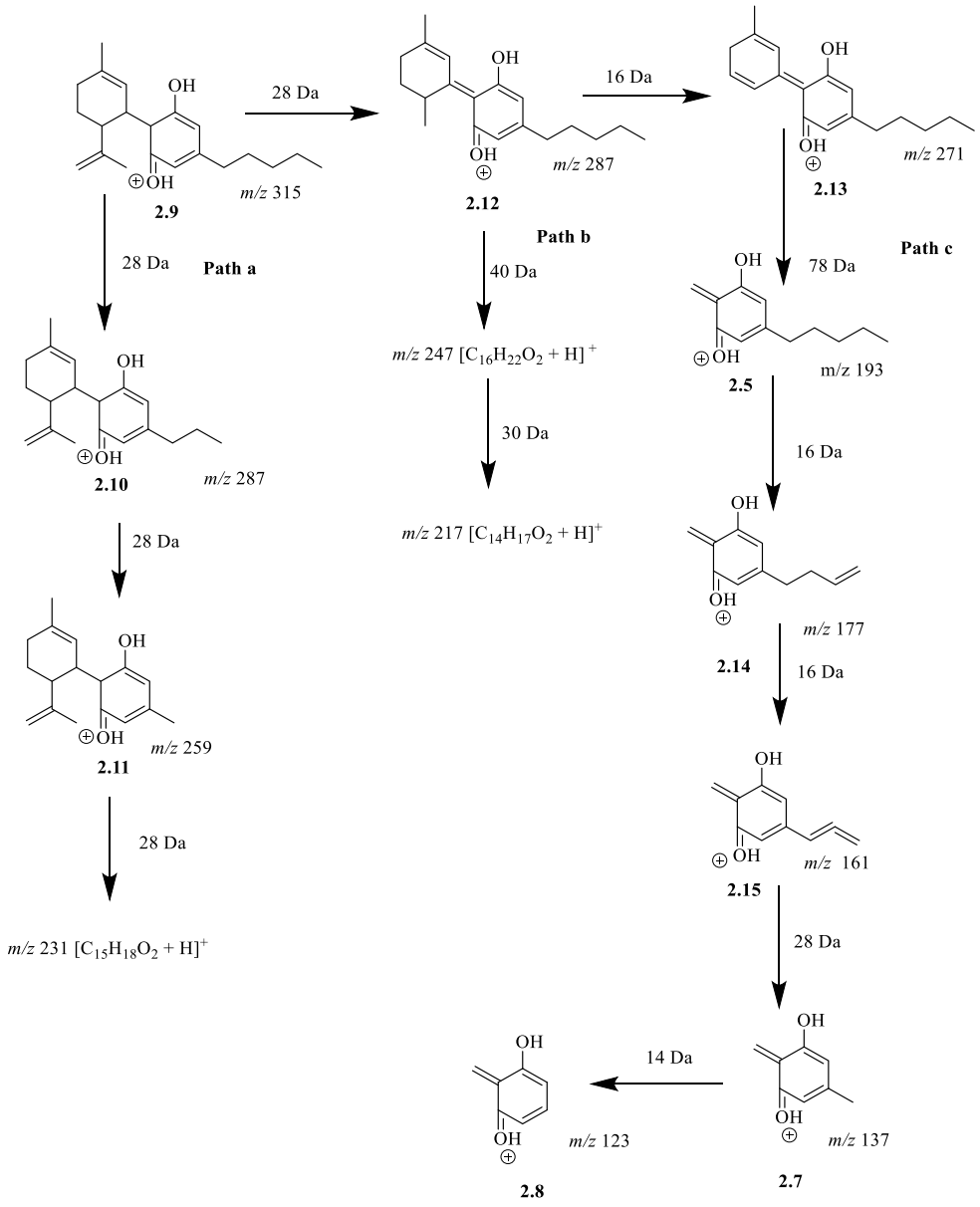

Scheme 2.2: Proposed fragment structures pathways of CBD precursor ion $[M + H]^+$ *m/z* 315.2320.

The CBD precursor ion of *m/z* 315 $[C_{21}H_{30}O_2 + H]^+$ (Structure **2.9**) produced fragments from the transition (*m/z* 315 → 123), either from several neutral losses or hydrogen rearrangement reactions shown in scheme 2.2 in paths a, b and c.

As seen in scheme 2.2, the production of the *m/z* 287 $[C_{19}H_{26}O_2 + H]^+$ fragment ion is dependent on the position where the fragmentation occurs in the *m/z* 315 precursor ion, where structure **2.9** could give structure **2.10** or **2.12**. This (*m/z* 315 → 287) transition in both cases could be due to a neutral loss of 28 Da (C_3H_6). Nonetheless, we proceeded to propose other fragment structures in the scheme, labelling paths as, the **path a** starting from structure **2.9** to **2.11**, **path b** from structure **2.9** to the *m/z* 217 ionised formula, and **path c** structure **2.9** to **2.8**. Path a, shows transitions (*m/z* 287 → 259) and (*m/z* 259 → 231) could be defined by the neutral losses of 28 Da (C_2H_4) and 28 Da (C_3H_6) resulting in the fragment ions *m/z* 259 $[C_{17}H_{22}O_2 + H]^+$ (Structure **2.11**) and *m/z* 231 $[C_{15}H_{20}O_2 + H]^+$ respectively. In path c, the transitions (*m/z* 287 →247) and (*m/z* 247 → 217), could be by the neutral loss of 40 Da (C_3H_4) and 30 Da (C_2H_6).resulting in the fragment ions *m/z* 247 $[C_{16}H_{22}O_2 + H]^+$ and *m/z* 217 $[C_{14}H_{17}O_2 + H]^+$ respectively.

The fragmentation path c continues from the fragment structure **2.12**, with the transition *m/z* 287 → 271 by the neutral loss 16 Da (CH_4), resulting in the *m/z* 271 $[C_{18}H_{22}O_2 + H]^+$ fragment ion (structure **2.13**). Following this, the (*m/z* 271 → 193) transition that may be due to the loss of 78 Da (C_6H_8, H_2), by bond cleavage and hydrogen rearrangement could produce the fragment ion *m/z* 193 $[C_{17}H_{22}O_2 + H]^+$ (Structure **2.5**). The pathway proceeds with the transitions (*m/z* 193→177→ 161) that may be characterized by the consecutive neutral loss of 16 Da (CH_4) resulting in the fragment ions *m/z* 177 $[C_{11}H_{12}O_2 + H]^+$ (structure **2.14**) and *m/z* 161 $[C_{10}H_8O_2 + H]^+$ (structure **2.15**) respectively. The transitions *m/z* (161 → 137 → 123) with the loss of 28 Da (C_2H_4), 14 Da (CH_2) resulting in the fragment ions *m/z* 137 $[C_8H_8O_2 + H]^+$ (Structure **2.7**) and *m/z* 123 $[C_7H_6O_2 + H]^+$ (Structure **2.8**) respectively.

2.3.4.3 Cannabidivarin

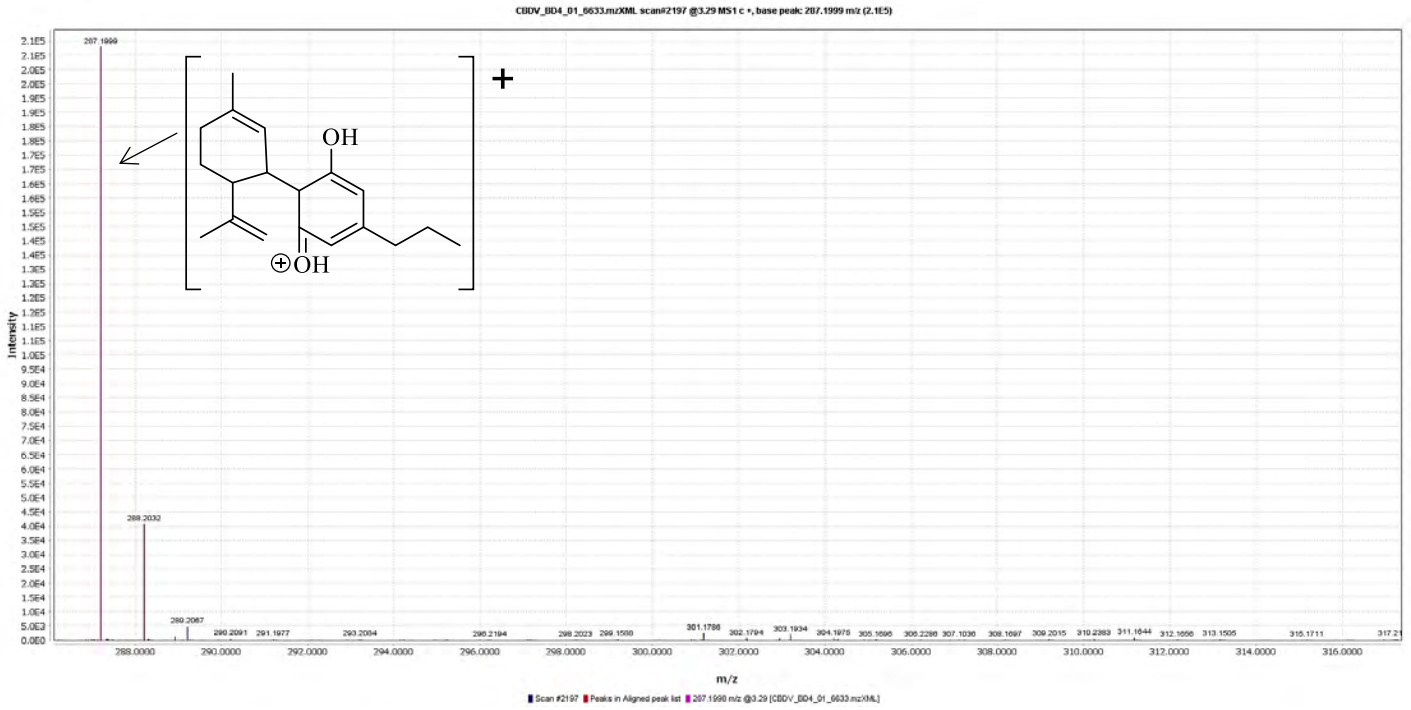

Figure 2.10: MS1 spectrum of Cannabidivarin $[M+H]^+$, precursor ion *m/z* 287.1999 obtained by LC-MS.

The $[M+H]^+$, precursor ion of CBDV is represented by the *m/z* 287.1999 signal in the spectrum. The signal m/z 288.2032m/z 289.2067 is also visible in relative abundances. The MS2 spectrum

in Figure 2.11 shows the fragmentations possible for the [M+H] $^{+}$ precursor ion.

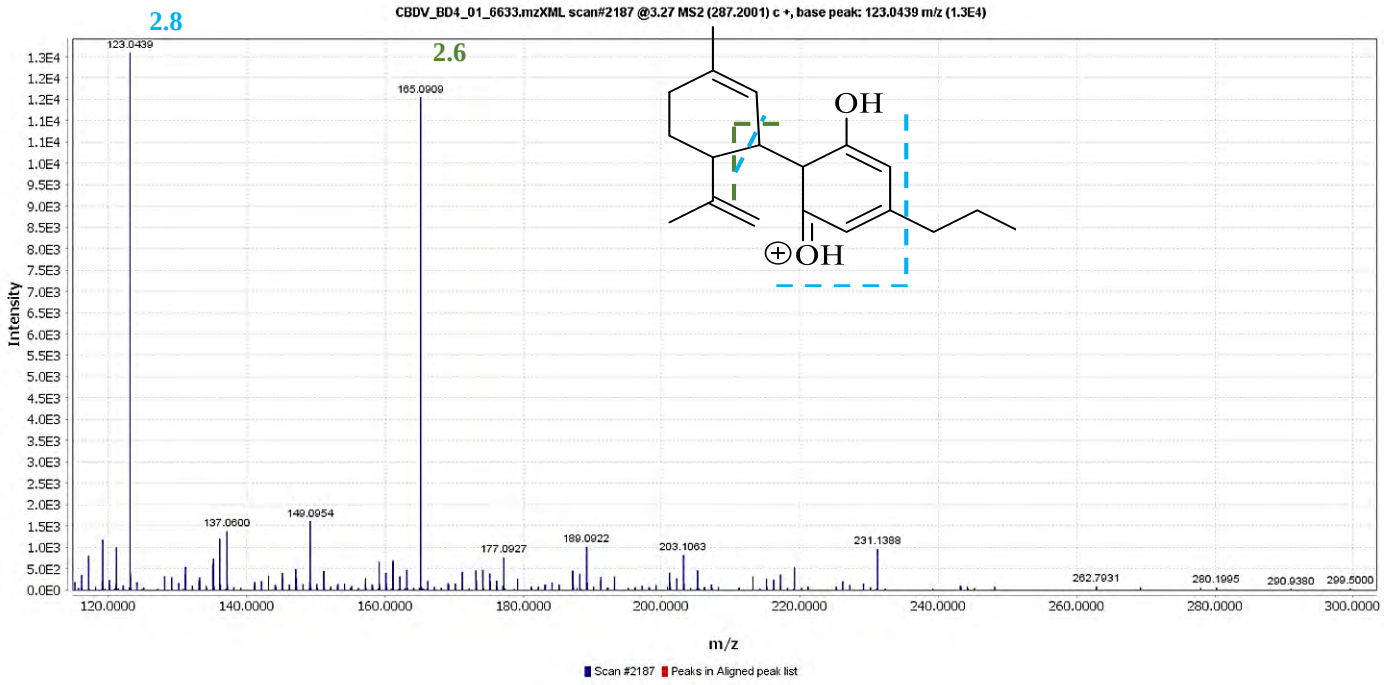

Figure 2.11: MS2 spectrum of Cannabidivarin [M+H] $^{+}$, precursor ion *m/z* 287. 1999 obtained by LC-MS/MS at 40 eV.

The precursor ion *m/z* 287 completely dissociated at collision energy 40 eV. This is expected because of the structure's similarity to CBD, under similar conditions, a comparable response is expected. The fragment ions for the CBDV precursor ion are predicted in Scheme 2.3.

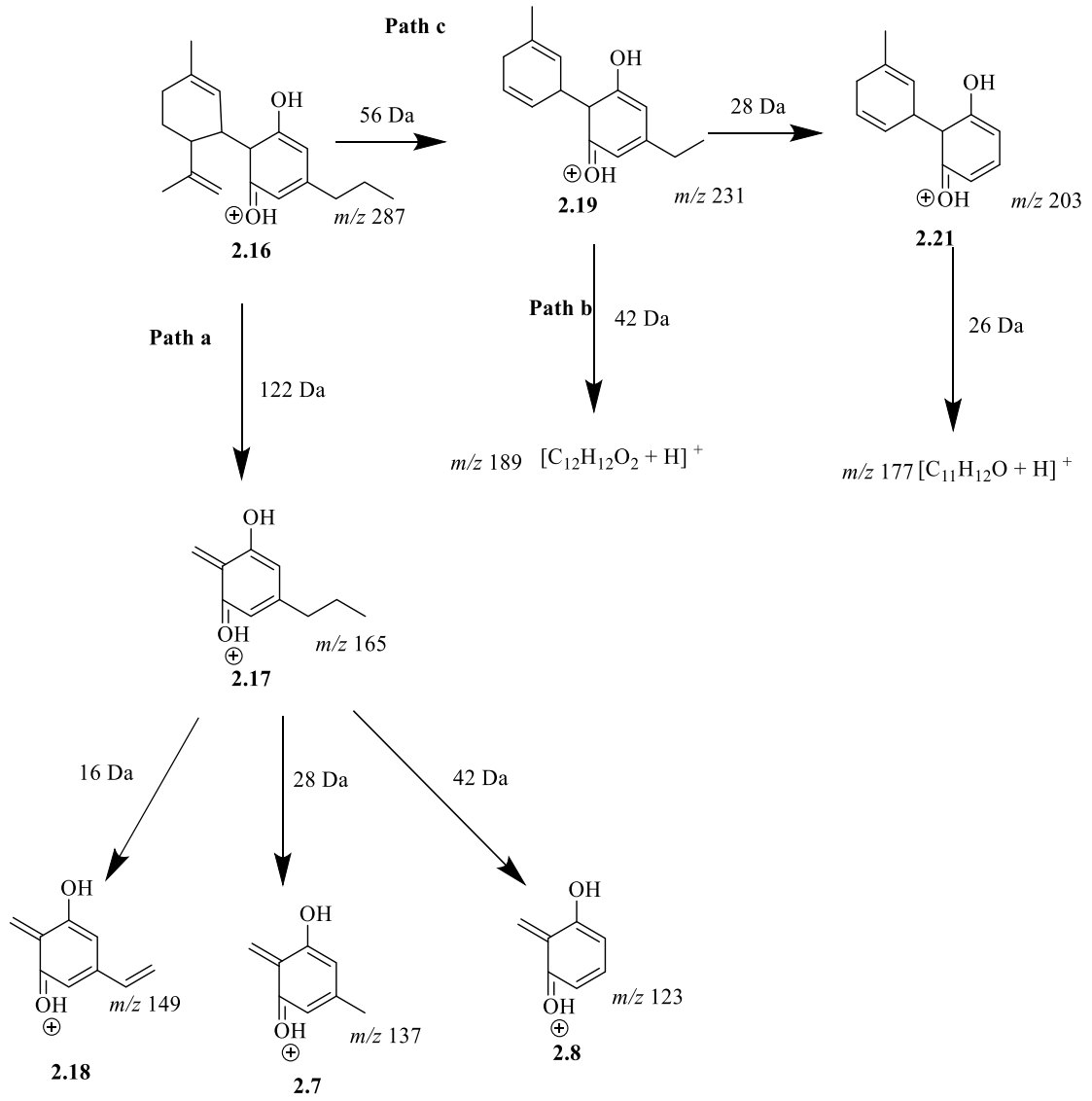

Scheme 2.3: Proposed fragment structure pathways of CBDV precursor ion [M + H] $^{+}$ *m/z* 287.1999.

Proposed above are fragment structures with pathways a b and c for the precursor ion m/z 287 [C19H26O2+H] + (Structure 2.16). Fragment ions observed in the CBDV MS2 spectrum (Figure 2.11), in comparison to the CBD MS2 spectrum (Figure 2.9), following the detection of m/z 287 were similar except for fragment ions m/z 203 [C13H14O2 + H]+ (structure 2.21), [C12H12O2 + H]+ m/z 189 (structure 2.20), m/z 165 [C10H12O2 + H]+ (structure 2.5) and m/z 149 [C9H8O2 + H]+ (structure 2.21). Interestingly we found the similar fragment m/z 165 [C10H12O2 + H] + present in THC MS2 (Figure 2.7, structure 2.25) showing a similarity with CBDV not only with

CBD but with its constitutional isomer THC. **Path a** start with the transition m/z 287 → 165 by the neutral loss of 122 Da (C9H14) resulting in the fragment ion m/z 165 [C10H12O2 + H] + (structure 2.5).

The transitions m/z 165 →149, m/z 165 →137 and m/z 165 →123 are characterized by the neutral loses 16 Da (CH4), 28 Da (C2H4) and (C3H8) respectively, resulting in the fragment ions m/z 149 [C9H8O2 + H] + (structure 2.21) , m/z 137 [C8H8O2 + H] + (Structure 2.6) and m/z 123 [C7H6O2 + H] + (Structure 2.7) respectively. **Path b**, the transition m/z 231→ 189 by the neutral loss of 42 Da (C3H8) resulting in the fragment ion m/z 189 [C12H12O2 + H] + ion. The transition m/z 287→ 231 → 203→177 , **path c**, characterised by the neutral losses of 56 Da (C4H8), 28 Da (C2H4), 26 Da (C2H2) resulting in the fragment ions m/z 231 [C15H18O2 + H] +(structure 2.18) m/z 203 [C13H14O + H] + (structure 2.19) and m/z 177 [C11H12O + H] + ion respectively.

2.3.4.4 Cannabigerol

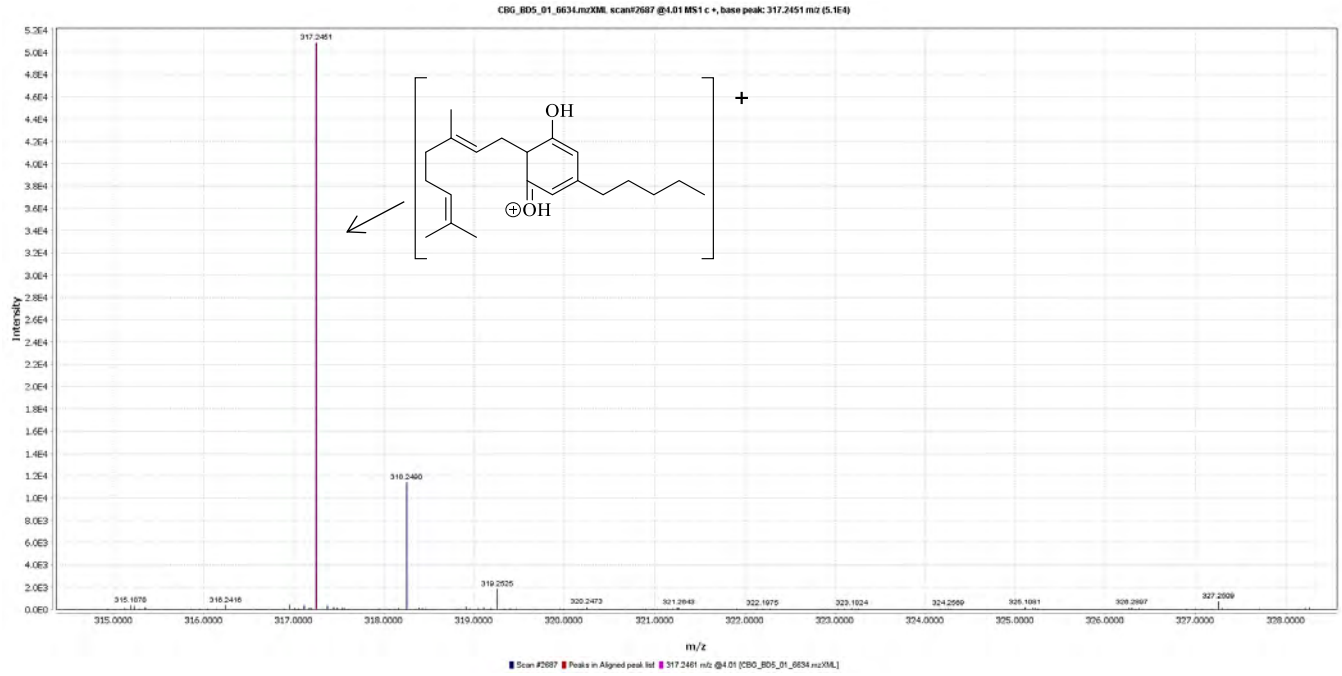

Figure 2.12: MS1 spectrum of CBG $[M+H]^+$, precursor ion *m/z* 317.2451 obtained by LC-MS.

Figure 2.12 is the spectrum of CBG showing the signal m/z 317.2451 as expected as the value of the CBG [M+H] + precursor ion. The signals *m/z* 318.2490 and m/z 319.2525 are also seen in this spectrum in their relative abundances.

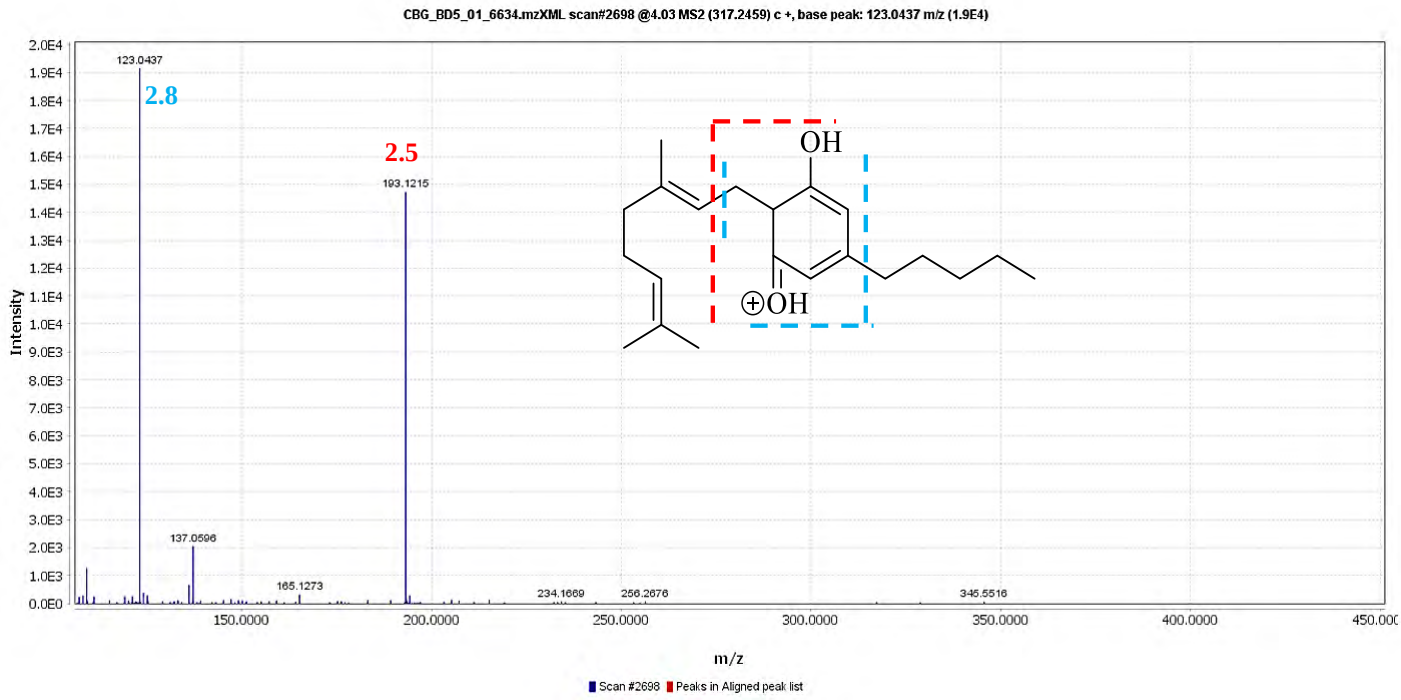

Figure 2.13: MS2 spectrum of CBG $[M+H]^+$ precursor ion *m/z* 317.2451 obtained by LC-MS/MS at 40 eV.

The MS2 spectrum of CBG shows a few signals, as a result of structure fragmentation. This structure has one aromatic ring, a simple fragmentation pathway could summarise the fragmentation that occurs (Scheme 2.4).

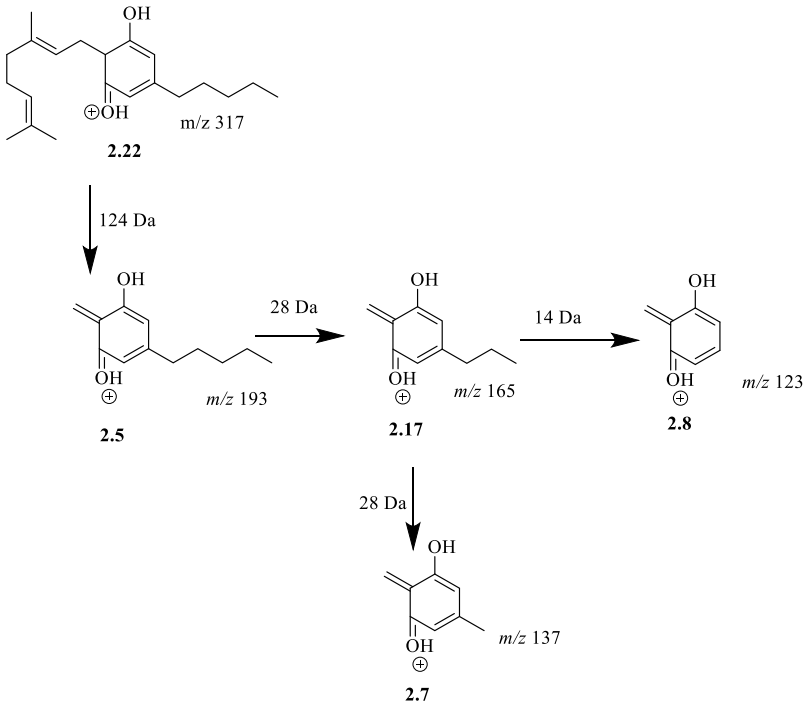

Scheme 2.4: Proposed fragment structures pathways of CBG precursor ion $[M + H]^+$ *m/z* 317.2451.

Fragments from the precursor ion *m/z* 317 $[C_{21}H_{32}O_2 + H]^+$(structure **2.22**, scheme 2.4) were *m/z* 315→193→ 165 → 137→123 with the neutral losses of 124 Da (C_9H_{16}), 28 Da (C_2H_4) ,28 Da (C_2H_4) and 14 Da (CH_4) respectively. The resulting fragment ions were *m/z* 193 $[C_{12}H_{16}O_2 + H]^+$ (structure **2.5**,), *m/z* 165 $[C_{10}H_{12}O_2 + H]^+$ (structure **2.17**) and *m/z* 137 $[C_8H_8O_2 + H]^+$ (structure **2.7**,) respectively. In the estimation of the fragment ion *m/z* 123 $[C_7H_6O_2 + H]^+$ (structure **2.8**), we explored the *m/z* 137 → 123 in previous schemes as opposed to the transition *m/z* 165 → 123, the latter has another logical neutral loss of 42 Da (C_3H_6).

2.3.4.5 Cannabinol

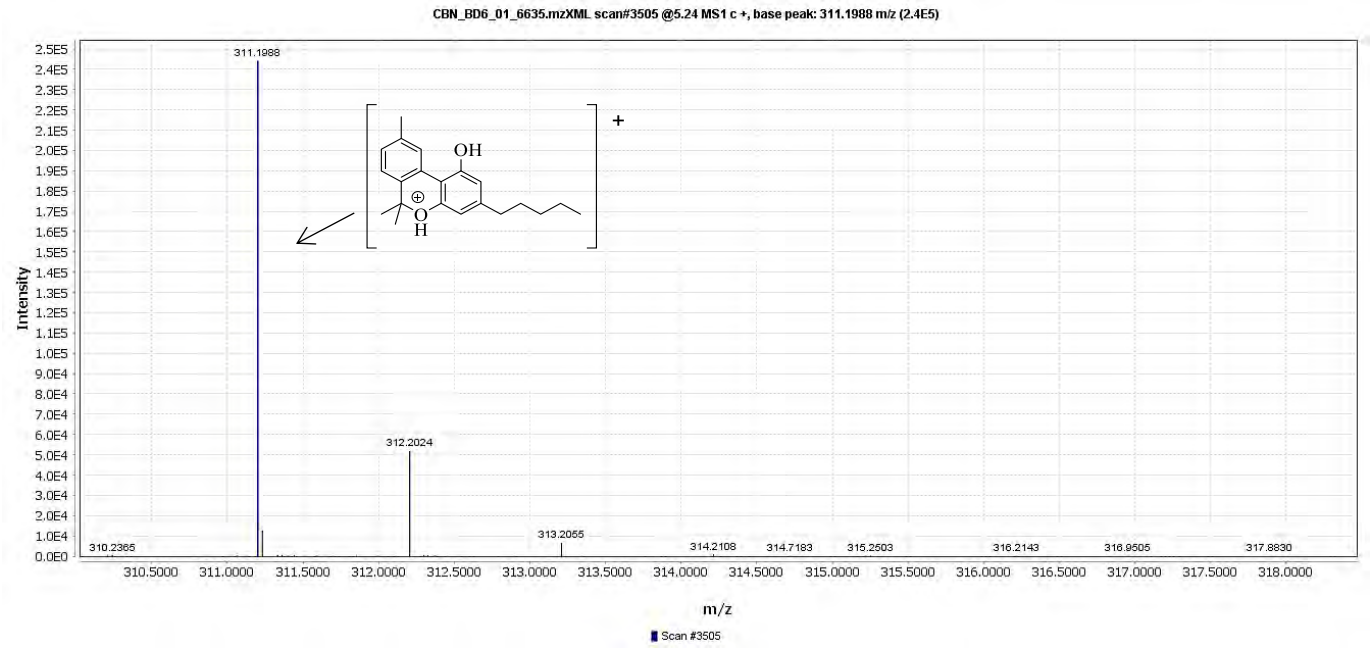

Figure 2.14: MS1 of CBN $[M+H]^+$, precursor ion *m*/*z* 311.1988 obtained by LC-MS.

Figure 2.14 shows the mass spectrum of CBN with the $[M+H]^+$, having the m/z 311.1988, having a higher intensity than the *m*/*z* 312.2024 and m/z 313.2055 signals.

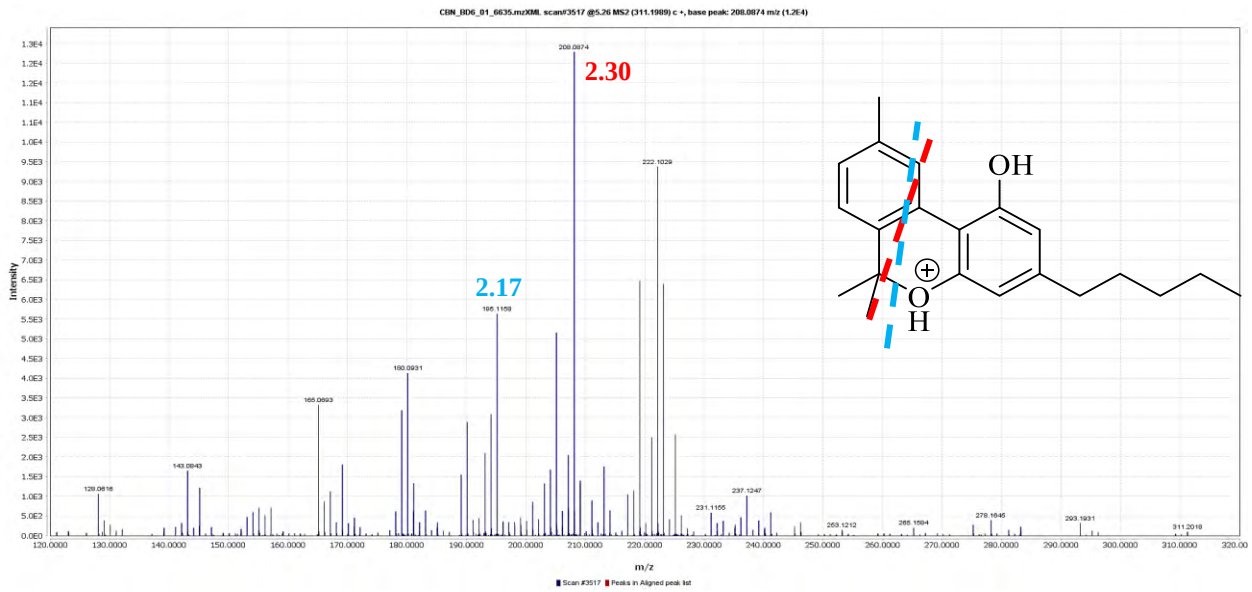

Figure 2.15: MS2 spectrum of CBN $[M+H]^+$ precursor ion *m/z* 311.1988 obtained by LC-MS/MS at 40 eV.

The CBN structure being an oxidative degradation product of THC and a tricyclic structure the *m/z* 311 precursor ion did not dissociate completely at 40eV. Observed in the MS2 spectrum, are fragment ions of intensities of *m/z* 128.0616, 180.0931, 208.0874 and 222,1029 that have higher intensities compared to the fragment ions of *m/z* 129.0714, 181.1001, 209.0945 and 223.1111. Although this is the case then for the former *m/z* values their fragment structures were not predicted, the latter were predicted. This reduced the complexity in the fragment structure identification. This confirmed the reports that the fragment structures with lower intensities are a product of remote hydrogen rearrangement and energetically favoured (27). These are the *m/z* values of fragment structures we were able to be predicted (Scheme 2.5).

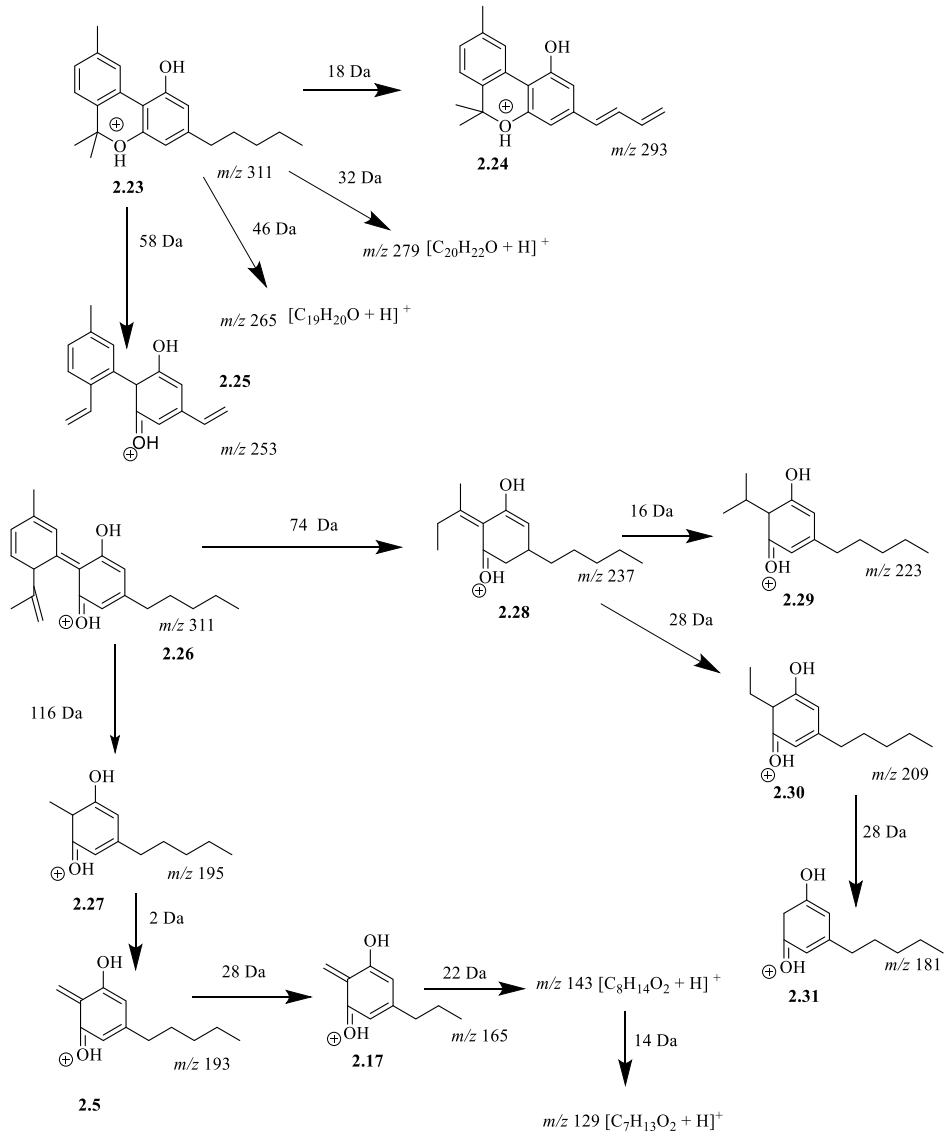

Scheme 2.5: Proposed fragment structures pathways of CBN precursor ion $[M + H]^+$ *m/z* 311.1988

The fragment ions prediction pathway represent in scheme 2.5, shows the transitions of *m/z* 311→129. The transition *m/z* 311 → 293 from the precursor ion *m/z* 311 $[C_{21}H_{26}O_2 + H]^+$ (structure **2.23**) by the neutral loss of 18 Da (H_2O), by hydrogen rearrangement resulting in the fragment ion *m/z* 293 $[C_{21}H_{24}O + H]^+$ (structure **2.24**). The transitions *m/z* 311 → 279, *m/z* 311 → 265, *m/z* 311 → 253 were predicted to occur by the neutral losses of 32 Da (CH_3OH), 46 Da (C_2H_5OH), and 58 Da (C_3H_5OH) these neutral losses lead to the fragment ions *m/z* 279 $[C_{20}H_{22}O + H]^+$ ionised structure. *m/z* 265 $[C_{19}H_{20}O + H]^+$ion and *m/z* 253 $[C_{18}H_{20}O + H]^+$ (structure **2.25**) respectively. Transition *m/z* 311 → 237 from the *m/z* 311 $[C_{21}H_{26}O_2 + H]^+$ (structure **2.26**)

precursor ion with the neutral loss of 74 Da (C_5H_{12}, H_2) resulting in the fragment ion *m/z* 237 $[C_{15}H_{24}O_2 + H]^+$ (structure **2.28**), this fragment ion *m/z* 237 was useful in the structure prediction of the fragments *m/z* 223 and *m/z* 209. The transitions *m/z* 237 → 223 and *m/z* 237 → 209 by the neutral losses 16 Da (CH_4) and 28 Da (C_2H_4) respectively, resulting the fragment ions *m/z* 223 $[C_{14}H_{23}O_2 + H]^+$ (structure **2.31**) and *m/z* 209 $[C_{13}H_{21}O_2 + H]^+$ (structure **2.32**). In the MS2 spectrum (Figure **2.15**), the detected ions *m/z* 209 and *m/z* 223 have a lower intensity than *m/z* 208 and *m/z* 222, we proposed structures for the former of *m/z* 223 (structure **2.31)** and *m/z* 209 (structure **2.32**)

The fragment ion *m/z* 181 $[C_{11}H_{17}O_2 + H]^+$ (structure **2.31**) proposed from the fragment ion *m/z* 209 (structure **2.30)**, with the neutral loss of 28 Da (C_2H_4) by cleavage and hydrogen rearrangement. The transition *m/z* 311 → 195 in our predictions is characterised by the neutral loss of 116 Da (C_8H_{20}) from the precursor ion *m/z* 311 $[C_{21}H_{26}O_2 + H]^+$ (structure **2.26** resulting in the fragment ion *m/z* 195 $[C_{12}H_{19}O_2 + H]^+$ (structure **2.27**), from this fragment ion the neutral loss of 2 Da (H_2) resulting in the fragment ion *m/z* 193 $[C_{12}H_{17}O_2 + H]^+$ (structure **2.5**) by hydrogen rearrangement. The transition *m/z* 193 → 165 by the neutral loss of 28 Da (C_2H_4) resulting in the fragment ion *m/z* 165 $[C_{10}H_{12}O_2 + H]^+$, (structure **2.17**). The transition of *m/z* 165 → 143 neutral loss of 22 Da (CH_4 ,$2H_2$) by hydrogen rearrangement resulting in the ion *m/z* 143 $[C_8H_{14}O_2 + H]^{+\cdot}$ and the transition of *m/z* 143 → 129 with the neutral loss of 14 Da (CH_2) in the ion *m/z* 129 $[C_7H_{13}O_2 + H]^+$.

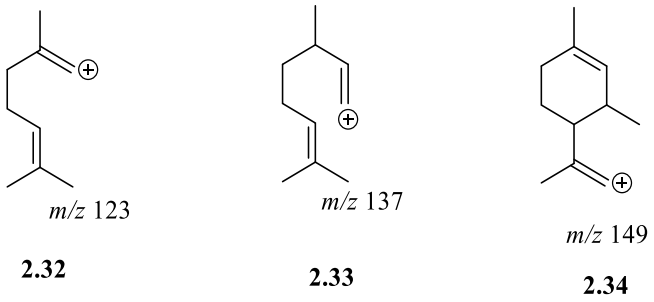

2.32 **2.33** **2.34**

Scheme 2.6: Alternative proposed fragment ion structures for *m/z* 123 and *m/z* 137

Fragment structures for the *m*/*z* values 123, 137 and 149 have been proposed in the schemes above relative to the MS2 spectra they appear in (see structures **2.7, 2.8** and **2.18**). Interest in proposed alternative fragment ion structures for these specific ions is due to the abundance of terpenes and terpenoids that have molecular weights of approximately 122 g/mol, 136 g/mol and 148 g/mol that could ionize to give ions *m*/*z* 123, *m*/*z* 137 and *m*/*z* 149 respectively. So far, the fragment ion structures predicted above (scheme 2.1 to 2.5) are mostly terpenoids, because of the oxygens in their structures while in scheme 2.6 we observe terpenes, they have no oxygens in their structures.

Fragmentation of structures could be likened to the degradation of compounds; hence it is important to consider the resulting fragments of alternative compounds (27). The elimination of small neutral molecules from precursors are preferred when fragment pathways are proposed. In this case, we took into consideration the possibility of the small molecules being ionized upon loss from the structure (9).

The neutral loss of 122 Da has been previously reported, as a small molecule loss in soft ionization fragmentation, there is a possibility that these fragment ion structures may represent the *m*/*z* 123 upon ionization. Generally, terpenes are small structures an example that inspired this is limonene with a molecular weight of approximately 136 g/mol, this structure has no oxygen but there is a possibility that these cannabinoid compounds like CBD may degrade breaking into the limonene or isomers of the limonene structure (11). Limonene has therapeutic effects and cannabinoids have been reported to have synergistic effects that assist in the therapeutic results observed with cannabinoids and other compounds in plants (11). The purpose of fragment structure predictions in this work to find scaffold for the creations of a fragment library (Chapter 3).

This is a fragment drug design approach whereupon synthesis the drugs would likely be detectable with the same LC-MS methods. The volatility of terpenes means they are difficult to detect meaning the design or synthesis of cannabinoid fragments that can mimic terpenes and terpenoids is essential. The design of these fragment drugs will be in line with keeping the same therapeutic properties of cannabinoids.

2.4 Conclusion

The LC-MS was used to successfully develop methods for qualitative analysis of cannabis products. Analysis of cannabis standards THC, CBD, CBDV, CBG, and CBN was completed with other cannabinoids detected cannabis samples followed by the detection of terpenes and terpenoids. However, a flaw of our method was the precursor ion mass accuracies being higher than the desired goal of being at least lower than 10 ppm. The effects of the mobile phase on precursor ions of the cannabinoid standards were explored. After observing that a higher intensity of the precursor ions resulted from the use of 80% methanol in 20% water (with 1% formic acid), it was applied in the final method with high-performance computing, giving us mass accuracies lower than 10 ppm. This mass accuracy was reasonable enough to continue with fragment structure predictions. Structures for some ions detected in the MS/MS were predicted, following suggestions of possible ESI fragmentation pathways available in the literature.

2.5 References

1. Urban J., Afseth N.K. and Štys D. Fundamental definitions and confusions in mass spectrometry about mass assignment, centroiding, and resolution. TrAC - Trends Anal Chem. 2014;53:126–36.

2. Parasuraman S.R.A, Balamurugan S, Muralidharan S, Kumar KJ and Vijayan V. An Overview of Liquid Chromatography-Mass Spectroscopy Instrumentation. *Pharm Methods*. 2014;5(2):47–55.

3. Crawford Scientific. Mass Spectrometry Fundamental LC-MS Introduction. 2004;1–24. Available from: www.chromacademy.com

4. Siuzdak G. An introduction to mass spectrometry ionization: An excerpt from The Expanding Role of Mass Spectrometry in Biotechnology, 2nd ed.; MCC Press: San Diego, 2005. *J Assoc Lab Autom*. 2004;9(2):50–63.

5. Sleno L, Volmer D.A. Ion activation methods for tandem mass spectrometry. *J Mass Spectrom.* 2004;39(10):1091–112.

6. Stevenson D.P. Modern Mass Spectrometry. *J Am Chem Soc*. 2005;76(2):636–636.

7. Karni M and Mandelbaum A. The 'Even-Electron Rule.' *Organic mass spectrometry* 1980;15(2):53–64.

8. Liigand P, Kaupmees K, Haav K, Liigand J, Leito I, Girod M, Antoine R, and Kruve A. Think Negative: Finding the Best Electrospray Ionization/MS Mode for Your *Analyte. Anal Chem*. 2017;89(11):5665–8.

9. dos Santos N.A, Tose L.V, Murgu M., Kuster R.M, Ortiz R.S, Camargo F.A.O and Vaz B.G. Analysis of Isomeric Cannabinoid Standards and Cannabis Products by UPLC-ESI-TWIM-MS: a Comparison with GC-MS and GC × GC-QMS. *J. Braz. Chem. Soc 2*019;30(1):60–70. complete title

10. Citti C, Linciano P, Panseri S, Vezzalini F, Forni F, Vandelli M.A, Cannazza Guiseppe.

Cannabinoid profiling of hemp seed oil by liquid chromatography coupled to high-resolution mass spectrometry. *Front Plant Sci.* 2019;10 (2):1–17.

11. Russo EB. Taming THC: Potential cannabis synergy and phytocannabinoid-terpenoid entourage effects. *Br J Pharmacol*. 2011;163(7):1344–64.

12. Alechaga É, Moyano E, and Galceran MT. Ion-molecule adduct formation in tandem mass spectrometry. *Anal Bioanal Chem*. 2016;408(4):1269–77.

13. Pavlovic R, Nenna G, Calvi L, Panseri S, Borgonovo G, Giupponi L, Cannazza G and Annamaria G. Quality traits of "cannabidiol oils": Cannabinoids content, terpene fingerprint and oxidation stability of European commercially available preparations. *Molecules.* 2018;23(5).

14. Rogerson D. Vegan diets: practical advice for athletes and exercisers. *J Int Soc Sports Nutr*. 2017;14(1):1–15.

15. Citti C, Battisti UM, Braghiroli D, Ciccarella G, Schmid M, Vandelli MA, and Cannazza G. A Metabolomic Approach Applied to a Liquid Chromatography Coupled to High-Resolution Tandem Mass Spectrometry Method (HPLC-ESI-HRMS/MS): Towards the Comprehensive Evaluation of the Chemical Composition of Cannabis Medicinal Extracts. *Phytochem Anal.* 2018;29(2):144–55.

16. Brenneisen R. Chemistry and Analysis of Phytocannabinoids and Other Cannabis Constituents. *Marijuana and the Cannabinoids.* 2007; (7):17–49. journal

17. Yermakov AI, Khlaifat AL. Characteristics Of The GC-MS Mass Spectra Of Terpenoids (C10H16). *Chem Sci J*. 2010;1(1):1–10.

18. Bergman ME, Davis B, and Phillips MA. Medically useful plant terpenoids: Biosynthesis, occurrence, and mechanism of action. *Molecules*. 2019;24(21):1–23.

19. Zwenger S and Basu C. Plant terpenoids: applications and future potentials. *Biotechnol. Mol. Biol. Rev.* 2008;3(2):1–7.

20. Shapira A, Berman P, Futoran K, Guberman O and Meiri D. Tandem Mass Spectrometric Quantification of 93 Terpenoids in Cannabis Using Static Headspace Injections. *Anal Chem.* 2019;91(17):11425–32.

21. Brenton AG and Godfrey AR. Accurate mass measurement: Terminology and treatment of data. *J Am Soc Mass Spectrom*. 2010;21(11):1821–35.

22. Patiny L and Borel A. ChemCalc: A building block for tomorrow's chemical infrastructure. *J Chem Inf Model*. 2013;53(5):1223–8.

23. Sargent M. Guide to achieving reliable quantitative LC-MS measurements. *RSC Analytical Methods Committee*. 2013.1–61.

24. Niessen WMA, Falck D. Introduction to Mass Spectrometry, a Tutorial. *Anal Biomol Interact by Mass Spectrom*. 2013;(1):1–54.

25. Ho, CS; Lam, CWS; Chan, MHM; Cheung, RCK; Law, LK; Lit, LCW; Ng, KF; and Suen M. Mechanism of electrospray ionisation. *Clin Biochem Rev*. 2003;24(2):3–12.

26. Steckel A and Schlosser G. An Organic Chemist's Guide to Electrospray Mass Spectrometric Structure Elucidation. *Molecules*. 2019;24(3):611.

27. Demarque DP, Crotti AEM, Vessecchi R, Lopes JLC, and Lopes NP. Fragmentation reactions using electrospray ionization mass spectrometry: An important tool for the structural elucidation and characterization of synthetic and natural products. *Nat Prod Rep*. 2016;33(3):432–55.

28. Eckel-Passow JE, Oberg AL, Therneau TM, and Bergen HR. An insight into high-resolution mass-spectrometry data. *Biostatistics*. 2009;10 (3): 481–500.

Chapter 3
Homology modelling and docking

3.1 Introduction

The activity of compounds like drugs and natural products versus the activity of fragments derived from these compounds are different but worthy of exploration. This is partly because fragments can be used in drug discovery and in biochemical tools to understand the disease. Fragments are, by their nature, smaller than their bioactive full molecule, and hence generally easier to synthesize and study (1). An understanding, therefore, of the relationship between hypothetical fragments and the intact compound would be very useful in guiding the design of a synthetic fragment library. In the previous chapter, we discussed fragment structure prediction from cannabinoids THC, CBD, CBDV, CBG and CBN using the LC-MS. This chapter will explore the differences in the binding energies of this group of compounds and their proposed fragment structures (2). The steps in the fragment structure prediction have been discussed in Chapter 2, but it's worthwhile highlighting the fact that these predicted structures may not be synthetically accessible or stable. The value here is to understand the relationship between structural features of fragments and the cannabinoid ligands from which they are derived.

This work has been inspired by fragment-based drug design (FBDD) approaches; because these fragments could encourage the design of synthetic fragment compound libraries (3). Fragment compounds are compounds low in molecular weight and chemical complexity, and an ideal fragment is one that binds in the active site of a target with high affinity. Fragments must have a molecular weight less than 300, logP < 3 and H-bond donors/acceptors <=3, they adhere to the "Rule-of-Three" derived from the Lipinski rule of five (3) (1).

Fragments are meant to be simpler, so they have fewer pharmacophore features even when derived from a pharmacophore, smaller fragments with functional groups from the pharmacophore can be

designed and linked rather than create a chemically complex compound with desirable activity (1). Characterization of fragment compounds after synthesis is the same as that of other organic synthetic compounds. The best way to gain insight on compound structures is by analysing them using different methods be it experimental or *in silico*, we chose the latter due to accessibility, the proposed fragment structures are not energetically favourable and may be difficult if not impossible to synthesize using standard methods (4). *In silico* methods require the usage of the software that is verified for research, we constructed a CB2 homology model and did docking studies. I-TASSER (Iterative Threading ASSEmbly Refinement) was our bioinformatics tool of choice for the construction of our model, which is an online server that implements iterative threading assembly refinement on amino acid sequences producing high-quality model predictions (4). A well-known purpose for homology modelling is to grow the protein data bank (PDB) leading to easy access for researchers, therefore improving drug discovery (5). Although this growth is noted there is a gap between known structures and known protein sequences, therefore some structures are not always readily available in databases. The problem can be bridged by *in silico* prediction of protein structures hence the prediction of our protein structure for the human cannabinoid receptor 2 (CB2). The main receptors used here were the human cannabinoid receptor 1 and 2 (Figure 3.1).

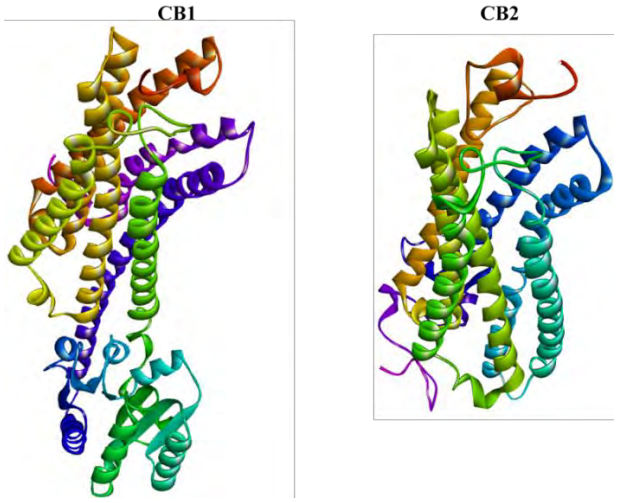

Figure 3.1: CB1 (5U09, from PDB) and CB2 (I-TASSER model) human receptor models.

We determined coordinates of the active site to give us the best binding energies on the CB2 (see section 3.3), for this, we used Maestro 11.2 software, CASTp 3.0 server and the suggested coordinates that came from I-TASSER. Caution is required when using these methods to obtain results that are almost as accurate as protein structures obtained by high-resolution studies (4). Computed atlas of surface topography of proteins (CASTp) is an online service that is used to locate the position of the active site three-dimensional proteins models (6). Maestro is a tool from the Schrödinger software package was also used in the determination of the active site, although it can be used for more, such as docking and visualization (7). The software of choice for docking studies was Autodock 1.5.6, this software is one of the most effective protein-ligand docking software (8) (4). An example of this success is a small protein α-lactalbumin in 1969, modelled using a structure of an egg-white lysozyme as a template (5). The structure of α-lactalbumin was then solved by X-ray crystallography, which then proved the model correct, despite this homology modelling is well established as an alternative or complement to structural biology (5).

The objective of this chapter is to develop molecular docking of THC, CBD, CBDV, CBG and CBN on the CB1 and CB2 human receptors to obtain information about their proposed (or suspected) active site interaction. Information about these ligand/protein interactions could lead to the design of better drugs and cannabinoid derivatives. In this work we did not explore the interactions of the fragment structures in detail since many of these fragments would not be synthetically accessible, but rather our main interest was the binding energies of the fragments to gauge whether the fragments are worth further exploration, and to better understand which structural features could be useful for fragment design.

3.2 Materials and method

Homology modelling

Retrieval and analysis target sequence: The cannabinoid receptor 2 (Homo *Sapiens*) sequence was retrieved from the UniProt (https://www.uniprot.org/uniprot/P34972). The sequence has 360 amino acids. The protein sequence was analyzed on BLAST, the same sequence was available on the NCBI database (https://www.ncbi.nlm.nih.gov/protein/NP_001832.1) with NCBI reference: NP _001832.1. CB2 protein structure refinement and homology modelling were performed with I-TASSER, an online tool. Using the Chrome browser we accessed the URL (http://zhanglab.ccmb.med.umich.edu/I-TASSER/), where we copied and pasted the sequence of human cannabinoid receptor 2 adapted from UniProt into the input box. The sequence was submitted then upon completion, the job results were received by email the following day. The results on I-TASSER were given the job id S409797.

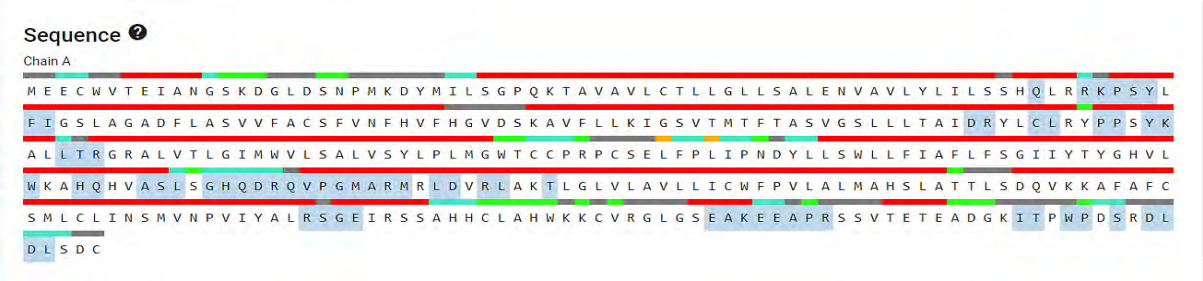

Figure 3.2: The CB2 receptor model sequence adapted from UniProt.

Determining the active site of the CB2 homology model: The active site of the homology model was predicted using I-TASSER. Protein binding site prediction using the cofactor algorithm using 5 proteins, the 5dhhB protein coordinates were used to activate site coordinates for the predicted CB2 homology model. We determined active site coordinates on Maestro11.2 software by putting the model through protein preparation, which involved pre-processing, optimization, removal of water and minimization. We then used Sitemap to determine the active site coordinates by selecting the dots in the map, upon selecting 3 of the dots we got the same coordinates to represent the active site coordinates for docking. CASTp 3.0: Active site determination by CASTp 3.0 was done by uploading the model produced by I-TASSER in the CASTp online server, (http://sts.bioe.uic.edu/castp/index.html?j_5ba0d77abf98b).

The summarized results containing details of the active site were emailed in a zip file. The files were ranked according to best to worst, we chose the best-proposed coordinates, according to their ranking.

Docking

All docking experiments were conducted with the AutoDock 1.5.6 using the Lamarckian Genetic Algorithm (LGA), to explore the human cannabinoid receptor 1 and 2 with cannabinoid compounds and predicted fragment structures. Although, as mentioned, above some coordinates were found using Maestro and CastP, no docking was performed using Maestro. The choice of LGA is informed by its ability to handle ligands with many degrees of freedom, making it reliable and efficient (9).The docking area selected for grid box construction size 40 × 40 × 40 points, centred at x, y and z coordinated of the CB1 and CB2 proteins. The coordinates used in docking in the CB1 protein were x: 21.500, y: 3.590 and z: -9.800 centred. Grid spacing (0.375 Å). As mentioned, we developed a homology model for CB2, the docking coordinated used were obtained from I-TASSER, Maestro, and CASTp. The coordinates from the I-TASSER results x: 6.540, y: 71,138 and 60.839. The active site coordinates found by using sitemap Maestro were x: 68.390, y: 71.870 and 57.420. CASTp, the position of the active site and the coordinates used x: 70,164, y: 70.619 and 88.157. The active site of the CB1 protein 5U09 was used as per the information is given in the publication coordinates used were Coordinates (x: 21.500 y: 3.590 z: -9.800). The docking parameters used for the LGA-based conformational searches are docking trials 150; population size 150; the maximum number of energy evaluations 25,000,000; the maximum number of top individuals to survive to next-generation 1; the rate of gene mutation 0.02; the rate of crossover 0.8; mean of Cauchy distribution for gene mutation 0.0; variance of Cauchy distribution for gene mutation 1.0 and number of generations for picking the worst individual 10. Our CB1 receptor for docking was adapted from PDB, the protein 5U09 was complex to ligand taranabant (Figure 3.5), upon removal of this ligand from the active site we proceeded to dock (10).

3.3 Results and discussion

Residues involved in interacting with ligands are being researched with multiple suggestions being made without certainty. Similarities between CB1 and CB2 receptors have been reported to be more than 48% in sequence and 68% within their transmembrane regions (10). We determined the coordinates for docking for the CB1 and CB2 models we used, the results for the CB2 model are summarised in Figure 3.3 and Figure 3.4 with a visual representation of the active site. Molecular docking was done to determine the binding energy values obtained when docking cannabinoids THC, CBD, CBDV, CBG and CBN on the CB1 and CB2 receptors (see Table 3.1 and Table 3.2). Fragment structures proposed in chapter 2, were docked to determine their resulting binding energies. The results of this docking are summarized in Table 3.3 to and are discussed to determine if they could be used as leads in FBDD of libraries. Molecular docking calculations yielded negative binding energy values indicating the docking systems are stable.

3.4 Human cannabinoid receptor 2 homology modelling.

The absence of a 3D structure CB2 homology model in the Protein Data Bank leads to our modelling of the CB2 protein with I-TASSER, giving the result of the 5 models ranked by C-scores, which is the confidence score given to a model. The best model being the first model, with a higher c-score of 0.02. (see Figure 3.3). The first model resembles the CB1 known crystal structure quite closely, which is another reason for our confidence in this model.

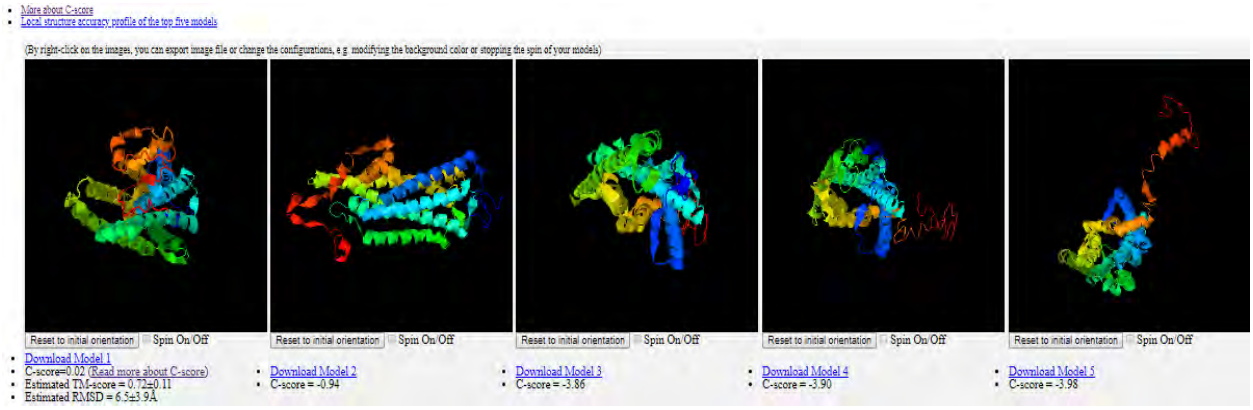

Figure 3.3: CB2 homology model predicted structures obtained from I-TASSER.

The confidence score of the model is reported as the C-score. Amongst the 5 models, model 1 has a C-score that falls within the (-5,2) with a c-score of 0.2, while the other predicted options have significantly smaller C-scores. The C-Score is based on the comparison between the 5dhhB protein and the binding site for the model in a similar region. Upon the development of the model, I-TASSER gives results along with the model of the possible binding site of the receptor.

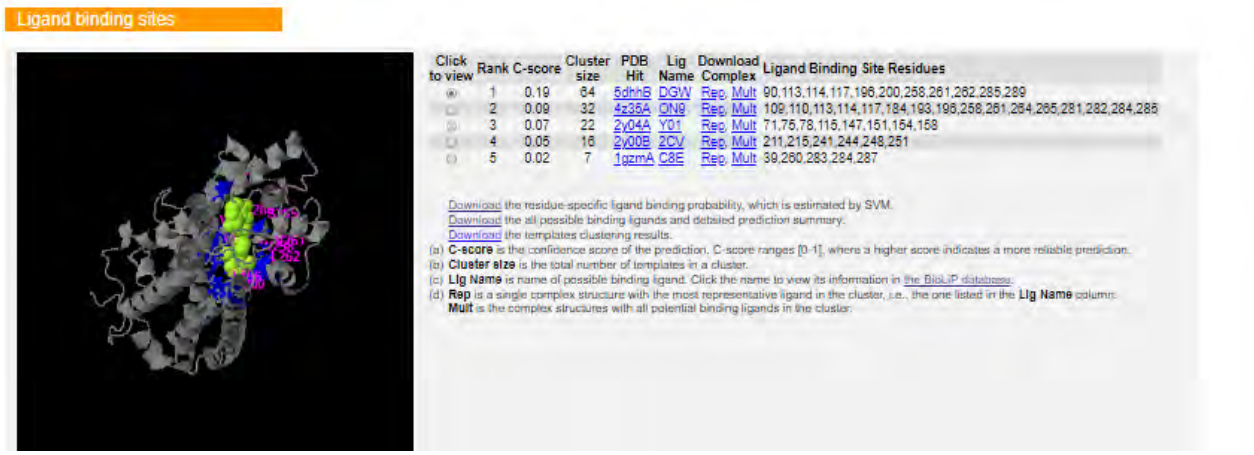

Figure 3.4: Ligand binding site predictions by I-TASSER.

The results in Figure 3.4 represent the ligand-binding site of CB2, with the binding sites ranked by C-scores, and the highest being 0.19 from the protein 5dhhB. The calculations by I-TASSER are an estimation (11). We supplemented the active site estimation of the I-TASSER active site prediction with the Maestro and CASTp 3.0. The different coordinates found using these reliable tools, were used to dock THC, CBD, CBDV, CBG, and CBN on the CB2 model, yielding varying binding energies (Table 3.2). Best lowest binding energies based on the coordinates of the active site means a more stable docking environment was achieved (12). This is an option to choose the best lowest binding energies for further docking experiments. The visual representation of the position of the active site as a result of the tools used to determine active site coordinates (Figure 3.5).

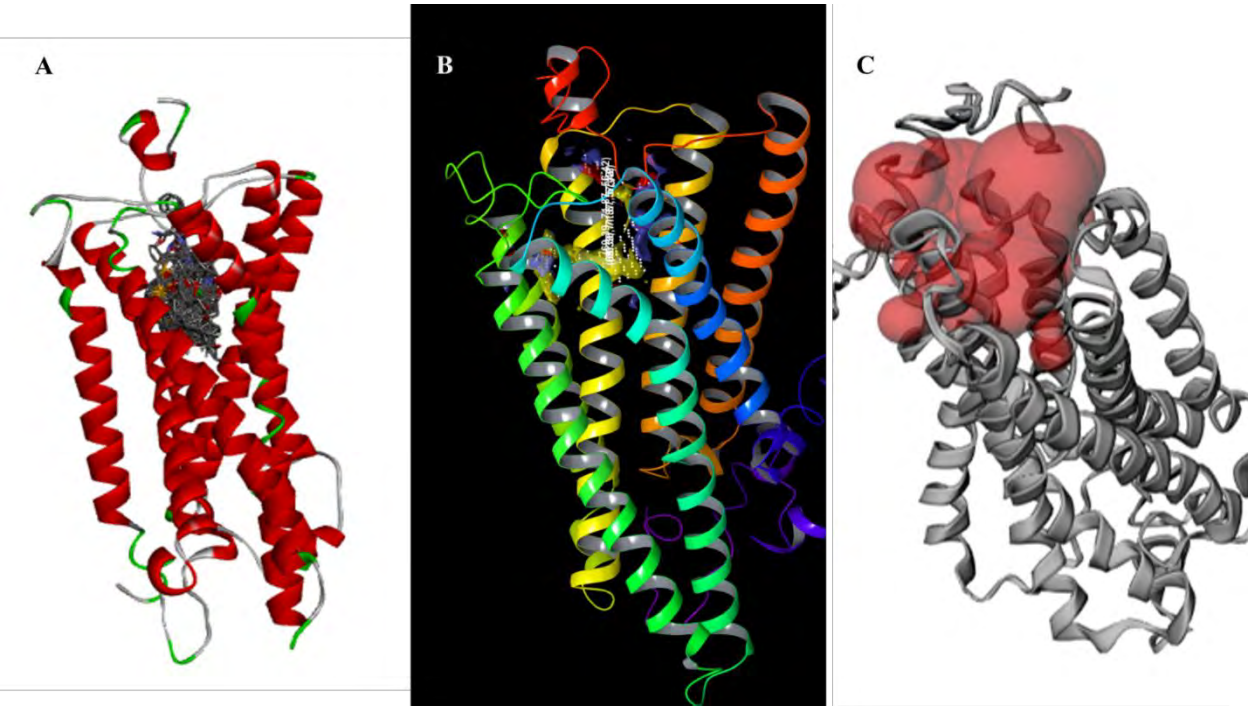

Figure 3.5: A visual representation of the active site position in the CB2 protein model, A: I-TASSER; B; Maestro; C: CASTp 3.0.

In the above figure, we observe the similarity in the position of placement of the active sites. The potential binding pocket of CB2 in A: I-TASSER is represented by the grey cluster of ligandlike structures, B: Maestro 11.2, the binding site is represented by a sitemap with the small white dots and finally, C: CASTp coordinates are represented by the red bubble.

3.5 Molecular docking

Docking the phytocannabinoids THC, CBD, CBDV, CBG, and CBN, and fragment structures gave binding energy results summarized in Table 3.1 and Table 3.2. The resulting binding energies are all more negative (stronger binding) than the minimum -5 kcal/mol requirement (13).

Table 3. 1:Binding energies obtained by docking CB1 with cannabinoids using Autodock 1.5.6

Compound	Protein	Binding Energy kcal/mol
CBD	CB1	-8.56
CBDV	CB1	-9.01
CBN	CB1	-9.23
CBG	CB1	-8.32
THC	CB1	-9.97

The binding energy for CBG (Table 3.1) is -8.32 kcal/mol, which is the lowest binding energy of the 5 cannabinoids, followed by CBD and CBDV, having binding energies of -8.56 kcal/mol and -9.01 kcal/mol, respectively. The structural difference between CBD and CBDV lies in the alkyl chain, this is an interesting observation that could lead to further investigation. The tricyclic cannabinoid compounds CBN and THC have relatively higher binding energies of -9.23 kcal/mol and -9.97 kcal/mol respectively.

Table 3. 2**:** Binding energies obtained by docking CB2 with cannabinoids using Autodock 1.5.6.

Compound	Protein	I -TASSER Binding Energy kcal/mol	Maestro Binding Energy kcal/mol	CASTp Binding Energy kcal/mol
CBD	CB2	-5.39	-7.54	-7.31
CBDV	CB2	-6.51	-7.46	-6.78
CBN	CB2	-6.82	-6.56	-7.01
CBG	CB2	-6.85	-7.22	-6.88
THC	CB2	-7.35	-7.77	-7.74

Table 3.2 summarizes the docking completed to find the most appropriate active site of the CB2 homology model we modelled with I-TASSER. As mentioned in Figure 3.5, the position of the active sites appears to be in the same part of the protein, hence the need for comparison that gives a clear distinction between achievable binding energies with the coordinates of each active site. The binding energies do show some strong correlation differing only in the last decimal points for some binding energies. and while there is a similarity, we found that CASTp 3.0 binding energies were more favourable in that they were giving the best lowest binding energies, CASTp 3.0 is specially designed for the determination of the active site of the specific modelled protein structure without having to estimate using other modelled structures (8). An interesting observation made was the consistency of THC in having the highest lowest binding energy in comparison to the other cannabinoids, in all the coordinates predicted for the CB2 homology model, this shows that all these results are valid.

3.6 Binding energies of predicted fragment structures

Proposed fragments from the MS fragmentation experiments were docked into the CB1 and CB2 proteins, to determine their binding energies in comparison to the phytocannabinoids compounds. We have used neutral versions of the predicted ionized fragment structures, to determine the binding energies. The fragment structures docked in Table 3.3, ranging from a molecular weight of 122 g/mol to 259 g/mol which is less than the 300 g/mol typically used as a cut-off range to be considered a “fragment” rather than a small molecule, although this distinction is somewhat arbitrary (4). The binding energies of fragment structures can be affected by how they fit into the binding pockets (1).

In Table 3.3 a general observation was most of the fragment structures docked in the CB1 human receptor were higher than those docked in the CB2 human receptor. A higher binding affinity of the cannabinoid compound to the CB1 human receptor would be favourable for therapeutic applications, due to the reported abundance of the CB1 receptor over the CB2 human receptor in the body (14).

Table 3.3: Binding energies for some proposed fragment structures docked on the cannabinoid receptors (software AutoDock 1.5.6).

Fragment Structure	Fragment *m/z*	CB1 Receptor kcal/mol	CB2 Receptor kcal/mol
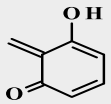	123	-5.12	-4.63
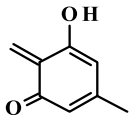	137	-5.45	-4.96
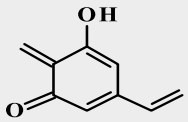	149	-5.91	-5.29
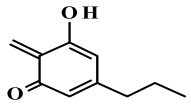	165	-6.77	-6.29
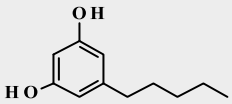	181	-5.95	-5.94
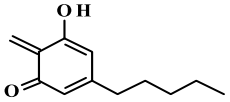	193	-6.62	-5.99
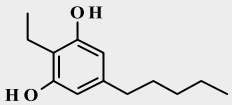	209	-7.31	-6.59
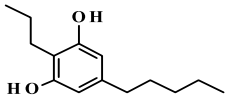	223	-7.71	-6.56
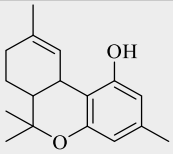	259	-9.62	-6.26

A neutral structure of the *m*/*z* 123 fragment ion in chapter 2 has a binding affinity of -5.12 kcal/mol CB1 human receptor and -4.63 kcal/mol in the CB2 human receptor. The size of structure 3.1 leaves room for further development to make it a better lead fragment. In comparison, the neutral structure of *m/z* 259 fragment has a binding affinity of -9.62 kcal/mol CB1 human receptor and -6.26 kcal/mol in the CB2 human receptor. This fragment was proposed to be as a result of the loss 56 Da (C_5H_{11}) this loss has not made a large difference in the binding energy in comparison to cannabinoid THC with a binding energy of -9.97 kcal/mol in the CB1 human receptor and -7.74 kcal/mol in the CB2 human receptor. On the one hand, this is not unusual, because it has much of the THC structure in place, including the "aromatic" moiety, the terpene moiety, and the intact ring joining these two (15). There is data showing that importance of the side chain in and how it is good binding – this leads on to the discussion about the importance of the side chain.

Although the binding energies of THC with the pentyl chain present are higher, the binding energies of the fragment structures still fall within a reasonable range (and all still a negative value). The pentyl chain has been reported to have significant in pharmacophores cannabinoids in general (7). The observation made from the binding energy structure might be enough to get the therapeutic benefits of THC. We observed that the large the compound structure the higher binding energies, this may be due to the binding pocket being slightly more filled leading to more interaction. Modifying the alkyl side chain in THC with aromatic structures has shown improved binding energies, may most likely make cannabinoids more potent improving the chances for chemists to produce more cannabinoids receptor-selective ligands (8). The fragment structures could be possible compound leads in the creation of fragment libraries to aid in the treatment of various diseases that cannabinoids been shown to treat. Beyond binding energies, ligand interactions with receptors are important to understand.

3.7 Active site and ligand interactions

According to Shao Z *et al* (2016), the CB1 receptor showed a conserved membrane-proximal N-terminal region, which is different from other lipid-activated GCPRs, and this is important for the binding pocket (10). To confirm this, the taranabant ligand and the THC ligand (as representatives of a successful synthetic ligand, and the phytocannabinoids, respectively), were docked into the binding pocket (10). We then also docked the CBN, CBD, CBDV and CBG ligands since they are also major cannabinoids detectable in most cannabis plant extracts. The interactions we observed in the CB1 binding pocket by docking the THC ligand were affected by the preferred docking pose.

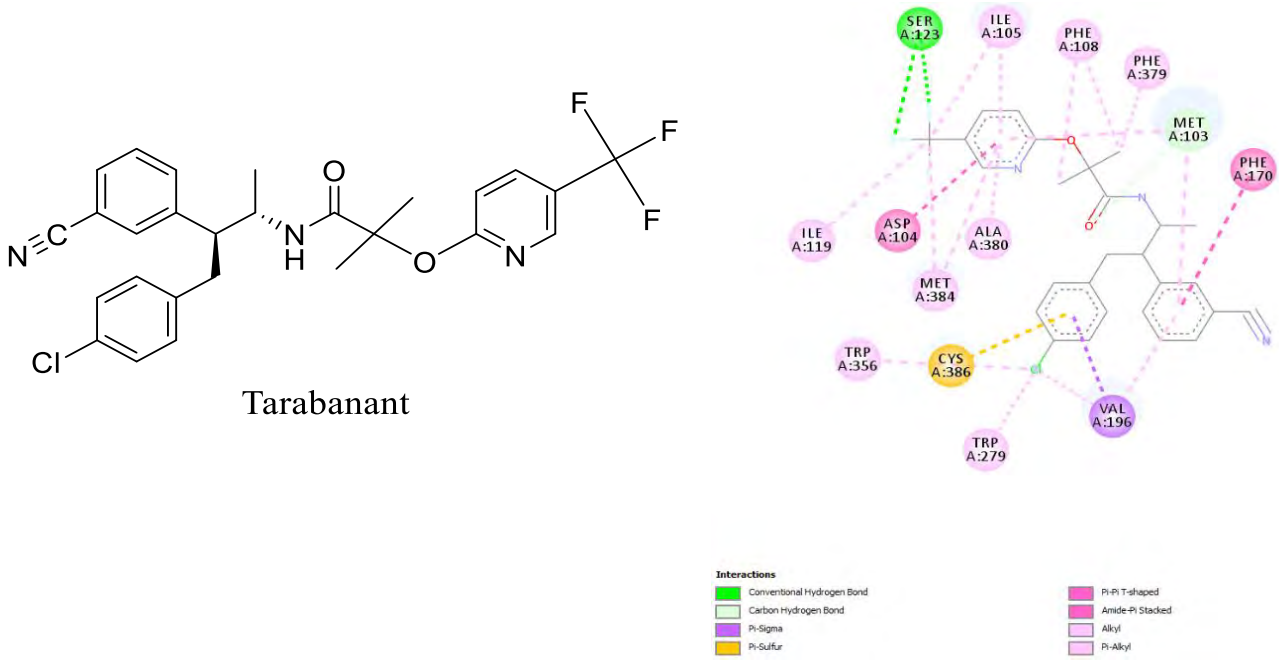

Figure 3. 6: Amino acids of the active site of the ligand in 5U09.

The interactions we observed in the pocket for THC were as expected, residues in proximity or contact with the THC at its preferred docking pose (10). Although a caveat has been put forward relating to using an inactive structure of CB1 predicting high-affinity agonist interactions, we are confident that the binding affinities still show reasonable affinity that propels, the understanding of cannabinoid receptor interactions going forward. The suggested significant residues Leu[193] and

Ser^{383} are observed in our interactions map (see Figure 3.7E). Although the residues are in proximity and not in contact with the THC ligand, we hoped to find the other cannabinoid ligands interacting with these ligands. The chemical structure of taranabant (Figure 3.6), is a structure acknowledged for being an inverse agonist for the treatment of obesity by appetite suppression. This compound reached clinical trials (phase III), it was discontinued in 2008 due to its side effects (16).

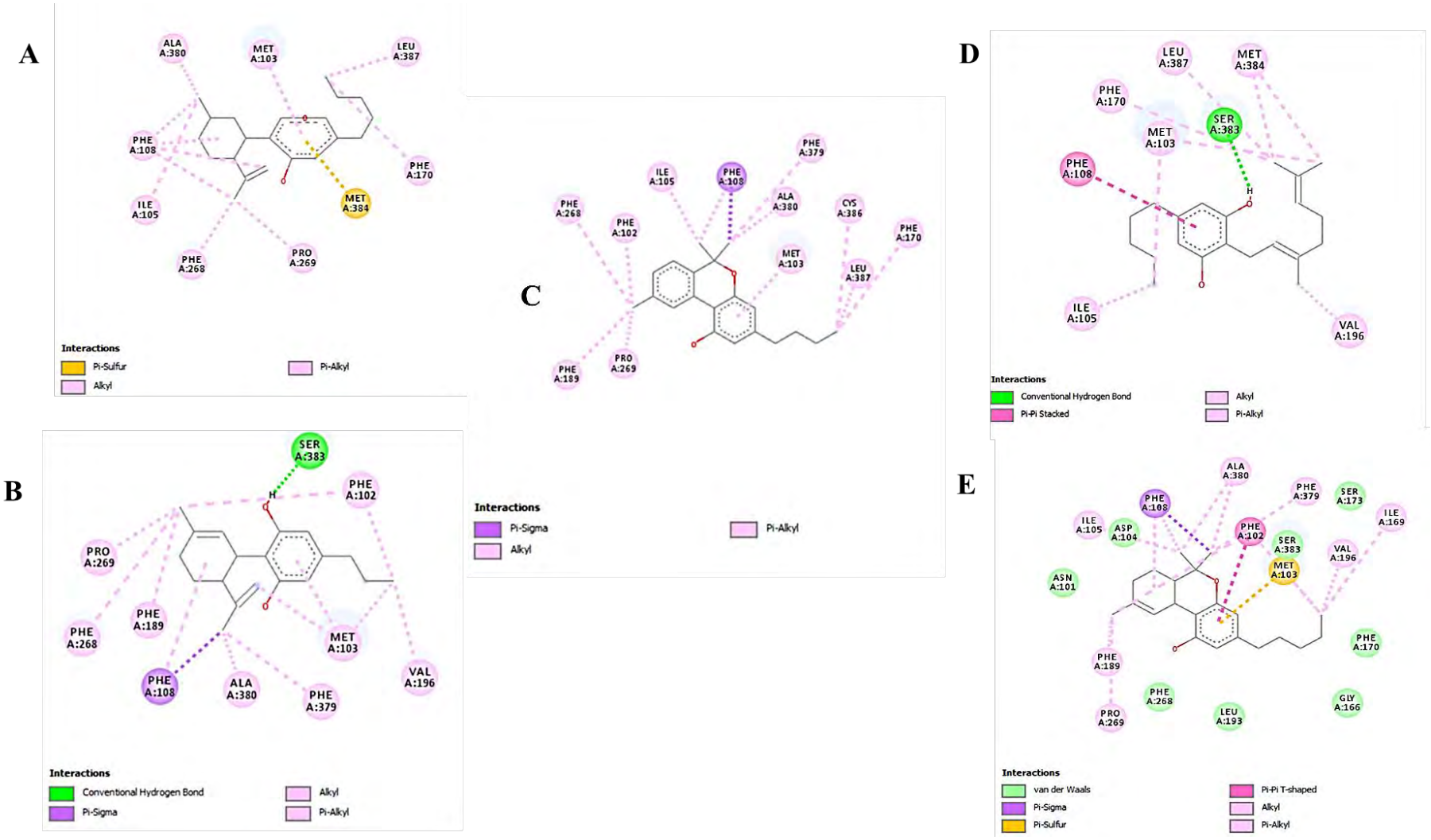

Figure 3.7: Amino acids of the active site of the CB1 human receptor PDB(5U09), A: CBD, B: CBDV, C: CBN, D: CBG, and E: THC.

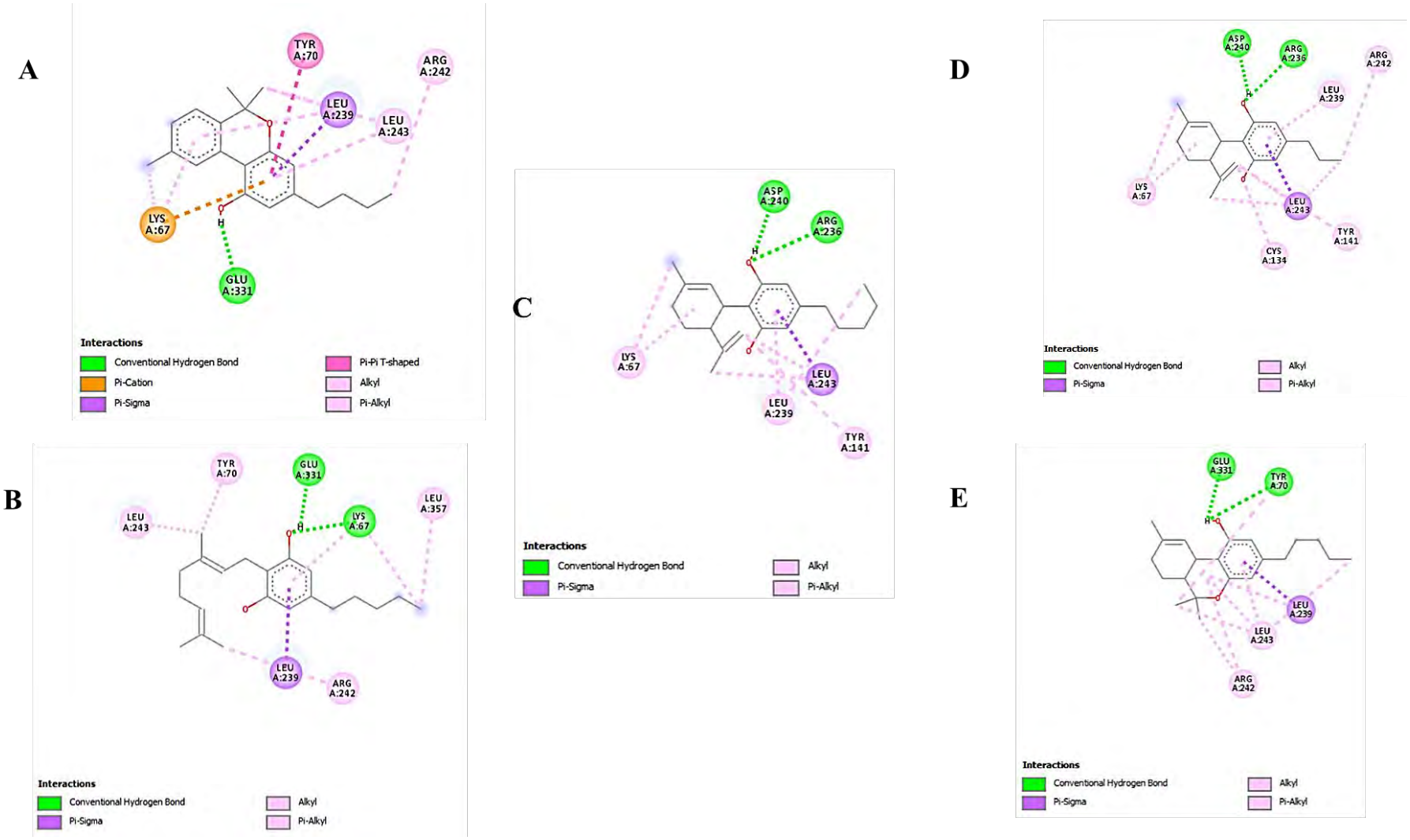

Figure 3.8: Amino acids of the active site of the CB2 human receptor, A: CBN, B: CBG, C: CBD, D: CBDV, and E: THC.

The interaction maps above show multiple cannabinoid ligand interaction with CB1 and CB2 receptors with interactions that include conventional hydrogen bonding used for the orientation of the molecule, interaction at the middle range (1.6 Å to 3.8 Å). Since proteins are surrounded by other proteins in a cell protein-ligand complexes could be attracted by electrostatic dipole interactions due to the presence of π – cation, π- π t-shaped, and π-π stacked interactions observed (13). These are long-distance and low energy effect, there needs to be more affinity for competitive docking (7). The presence of π – alkyl and alkyl interactions is associated with hydrophobic interactions, they have the shortest distance between the ligand and protein, this would mean high binding affinity (3) (17). Although, the dockings must be validated by wet-lab assays (17).

CB1 receptor interactions: Two of the 5 cannabinoids showed conventional hydrogen bonding with the Ser^{383} residue, which is a significant residue for bonding suggested also by Shao *et al*, (2016). Another common residue that interacted with all the ligands is Met^{103}. The ligand interaction in Figure 3.7, shows the amino acids present in the binding pocket of the CB1 protein with the taranabant ligand docked in the site (10). In Figure 3.7 cannabinoid ligands are docked in the binding pocket of the CB1 receptor. CBD has a π – sulfur bond with Met^{384}, π – alkyl interaction with Met^{103} and alkyl interactions with the other residues in contact with CBD (Figure 3.7A). In the CBDV interaction map, we observed conventional hydrogen bonding with an OH-group on the aromatic ring with residues Ser^{383}, other π-sigma interactions with Phe^{108}, π – alkyl and alkyl interactions (Figure 3.7B). The tricyclic CBN ligand showed more π – alkyl, alkyl, and π – sigma, with the π – sigma interaction in the interaction map (Figure 3.7C). The Ser^{383} residue showed a conventional hydrogen bond at the OH-group in the CBG structure, and a π-π stacked interaction with the aromatic ring (Figure 3.7D). The interactions with the THC model showed direct alkyl interactions with the residues Ile^{169}, Ala^{380}, and Phe^{189}. Met^{103} displayed a π – sulfur interaction with THC, while the Phe^{102} residue showed π-π T-shaped interactions and the Asp^{104} residue showed van der Waals interactions that may also be important in stabilizing ligands – recall the changes seen in binding in the presence and absence of alkyl chains on the ligand (Figure 3.7E).

CB2 receptor interactions: In Figure 3.8, are interactive maps of cannabinoid ligands THC, CBD, CBDV, CBN, and CBG. The CB2 model did not have a pre-existing ligand binding. Interestingly we noticed the cannabinoids had conventional hydrogen interaction in the CB2 model binding pocket. Leu^{239} common in all interactions. The CBN ligand OH- group in the aromatic ring has a convention hydrogen bond the Glu^{331}. This π – cation interaction with the Lys^{67} residue, differing with the other cannabinoids while it has alkyl interactions with CBD (Figure 3.8C) and CBDV (Figure 3.8D) in the same position (Figure 3.8A). CBG shows conventional hydrogen bond interaction Glu^{331} and Lys^{67} with the OH-group on the aromatic ring. The CBG ligand has a π - sigma interaction with the Leu^{243} and alkyl interaction with Arg^{242}, Leu^{239}, Tyr^{141}, Cys^{134}, and Lys^{67}. (Figure 3.8B). Based on the structural similarities in the CBD and CBDV structure, similar interactions were observed in the interaction maps (Figure 3.8C and 3.8D. The interaction residues Asp^{240} and Arg^{236} with conventional hydrogen bond, alkyl, and π – alkyl interactions with the residues Lys^{67}, Leu^{234}, Tyr^{141}, with the exception Cys^{134} and Arg^{242}, which are alkyl interactions observed in CBD interaction maps. This is also the major difference in the interactive maps. The residue Leu^{243} had π – sigma with the aromatic ring in both CBD and CBDV (Figure 3.8C and 3.8D. The THC ligand in the CB2 pocket has few interactions with the hydrogen bond interactions with OH-group on the in the aromatic ring, with Glu^{331} and Tyr^{70} residues (Figure 3.8E).

3.8 Conclusion

The CB2 receptor homology model was successfully modelled using I-TASSER, this was essential for receptor-ligand interactions, determining active site coordinates for the model, using I-TASSER Maestro and CastP. The best highest binding energies were obtained when the cannabinoids THC, CBD, CBDV, CBG and CBN were docked using CastP coordinates. Some of the receptor-ligand interactions of cannabinoids with the CB1 and CB2 receptors were consistent with the findings in the literature, with the most essential residues visible in the ligand-interaction maps. The best lowest binding energies were from docking with the CB1 receptor in the case of both phytocannabinoids and fragment structures. Resulting binding energies from the docking showed were satisfactory showing that, combining LC-MS fragment structure prediction and molecular docking has proven to be a promising interdisciplinary approach to fragment-based drug design

3.9 References

1. Murray C.W and Rees D.C. Opportunity Knocks Organic Chemistry for Fragment-Based Drug Discovery (FBDD). *Angew Chemie - Int Ed*. 2016;55(2):488–92.

2. Chen J.Z, Wang J, and Xie X.Q. GPCR structure-based virtual screening approach for CB2 antagonist search. *J Chem Inf Model.* 2007;47(4):1626–37.

3. Murray C.W and Blundell T.L. Structural biology in fragment-based drug design. *Curr Opin Struct Biol*. 2010;20(4):497–507.

4. Kumar A, Voet A, and Zhang K.Y.J. Fragment-based drug design: from experimental to computational approaches. *Curr Med Chem*. 2012;19(30):5128–47.

5. Di Luccio E and Koehl P. A quality metric for homology modelling: The H-factor. *BMC Bioinformatics*. 2011;12 (1):48.

6. Binkowski T.A, Naghibzadeh S, and Liang J. CASTp: Computed Atlas of Surface Topography of proteins. *Nucleic Acids Res*. 2003;31 (13):3352–5.

7. Chen H, Lyne P.D, Giordanetto F, Lovell T and Li J. On evaluating molecular-docking methods for pose prediction and enrichment factors. *J Chem Inf Model*. 2006;46(1):401–15.

8. Forli S, Huey R, Pique M.E, Sanner M, Goodsell D.S, and Olson A.J. Computational protein-ligand docking and virtual drug screening with the AutoDock suite. *Nat Protoc.* 11(5): 905–919.

9. Zemla A. LGA: A method for finding 3D similarities in protein structures. *Nucleic Acids Res.* 2003;31(13):3370–4.

10. Shao Z, Yin J, Chapman K, Grzemska M, Clark L, Wang J and Rosenbaum D. High-resolution crystal structure of the human CB1 cannabinoid receptor. *Nature*. 2016;540(7634):602–6

11. Khetrapal N. Cognition meets assistive technology: Insights from load theory of selective attention. *Handb Res Hum Cogn Assist Technol Des Access Transdiscipl Perspect*. 2010;96–108.

12. John Harris C, D. Hill R, W. Sheppard D, J. Slater M, F.W. and Stouten P. The Design

and Application of Target-Focused Compound Libraries. *Comb Chem High Throughput Screen*. 2011;14(6):521–31.

13. Abdel-Hamid M.K and McCluskey A. *In Silico* docking, molecular dynamics and binding energy insights into the bolinaquinone-clathrin terminal domain binding site. *Molecules*. 2014;19(5):6609–22.

14. Russo EB. Cannabinoids in the management of difficult to treat pain. *Ther Clin Risk Mana*g. 2008;4(1):245–59.

15. Citti C, Linciano P, Panseri S, Vezzalini F, Forni F, Vandelli MA Gigli G, Aldo Lagana`, A Carmela Maria C Montone CM,〃 and Cannazza G. Cannabinoid profiling of hemp seed oil by liquid chromatography coupled to high-resolution mass spectrometry. *Front Plant Sci.* 2019;10(2):1–17.

16. Hagmann WK. The discovery of taranabant, a selective cannabinoid-1 receptor inverse agonist for the treatment of obesity. *Arch Pharm* (Weinheim). 2008;341(7):405–11.

17. Li, X, Hua T, Vemuri K, Ho J.H, Wu Y, Wu L, Popov P, Benchama O, Zvonok, N, Locke, K, Qu L, Won Han G, Iyer M.R, Cinar R, Coffey N.J, Wang J, Wu M, Katritch V, Zhao S and Kunos G.Crystal Structure of the Human Cannabinoid Receptor CB2. *Cell*. 2019;176(3):459-467.e13.

18. Song Z.H, Slowey C.A, Hurst D.P, and Reggio P.H. The difference between the CB1 and CB2 cannabinoid receptors at position 5.46 is crucial for the selectivity of WIN55212-2 for CB2. *Mol Pharmacol.* 1999;56(4):834–40.

19. Crowther G.J, Van Voorhis WC, and Quinn RJ, Fragment-Based Screening of a Natural Product Library against 62 Potential Malaria Drug Targets Employing Native Mass Spectrometry. *ACS Infect Dis*. 2018;4(4):431–44.

Chapter 4
Concluding remarks and Future work

4.1 Concluding remarks

The advancement of cannabinoid research influenced our interest in understanding the endocannabinoid system, endocannabinoids and phytocannabinoids, and their impact on pain and inflammation. In reviewing these concepts, it was found that the existing research has made progress in arguing for the possibilities of cannabinoids use as analgesics. To date, it is well known that several cannabinoid-infused products have some therapeutic effects around relaxation, pain and inflammation, due to the strategic distribution of the components of the endocannabinoid system along the CNS and PNS.

This research forms part of the body of research that argues for the medicinal significance of the cannabis plant and reduction of the stigma surrounding it, also providing a well-researched understanding of the cannabinoid system, endocannabinoids, phytocannabinoids, terpenes and terpenoids. Methods for qualitative analysis of cannabinoids, assessing chromatographic condition effects on precursor ions and a method that gives more accurate precursor ion masses for fragment structure elucidations were developed in this work. The mass accuracies of cannabinoids analysed were less than 10 ppm, which was the desired value. Although some of the fragment structures would prove difficult to synthesize, they give an insight into the binding affinities that can be obtained from docking fragments in the CB1 and CB2, and they indicate structural features that might be important in the fragments such as the aromatic moiety and the alkyl side-chain. Although we expected higher binding energies with bigger fragment we did not expect the -5.12 kcal/mol from docking on the CB1 receptor structure, showing the the "aromatic" moiety common in all the cannabinoid structures used in this work, has a high impact on binding affinity. Overall the binding energies of the fragment structures showed good binding to the CB1 and CB2 receptor, that also leads to the interesting observation of the increase of binding energies as the length of the alky side chain on the fragments is increased, but that this trend only applies to 5 carbons.

4.2 Future work

In terms of future work concerning this study, it would be interesting to consider a quantitative and qualitative analysis of other cannabinoid-infused products with alternative cannabinoid standards as well as terpene standards. A study on the appropriate collision-induced dissociation for some cannabinoids would help design improved methods or cannabinoid analysis, avoiding the complete dissociation of cannabinoid precursor ions. Synthesis and analysing of synthetic cannabinoids or cannabinoid related fragment structures can be considered in the future, along with performing bioassay on the compounds.

In silico studies in future can be used to view the interactive maps of the performed dockings and use some of them as the starting point for designing fragment libraries for high-throughput virtual screening. Although we discussed fragment structures based on the structure elucidations made from the MS data, in the future we hope to predict structures that could be good binders from these fragment structures. Relating to pain and inflammation, considering docking cannabinoids on other known receptors studied for their impact on pain and inflammation besides the cannabinoid receptors lead to interesting findings on how cannabinoids perform as ligands in other receptors.